

# Determining the killer whale gut microbiome and its genetic ability to degrade persistent organic pollutants

**Cédric THIENPONT**

Promotor: Prof. Dr. Ellen Decaestecker  
Laboratory of Biology - MicrobiomeEcoEvo

supervisor: Broos Van de Moortel  
Laboratory of Biology - MicrobiomeEcoEvo

Thesis presented in fulfillment of the  
requirements for the degree of Master of  
Science in Biology

Academic Year 2024-2025

---

© Copyright by KU Leuven

Without written permission of the promotors and the authors it is forbidden to reproduce or adapt in any form or by any means any part of this publication.

Requests

for obtaining the right to reproduce or utilize parts of this publication should be addressed to KU Leuven, Faculteit Wetenschappen, Celestijnenlaan 200H - bus 2100,

3001 Leuven (Heverlee), Telephone +32 16 32 14 01.

A written permission of the promotor is also required to use the methods, products, schematics and programs described in this work for industrial or commercial use, and for submitting this publication in scientific contests.

## Acknowledgements

First of all, I would like to thank my promotor Prof. Dr. Ellen Decaestecker for granting me the opportunity to perform my master thesis on this pioneering topic. Secondly, I would like to express my sincere gratitude and respect to my supervisor, Broos van de Moortel, for his invaluable guidance throughout this journey. His patience, constructive feedback on my scientific writing, and willingness to share his expertise in the research field have been deeply appreciated.

I also wish to thank Loro Parque Zoo (Nakita Camara, Marta Canchal and Javier Almunia) for their important contribution to this study, particularly for providing stool samples from four of their killer whales. Likewise, I am grateful to Thierry Jauniaux for directing the sampling of the killer whale stranded at De Panne, to Lonneke IJsseldijk for sharing the stool sample from the killer whale stranded at Cadzand, and to Eve Jourdane for providing the sample from the stranded killer whale at Sognefjord. Finally, I extend my thanks to Prof. Dr. Dirk Springael and Dr. Rakeshkumar Yadav for conducting the Oxford Nanopore sequencing and kindly guiding us through this procedure.

The resources and services used in this work were provided by the VSC (Flemish Supercomputer Center), funded by the Research Foundation - Flanders (FWO) and the Flemish Government.

# Tablet of Contents

<b>1. Summary</b> .....	<b>vi</b>
<b>2. Introduction</b> .....	<b>1</b>
2.1. <i>Persistent Organic Pollutants (POPs)</i> .....	1
2.1.1 POP properties .....	1
2.1.2 POP bioaccumulation and biomagnification .....	1
2.1.3. Legacy and emerging POPs.....	1
2.1.4. POP effects on reproduction .....	2
2.1.5. POP effects on development and growth .....	2
2.1.6. POP effects on immune system .....	3
2.2. <i>POP accumulation in killer whales</i> .....	3
2.3. <i>Gut microbiome</i> .....	4
2.3.1. Acquisition of gut microbiome.....	4
2.3.2. Factors influencing gut microbiome composition .....	4
2.3.3. Microbiome functions.....	5
2.3.4. Absorption of POPs .....	7
2.3.5. Host biotransformation of POPs.....	7
2.3.6. POP microbial degradation and metabolism by the gut microbiome .....	7
2.4. <i>Cetacean gut microbiome</i> .....	17
2.5. <i>Techniques to study gut microbiome functions</i> .....	17
2.5.1. 16S rRNA amplicon sequencing .....	17
2.5.2. Metagenomic sequencing.....	18
<b>3. Objectives</b> .....	<b>18</b>
<b>4. Materials &amp; Methods</b> .....	<b>19</b>
4.1. <i>Sample collection</i> .....	19
4.1.1. Gut content sampling from wild killer whales .....	19
4.1.2. Gut content sampling from captive killer whales .....	20
4.2. <i>Microbial DNA extraction and quantification</i> .....	20
4.2.1. Microbial DNA extraction   PowerFecal Pro kit.....	20
4.2.2. Host DNA depletion and microbial DNA extraction   HostZero Microbial DNA kit .....	20
4.2.3. DNA quantification   Qubit dsDNA High Sensitivity Assay kit .....	20
4.3. <i>16S amplicon sequencing</i> .....	21
4.3.1. Full-length 16S rRNA gene sequencing   PacBio Revio.....	21
4.4. <i>Metagenomic Sequencing</i> .....	21
4.4.1. Shotgun sequencing   Illumina NovaSeq .....	21
4.4.2. Long read sequencing   Oxford Nanopore .....	22
4.5. <i>Bioinformatics</i> .....	22
4.5.1. 16S amplicon sequencing .....	22
4.5.2. Metagenomic sequencing.....	22
4.6. <i>Data Analysis</i> .....	23
4.6.1. 16S amplicon sequencing data analysis .....	23
4.6.2. Short read assembly vs hybrid assembly.....	25
4.6.3. Metagenomic data analysis .....	25
<b>5. Results</b> .....	<b>26</b>
5.1. <i>16S amplicon sequencing results</i> .....	26

5.1.1. Gut microbiome diversity along the intestinal tract of killer whale De Panne.....	26
5.1.2. Gut microbiome composition along the intestinal tract of killer whale De Panne.....	26
5.2. Short read assembly vs hybrid assembly.....	30
5.3. Metagenomics results.....	33
5.3.2. POP-degrading gene diversity and pathway completeness in gut microbiome of Killer whale De Panne.....	33
5.3.3. POP-degrading gene diversity in stranded vs captive killer whales.....	41
<b>6. Discussion.....</b>	<b>43</b>
6.1. The gut microbiome of killer whale De Panne displays an increasing gradient in $\alpha$ -diversity along the intestinal tract.....	43
6.2. Microbiome composition varied along the intestinal tract of killer whale De Panne.....	44
6.3. Comparison of short read and hybrid assembly.....	45
6.4. The gut microbiome of killer whale De Panne exhibits the ability to degrade a wide range of POPs, highlighting enhanced degradation potential for DDT, HBCD, and HCH compounds.....	46
6.5. The wild killer whale gut microbiome exhibits the ability to degrade a wider range of POPs, while the captive killer whale gut microbiome shows higher abundances of specific POP-degrading genes.....	48
6.6. Limitations of the study.....	48
<b>7. Conclusions and future perspectives.....</b>	<b>49</b>
<b>8. References.....</b>	<b>50</b>
<b>9. Addendum.....</b>	<b>A</b>
A. Risk Assessment.....	A
General safety.....	A
Chemical risks.....	A
Physical risks.....	A
Environmental.....	A
B. Supplementary content.....	B

## LIST OF ABBREVIATIONS:

1,4-TCDN	1,3,4,6-Tetrachloro-1,4-Cyclohexadiene
2,5-DCHQ	2,5-Dichlorohydroquinone
2,5-DDOL	2,5-Dichloro-2,5-cyclohexadiene-1,4-diol
4-CBA	4-Chlorobenzoic Acid
ASD	Autism Spectrum Disorder
ASV	Amplicon Sequence Variant
BDE-3	4-Monobromodiphenyl Ether
CDT	Cyclododecatriene
CYP	Cytochrome P450
DCBE	2-Chloro-1,4-Benzenediol

DDA	2,2-Bis(p-chlorophenyl)acetic Acid
DDD	Dichlorodiphenyldichloroethane
DDE	Dichlorodiphenyldichloroethylene
DDM	1-Chloro-2,2-Bis(p-chlorophenyl)ethane
DDMU	1,1-Bis(p-chlorophenyl)-2-Chloroethene
DDNU	2,2-Bis(p-chlorophenyl)nitroethane
DDT	Dichlorodiphenyltrichloroethane
GLM	Generalized Linear Model
HBCD	Hexabromocyclododecane
HCB	Hexachlorobenzene
hCG/LHR	human Choriogonadotropin/Luteinizing Hormone Receptor
HCH	Hexachlorocyclohexane
Iga	Immunoglobulin A
MAMPs	Microbe-Associated Molecular Patterns
OHCTT	1-(2-hydroxy-2,2,2-trichloroethyl)-4- Chlorobenzene
OTU	Operational Taxonomic Unit
PAH	Polycyclic Hydrocarbon
PBCDE	Pentabromocyclododecene
PBCDOH	Pentabromocyclododecanol
PBDE	Polybrominated Diphenyl Ether
PCB	Polychlorinated Biphenyl
PCBe	Pentachlorobenzene
PCDD	Polychlorinated Dibenzo-p-Dioxins
PCDF	Polychlorinated Dibenzofuran
PCoA	Principal Coordinate Analysis
PCP	Pentachlorophenol
PGE2	Prostaglandin E2
PGF2 $\alpha$	Prostaglandin F2 Alpha
POP	Persistent Organic Pollutant
PRR	Pattern Recognition Receptors
SCFAs	Short Chain Fatty Acids
TCA	Tricarboxylic Acid
TeCH	Tetrachlorohydroquinone
TLR	Toll-Like Receptors

## 1. Summary

In this study, we characterized the microbiome composition along the full length of the intestinal tract (duodenum, jejunum, ileum, colon, and rectum) of a killer whale (*Orcinus orca*) stranded in De Panne, Belgium. While the overall microbiome composition showed strong similarities to that of other cetacean species, distinctions were observed. Microbial community composition varied significantly along the intestinal tract; however, no significant pairwise differences were detected between specific regions, likely due to the limited number of replicates ( $n = 3$ ). In contrast, alpha diversity showed a significant increase along the tract, with significant pairwise differences identified between all regions for Shannon and inverse Simpson Diversity. We further assessed the genetic potential of the killer whale gut microbiome to degrade persistent organic pollutants (POPs), comparing stranded (wild) ( $n = 2$ ) and captive ( $n = 2$ ) individuals. Both microbiomes harboured genes associated with the degradation of a broad range of POPs, with notable enrichment for genes involved in the degradation of DDT, HBCD, and HCH. Interestingly, the captive killer whale microbiome contained higher overall abundances of POP-degrading genes, whereas the stranded killer whale microbiome exhibited the genetic capacity to degrade a broader range of POPs. We compared Nanopore-Illumina hybrid metagenome assembly to Illumina-single assembly. Hybrid assembly did not result in the detection of any additional POP-degrading genes, likely due to low Nanopore sequencing depth. To our knowledge, this study represents the first comprehensive characterization of the killer whale gut microbiome and provides a comparative analysis of microbial composition across distinct gut regions in this species.

## 2. Introduction

### 2.1. Persistent Organic Pollutants (POPs)

#### 2.1.1 POP properties

Persistent organic pollutants (POPs) are anthropogenic organic chemicals strongly resistant to degradation due to their chemical and physical properties. They are typically characterized by a low water solubility value, due to their high molecular weight, and by both a high octanol water partition coefficient ( $K_{ow}$ ) (meaning they are lipophilic) and high organic carbon water partition coefficient ( $K_{oc}$ ) value (meaning they are absorbed by and accumulate in soil when present in groundwater), due to their high degree of chlorination and bromination (O'Sullivan & Megson, 2014). A range of POPs, including industrial chemicals, such as polychlorinated biphenyls (PCBs) and polycyclic aromatic hydrocarbons (PAH's), organochlorine pesticides, such as dichlorodiphenyltrichloroethane (DDT), hexachlorocyclohexane (HCH) and hexachlorobenzene (HCB), and brominated flame retardants, such as polybrominated biphenyl ethers (PBDEs) and hexabromocyclododecane (HBCD), enter the environment through incineration, industrial leaks, pesticide use in agriculture, etc.. Many POPs are semi-volatile, at higher temperatures they partition to the atmosphere either in the gas phase or as particles associated to atmospheric particles (O'sullivan and Megson 2014). Once in the atmosphere, they are deposited when temperatures lower to values specific for each POP. Cycles of partitioning between atmosphere and surface, referred to as the 'grasshopping' effect, result in long-range atmospheric transport to high latitude regions (Gouin et al. 2004). (Jones & De Voogt, 1999).

#### 2.1.2 POP bioaccumulation and biomagnification

POPs enter the marine environment through atmospheric wet- or dry deposition or by river runoff through particulate organic matter binding. Subsequently, they are absorbed by phytoplankton and zooplankton or deposited in marine bottom sediments (Ilyina et al. 2006). The combination of their lipophilic nature and resistance to metabolism leads to strong POP bioaccumulation (Guo et al. 2019). As these pollutants are transferred through the food web, they undergo biomagnification, with concentrations increasing 1- to 100-fold at each trophic level (Chen et al., 2023, chapter 13). Chronic accumulation of POPs in animals causes detrimental endocrinologic deficiencies often leading to a fatal outcome.

#### 2.1.3. Legacy and emerging POPs

The production of POPs has been globally banned by the Stockholm convention in 2004, yet their persistence in terrestrial and aquatic ecosystems remains a major concern. Oceanic concentrations have declined on a global scale although the arctic ocean acts as an important reservoir and shows increasing POP accumulation through oceanic currents (Zhang et al. 2024a). Furthermore, the chemical industry continues to develop structurally modified compounds that mimic the functionality of POPs - such as for use as pesticides or flame retardants - allowing them to bypass existing regulations and necessitating frequent legislative updates. These new substances, referred to as emerging organic pollutants, contrast with legacy POPs, which have been banned for decades.

#### 2.1.4. POP effects on reproduction

POPs are known to be endocrine disruptors, i.e., they disrupt hormonal function through mimicking hormones, competitively binding to receptors and affecting hormone transport or synthesis. Consequently, they cause a wide range of health defects, including reproductive defects. For example, *in vitro* DDT contamination reduces the potency of human chorionic gonadotropin/luteinizing hormone receptor (hCG/LHR) which is a G protein coupled receptor mediating cAMP production (Munier et al. 2021). Proper functioning of the hCG/LHR is necessary for ovulation and sustaining pregnancy during the first trimester (Ascoli, Fanelli, and Segaloff 2002). Furthermore, DDT is both an estrogenic receptor beta agonist, at low doses, and antagonist, at high doses, influencing oestradiol secretion accordingly. In ovarian granulosa cells of rats, low doses of DDT suppress ovarian gene expression and lead to reduced prostaglandin E2 (PGE2) production (Liu et al. 2012). In cows, as a result of DDT contamination, PGE2 secretion from endometrial cells decreased whilst prostaglandin F2 alpha (PGF2 $\alpha$ ) secretion increased. The PGF2 $\alpha$ :PGE2 ratio shifted from 1:1 to 1:4-10. This altered prostaglandin ratio may induce myometrial contractions, increasing the risk of premature birth, whilst accelerating luteum regression. In addition, luteal regression stimulates oxytocin secretion which further stimulates PGF2 $\alpha$  production, creating a positive feedback loop (Wrobel, Mlynarczuk, and Kotwica 2009). A study on Baltic grey seals revealed the association of PCB contamination and uterine leiomyomas prevalence, indicating an imbalance in uterine-associated hormones (Bredhult et al. 2008). In harbour porpoises, PCB exposure has been associated with increased reproductive failure (Murphy et al. 2015). In summary, persistent organic pollutants (POPs) are associated with a wide range of reproductive disorders, and it is highly probable that additional, as yet unidentified, POP-related reproductive impairments remain to be discovered.

#### 2.1.5. POP effects on development and growth

In addition to reproductive disorders, POPs have been revealed to impair growth and neurological development. In humans, PCB exposure during pregnancy leads to an impaired neurological development of the child. Children whose mother was exposed to POPs during pregnancy had a lower full-scale IQ compared to a control group and an impaired cortical development demonstrated by longer P300 latencies and reduced P300 amplitude (Chen & Hsu, 1994). In addition, prenatal exposure to PCBs and related contaminants is associated with reduced cognitive functioning and reduced psychomotor activity during early childhood (Koopman-Esseboom et al. 1996; Oseph, Acobson, and Acobson 1996). One of the mechanisms for cognitive impairment is the disruption of thyroid hormones. Hydroxymetabolites formed by PCB, Polychlorinated dibenzo-p-dioxin (PCDD) and Polychlorinated dibenzofuran (PCDF) metabolism have been shown to compete with T4 for binding to transthyretin and thyroxine-binding globulin. As these are the main T4 transporting proteins, competitive binding results in defective thyroid hormone transport (Lans et al. 1994). Hypothyroidism (underactive thyroid) during early development causes impaired brain development (Nicholson An and Altman 1972). PCB and DDT contamination has also been associated with reduced thyroid hormone transport in juvenile California sea lions (Debieer et al. 2005). In bottlenose dolphins, PCB exposure was correlated to anaemia due to iron deficiency as a result of hypothyroidism (Schwacke et al. 2011). In summary, POPs induce drastic neurological impairments through disruption of thyroid hormones.

### 2.1.6. POP effects on immune system

POPs are suspected to impair the immune response leading to increased susceptibility to pathogens. Although the mechanisms responsible for these immune defects are unknown, some correlations between contamination of specific POPs and immune disruption have been studied. Concrete evidence of POP-induced immunotoxicity in humans remains limited. However, long-term HCB exposure has been linked to reduced interferon gamma, a cytokine secreted by T-lymphocytes upon pathogen infection, production (Daniel et al. 2001). In harbour seals, the consumption of PCB- and DDT-contaminated food has been linked to reduced natural killer cell activity, reduced lymphocyte response to mitogens, such as concanavalin A, pokeweed mitogen and phytohaemagglutinin-M, and an increase in haemolytic granulocyte concentration. Furthermore, PCB and DDT contamination resulted in decreased lymphocyte proliferation (Swart et al. 1994). In addition, reduced *in vitro* lymphocyte proliferation and monocyte and neutrophil phagocytosis as a result of PCB and 2,3,7,8-TCDD exposure was revealed for multiple dolphin species, including killer whales (*Orcinus orca*, Linnaeus, 1758) (Levin et al. 2005; Mori et al. 2006). These findings suggest a decrease in both lymphocyte quantity and quality as a result of PCB and DDT contamination (Mos et al. 2006). In contrast, PCB-contaminated seals and cetaceans also showed increased respiratory bursts in leukocytes, which suggests an enhancement of the immune response (Desforages et al. 2016). To summarize, POPs affect both the innate and acquired immunity of exposed individuals causing an increased susceptibility to diseases.

### 2.2. POP accumulation in killer whales

Marine mammals are among the most contaminated mammals in the world due to their position at the top of the marine food web, substantial blubber reserves and long lifespans. Killer whales, in particular, are considered the most heavily contaminated marine mammals in terms of persistent organic pollutant accumulation. (Desforages et al. 2018). In Canadian arctic killer whales the DDT concentration is 390.000 times higher in their blubber (80mg/kg lw (lipid weight)) than in arctic oceanwater (205 pg/liter) (Desforages et al. 2024; Zhang et al. 2024b). Some of the most prevalent POPs within killer whales are organochloride pesticides like DDT, HCH and HCB, flame retardants like PBDEs and industrial chemicals like PCBs. In Canadian killer whale populations, POP concentrations in blubber tissue reach: 80 µg/g lw DDT, 0.6 µg/g lw HCH, 1.1 µg/g lw  $\Sigma$ CLBz (HCB), 40 µg/g lw PCB and 1.0 µg/g lw PBDE and in Norwegian populations they reach significantly lower concentrations of 26.8 µg/g lw DDT, 0.08 µg/g lw HCH, 0.29 µg/g lw HCB, 48.2 µg/g lw PCB and 1.38 µg/g lw PBDE (Andvik et al. 2020; Desforages et al. 2024; Rayne et al. 2004). Populations from Norway that feed on marine mammals accumulate more pollutants than fish-eating populations driving them past pollution effect thresholds (Andvik et al. 2020). Similarly, in populations from the Northeast pacific, PCB concentrations were found to be at least tenfold greater in marine mammal-eating killer whales compared to fish-eating individuals (Herman et al. 2005). Furthermore, mothers offload POPs to their progeny via gestation and lactation perpetuating contaminants and their associated health effects across generations (Frouin et al. 2012; Greig et al. 2007). Consequently, all marine mammal-eating killer whale populations are currently predicted to be at a risk of collapse due to chronic POP exposure (Desforages et al. 2018). Although animals possess limited capacity of metabolising POPs and their metabolites, certain bacteria have shown the capacity to degrade specific xenobiotic pollutants, making them an interesting subject to study, as they might potentially contribute to pollutant metabolism.

## 2.3. Gut microbiome

### 2.3.1. Acquisition of gut microbiome

The early microbiome is vertically inherited from the mother. While it was once thought that microbiome acquisition occurred exclusively during and after birth, recent research has revealed the presence of microbiota in the placenta, previously thought to be sterile, suggesting that microbiome acquisition starts *in utero*. However, researchers have yet to reach consensus on this matter (Miller et al. 2024; Perez-Muñoz et al. 2017). Early colonisation of gut microbiota is critical for development of the immune response (Arrieta et al., 2015). The important role of birth in microbiome colonisation is underlined by the reduced microbial diversity of infants born via caesarean section compared to vaginal delivery (Diniz Pinto Coelho et al. 2021). Moreover, infants born via C-section are more susceptible to development of chronic immune diseases, including asthma, inflammatory bowel disease and leukaemia (Sevelsted et al. 2015). Post-birth, microbiota structure is further modified through breastfeeding. Breast milk is rich in probiotics, including *Bifidobacterium* and *Lactobacillus* strains, crucial for pathogen resistance (Lyons et al. 2020). Moreover, in humans, breastfeeding has been shown to provide the infant with prebiotics, specifically human oligosaccharide, which stimulate the development of a healthy and diverse microbiome (Vandenplas et al. 2020). It is not known whether marine mammals also acquire their microbiota during birth although similar mechanisms as in terrestrial mammals seem evident as both share a placental viviparity reproductive strategy. Next to vertical transmission, gut microbiota can be shaped through horizontal transmission, defined as the acquisition of microbes coming from the environment throughout the hosts life span (Rosenberg and Zilber-Rosenberg 2022). Some interesting observations of horizontal microbiota transfer are the acquisition of microbes boasting antibiotic resistance genes by lettuce grown in soil containing manure of cattle treated with antibiotics, as well as microbial transfer from pets to humans (Song et al. 2013; Sun et al. 2021). Although all adult gut microbiome composition are unique, certain bacterial taxa/species are consistently found across individuals, referred to as the core microbiome, opposed by the transient microbiome which is determined by environmental factors but also host genetics (Sharon et al. 2022). Dissimilarities across individuals stem from various factors that influence gut microbiome composition.

### 2.3.2. Factors influencing gut microbiome composition

Microbiome compositions among conspecifics are similar yet host-specific, suggesting the existence of various factors influencing microbiota structure. These factors range from genetic to environmental origin. In humans, a genome-wide association study revealed the association of at least 8 bacterial taxa and single nucleotide polymorphisms in the host genome, demonstrating the role of genetics in microbiome composition (Davenport et al. 2015). An increasing pool of data demonstrate this impact of host genetics on microbiome composition although knowledge regarding the responsible mechanisms remains limited (Dabrowska and Witkiewicz 2016). It is suspected that host immune response shapes the microbiome through anti-microbial peptide production, induced by signalling between host and gut microbiome. For instance, recognition of microbe-associated molecular patterns (MAMPs) regulates the production of intestinal mucus which transports antimicrobial substances such as immunoglobulin A (Chairatana and Nolan 2017). This suggests a pronounced co-evolution of host and their core gut microbiota (Tasiemski et al. 2015). An additional factor that impacts gut microbiome structure is sex. In humans, gut microbiome function and composition can differ according to the sex of the host (Markle et al. 2013). In marine mammals, however, sex does not seem to significantly affect microbiome

composition as studies on several species, including leopard seals, dugongs, manatees, bottlenose dolphins and both dwarf- and pygmy sperm whales, found no significant differences between males and females (Bik et al. 2016; Denison et al. 2020a; Eigeland et al. 2012; Merson et al. 2014; Nelson et al. 2013). Indigestible food is fermented by gut microbes, therefore the sculpting role of diet on microbiome is evident. Consumption of an unbalanced diet can lead to dysbiosis, a condition characterized by a disturbed microbiome composition (Zhang 2022). Similarly, in marine mammals, diet is suspected as a primary driver for microbiota structure (Nelson et al. 2013). Furthermore, in humans, microbiome composition varies between age cohorts. Research suggests that, in humans, up to the age of 20 the microbiome matures whilst from the age of 70 onward it transitions to a typical elderly microbiome composition (Odamaki et al. 2016). Similar age related effects were found in marine mammals. In harbour seals, age was determined as the predominant driver for microbiome composition. However, these age related differences in microbiome might be the result of the difference in diet of pup and adult seals (Pacheco-Sandoval et al. 2022). Abundance of Bacillota bacteria seems to positively correlate with latitude whilst the Bacteroidetes phylum correlates negatively with latitude, suggesting a role of geographic location on microbiome composition in humans (Suzuki and Worobey 2014). Likewise, gut microbiome composition has been revealed to vary within marine mammal species across geographical locations. This geographical diversity is likely caused by factors such as exposure to pollutants and differences in diet (Delpont et al., 2016). Another microbiome defining factor is exposure to conspecifics, which mediates transmission of bacterial taxa. For example, Southern elephant seals, which are social animals, harbour a greater gut microbiome species diversity compared to solitary leopard seals (Nelson et al. 2013). However, additional differences between both species, such as genetics, could be responsible for the observed microbiome diversity differences.

### 2.3.3. Microbiome functions

#### 2.3.3.1. Nutrient synthesis

The gut microbiome aids in metabolism of various macronutrients, most of which are typically undigestible to the host, essentially expanding the host's dietary niche (Rowland et al. 2018). In the distal gut, carbohydrates are metabolized by microbiota to short chain fatty acids (SCFA), such as butyrate, acetate and propionate. These play important roles for the host including: acting as a source of energy, inducing gluconeogenesis, inducing satiation and acting as a co-factor for additional gut microbiota growth (Duncan et al. 2004; Kaji and Kuwahara 2008; De Vadder et al. 2014). Similarly, the gut microbiome is capable of fermenting proteins and amino acids, resulting in synthesis of SCFAs and branched-chain fatty acids, phenols, indoles, polyamines and more (Davila et al. 2013). Furthermore, microbiota can synthesize vitamin K and B. In human studies, subjects that were treated with broad-spectrum antibiotics and followed a diet low in vitamin K experienced decreased plasma prothrombin levels (Frick et al. 1967). In addition, the gut microbiome can alter host metabolism through modification of bile acids. Bile acids facilitate the absorption of lipids. They also act as signalling molecules, regulating their own production in addition to modulating lipid and glucose metabolism (Hirokane et al. 2004; Pircher et al. 2003; Stayrook et al. 2005). Modification of their composition could possibly affect lipid absorption and host metabolism (Rowland et al. 2018).

#### 2.3.3.2. Maturation of immune system

Early-life intestinal colonisation is important for maturation of the immune system. This is demonstrated by the higher prevalence of immune diseases in infants delivered by

caesarean section compared to vaginal delivery (Sevelsted et al. 2015). Gut microbiota aid in the maturation of the host immune system through a multitude of mechanisms. T-cell production is induced through sensing of microbial metabolites, such as SCFAs and indoles, by dendritic- and/or T-cells. Moreover, SCFAs can reduce inflammation through inhibition of neutrophil activity (Belkaid and Hand 2014). Host cells can detect MAMPs via binding to pattern recognition receptors (PRR), mostly present in cells contributing to innate immunity. These receptors include toll-like receptors (TLRs) and C-type lectins. *Bacteroides fragilis*, a commensal gut bacterium, produces and secretes polysaccharide A (PSA). Recognition of PSA by TLR2 induces regulatory T cells whilst suppressing interleukin 17-producing T cells (Round et al. 2011). In mice, this ultimately leads to protection against inflammatory bowel disease, induced by *helicobacter hepaticus*, and innate recognition of *B. fragilis* as a beneficial bacterium (Mazmanian, Round, and Kasper 2008). Germ-free mice demonstrated disrupted lymphoid structures, suggesting a microbial role in development of proper lymphatic tissues (Bauer et al. 1963). Colonisation of the gut microbiome in said germ-free mice results in restoration of intestinal Immunoglobulin A (IgA) levels and interleukin 17 producing cells which maintain homeostasis of intestinal epithelial cells (Hapfelmeier et al. 2010; Ivanov et al. 2009). All together, these findings illustrate the importance of gut microbiota in the development and proper functioning of the immune system.

#### 2.3.3.3. Pathogen protection

The gut microbiome protects the host from pathogens by promoting colonisation resistance (Horrocks et al. 2023). Beneficial gut bacteria compete with pathogens through various mechanisms, including direct nutrient competition which restricts pathogen colonisation and growth. Additionally, microbial production of SCFAs inhibits pathogen growth (Sorbara et al. 2019).

#### 2.3.3.4. Behaviour

Gut microbiota can affect host behaviour through interaction with the gut-brain axis, defined as the “bidirectional communication between the central and the enteric nervous system” (Carabotti et al. 2015). Gut microbiome dysbiosis has been shown to disrupt neurogenesis. Germ-free mice display increased neurogenesis in the dorsal hippocampus, upregulated expression of genes related to myelination in the prefrontal cortex, increased motor activity and reduced anxiety and dysregulated expression of genes related to microglia maturation (Heijtz et al. 2011; Hoban et al. 2016; Kim and Shim 2023; Matcovitch-Natan et al. 2016; Ogbonnaya et al. 2015). Composition of the gut microbiome can alter the release of neurotransmitters (Hooper et al. 2001). Moreover, gut bacteria can produce molecules that function as neurotransmitters (Asano et al. 2012). Mice treated with *Lactobacillus rhamnosus* displayed reduced stress-, anxiety- and depression-related behaviour. Vagotomy of previous mentioned mice led to disappearance of the effects, suggesting the vagus nerve as a communication pathway between gut bacteria and the brain (Bravo et al. 2011). In addition, gut bacteria can affect the gut-brain axis via metabolites. For example, autism spectrum disorder (ASD) mice that were fed beneficial bacterial metabolites exhibited improved behavioural symptoms (Sharon et al. 2019). Furthermore, children suffering from ASD exhibit a reduced butyrate producing gut microbiome (Liu et al. 2019). In conclusion, gut microbiota can affect the gut-brain axis in various ways. Gut dysbiosis is suspected to be involved in several neurological disorders, including Parkinson’s disease, Alzheimer’s disease and ASD (Kowalski and Mulak 2019; Liu et al. 2019; Tan, Lim, and Lang 2022).

#### 2.3.3.5. Toxicant metabolism

The gut microbiome can digest various toxicants thus serving another beneficial role for the host. One example of gut bacterial toxicant metabolism can be found in the coffee berry borer. This beetle feeds on coffee berries and appears resistant to the toxic effects caffeine has on herbivore insects. This caffeine resistance is mediated by *Pseudomonas fulva*, present in the beetle's gut, as it demethylates caffeine (Ceja-Navarro et al. 2015). Another example of gut microbiome mediated toxicant resistance is that of the fall armyworm. The caterpillar can freely feed on maize as gut bacteria, specifically *Pantoea dispersa*, metabolize the toxic benzoxazinoids (Qi et al. 2024). Furthermore, mammals also show examples of gut microbiome mediated detoxification. For example, koalas host gut bacteria, such as *Lonepinella koalarum*, are capable of metabolising Tannins and Tannin-protein complexes. Tannins form strong bonds with proteins which impedes their metabolism (Osawa et al. 1995). In camels, a large share of ingested indospicine, a known hepatotoxin, is metabolised by microbes in the foregut. However, a significant part remains unmetabolized and accumulates in the camel's tissues (Tan et al. 2017).

#### 2.3.4. Absorption of POPs

Once ingested, POPs are transported to the intestines. In the small intestines, they bypass the unstirred water layer with the help of bile salt micelles after which they are transferred through the membrane of enterocytes (Kelly, Apc Gobas, and Mclachlan 2004). In the epithelial cells, POPs can be transported through the cytoplasm or by lipoproteins (Dulfer, Govers, and Groten 1998). They are subsequently transported into the lymph or venous blood through exocytosis (Amutova et al. 2021). In the blood vessels, POPs are transported throughout the body and deposited in lipid-rich organs (Amutova et al. 2021).

#### 2.3.5. Host biotransformation of POPs

POPs in the blood stream can be partially degraded by the liver, generally, by cytochrome P450 (CYP) enzymes. PCBs are biotransformed to OH-PCB and MeSO<sub>4</sub>-PCB metabolites by phase I and phase II enzymes (Routti et al. 2008). DDT is biotransformed to Dichlorodiphenyldichloroethane (DDD) and Dichlorodiphenyldichloroethylene (DDE) by CYP enzymes. In rats, DDD can be converted to 2,2-bis(p-chlorophenyl)acetic acid (DDA) which is excreted through urine (IARC, 2018). DDE and DDD show reduced toxicity and increased solubility (Zhang et al. 2021). In rats, HCB is degraded to pentachlorophenol (PCP) and tetrachlorohydroquinone (TeCH). This reaction is catalysed by cytochrome P450 enzymes and is considered as bioactivation, defined as a the production of a more reactive chemical compound, since metabolism of HCB to PCP and TeCH results in accumulation of hepatic porphyria (Van Ommen et al. 1989). Alternatively, pentachlorothiophenol can be produced by glutathione conjugation of HCB (Charbonneau 1992). An *in vitro* study on human liver cells revealed metabolism of the PBDE congener BDE-99 by CYP enzymes. However, the resulting metabolites showed greater toxicity than the parent congener itself (Stapleton et al. 2009). HCHs are metabolised by hepatic CYP enzymes to primary metabolites such as chlorophenols and 1,2,4-trichlorocyclohexane-4,5-epoxide (ATSDR 2024).

#### 2.3.6. POP microbial degradation and metabolism by the gut microbiome

Microorganisms have been known for their potential to degrade organic pollutants in soils and are therefore often used as agents for bioremediation (Marinescu, Dumitru, and Lăcătușu 2009). The following section will give a summary of known microbial

biodegradation pathways of the most prevalent POPs accumulating in marine mammals and what is known about their metabolism by the gut microbiome. Note that there is not one universal pathway for any POP compound and proposed pathways can differ for each species.

#### 2.3.6.1. Polychlorinated biphenyls (PCB)

PCBs consist of two benzene rings which are chlorinated to a strong degree (varies by congener). They used to be produced to be applied for various functions, such as electrical insulating-, hydraulic- and heat transferring fluids (Erickson and Kaley 2011). PCBs have two microbial biodegradation pathways, one aerobic and the other anaerobic. In the aerobic pathway, bacteria open the aromatic ring via Biphenyl-2,3-dioxygenase producing chlorobenzoic acid and 2-hydroxy-penta-2,4-dienoic acid (Xiang et al. 2020) (Fig. 1). Most bacteria cannot metabolize chlorobenzoic acid and 2-hydroxy-penta-2,4-dienoic acid, resulting in their accumulation during PCB metabolism. Chlorobenzoic acids are toxic to microorganisms as they interact with their cell membrane. Therefore their accumulation reduces ongoing PCB degradation (Wójcik et al. 2020). A limited number of bacteria have been identified capable of fully metabolizing chlorobenzoic acid. In addition, *Paraburkholderia xenovorans* LB400 has been revealed to degrade 2-hydroxy-penta-2,4-dienoic acid, producing acetyl-CoA (Xiang et al. 2020). In the anaerobic pathway, PCBs are degraded via dichlorination, resulting in less chlorinated biphenyls (Borja et al. 2005) (Table 1). This reduces their toxicity as less chlorinated biphenyls appear to be less carcinogenic (Moore 2000). In addition, less chlorinated biphenyls display lower affinity for the dioxin receptor (Borja et al. 2005).

**Table 1 | Overview of general PCB microbial degradation steps.** Table shows the general microbial PCB degradation steps with their respective enzyme types and examples of encoding genes.

Reaction type	Reaction step	Enzyme type	Gene examples
Anaerobic	Reductive dechlorination	dehalogenases	PceA, CprA, DcbA
Aerobic	Biphenyl Dioxygenation	Biphenyl Dioxygenases	bphA
Aerobic	Dihydrodiol Dehydrogenation	Dihydrodiol Dehydrogenases	bphB
Aerobic	Ring Cleavage	Ring-cleaving dioxygenase	bphC
Aerobic	Hyrdolysis and further downstream metabolism	Hydrolases, isomerases, and aldolases	bphD

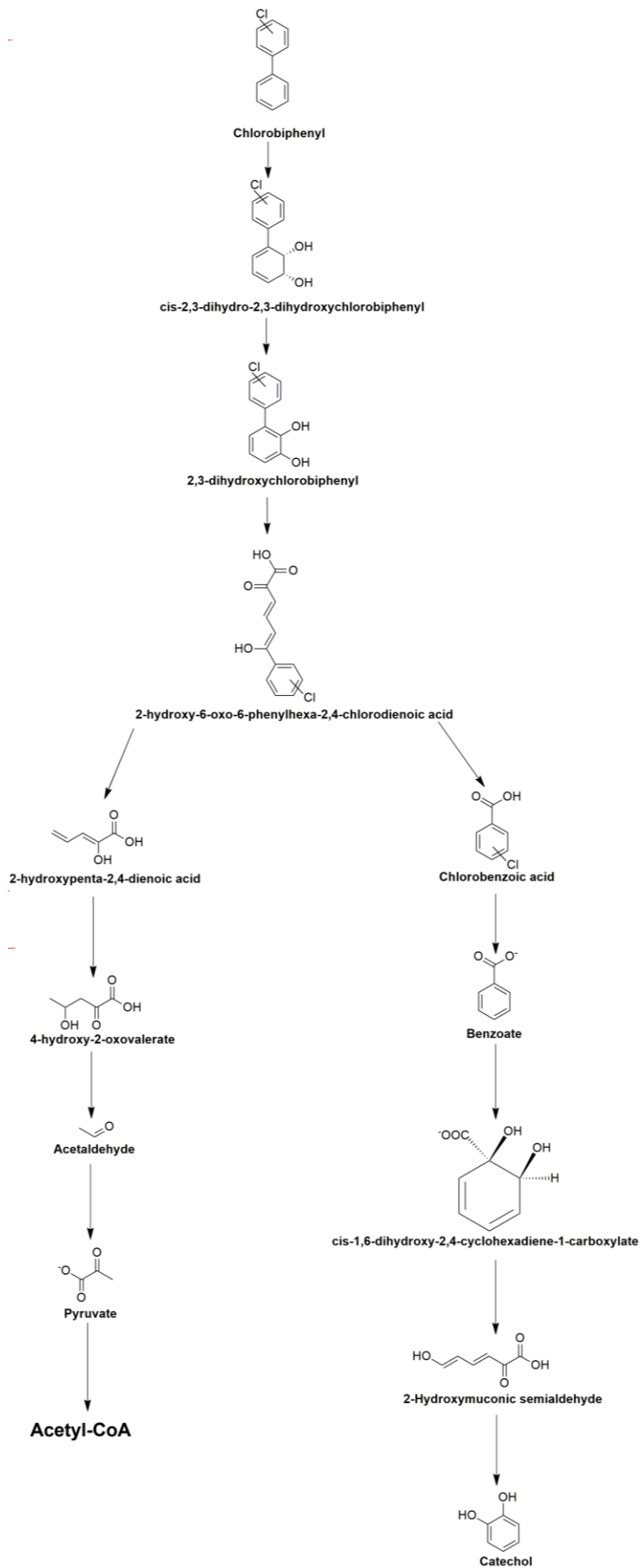


Fig. 1 | Proposed aerobic PCB microbial degradation pathway. (Source: <http://mibpop.genome-mining.cn/>)

### 2.3.6.2. Dichlorodiphenyltrichloroethane (DDT)

DDT is an organochlorine pesticide, banned since the 70's and part of the 12 original POPs adopted in the Stockholm convention, "The Dirty Dozen" (Xu, Wang, and Cai 2013). DDT is most efficiently microbially degraded in anoxic conditions, although both aerobic and anaerobic enzymes are required for complete mineralization. DDTs are reductively dechlorinated to DDD and aerobically dehydrochlorinated to DDE (Chen et al. 2013; Suman and Tanuja 2021) (Fig. 2) (Table 2). Subsequently, these metabolites are further dechlorinated to 1,1-Bis(p-chlorophenyl)-2-chloroethene (DDMU) which is then eventually metabolized to 4-chlorobenzoic acid (4-CBA) (Neerja et al. 2016). As previously mentioned, Chlorobenzoates are toxic to microorganisms and there are a limited number of bacteria known that can metabolize them (Xiang et al. 2020).

**Table 2 | Overview of general DDT microbial degradation steps.** Table shows the general microbial DDT degradation steps with their respective enzyme types and examples of encoding genes.

Reaction type	Reaction step	Enzyme type	Gene examples
Anaerobic	Reductive Dechlorination	Reductive dehalogenases	rdhA, pceA, cprA, dcaA
Aerobic	Dehydrochlorination	Dehydrochlorinase	linA
Aerobic	Hydroxylation/oxidation	Dehydrogenases/Dioxygenases	bphA, bphB
Aerobic	Ring cleavage	Dioxygenases	bphC
Aerobic	Further downstream metabolism	Hydrolases	bphD

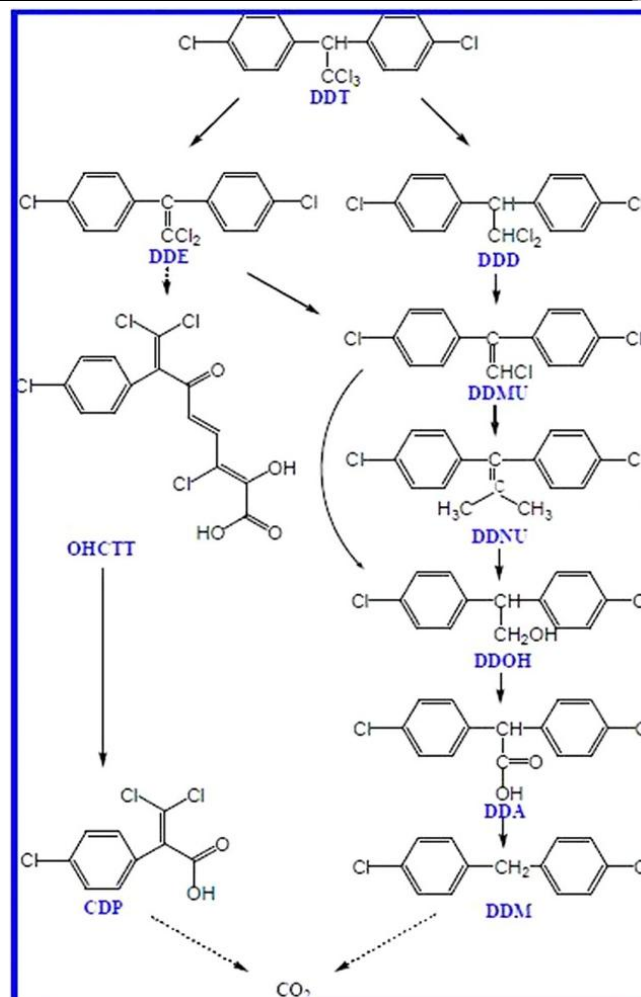


**Fig. 2 | Proposed DDT microbial degradation pathway.** (Adapted from (Pan et al. 2016))

### 2.3.6.3. Hexachlorobenzene (HCB)

HCB consists of a fully chlorinated benzene ring. It was historically used as a pesticide until it was adopted by the Stockholm Convention as one of the 'Dirty Dozen' in 2001 (Kumar, Kumar, and Kalaichelvan 2013). HCB is degraded most efficiently in anaerobic conditions. In these conditions it is generally dechlorinated to benzene after which it can be mineralized (Taş et al. 2011). In aerobic conditions, HCB is dechlorinated to PCP or pentachlorobenzene (PCBe) (Fig. 3) (Table 3) (Ito et al. 2017; Van Ommen et al. 1989). Subsequent degradation steps vary across strains. For example, *Acinetobacter sp.* catalyses an ortho ring cleavage pathway resulting in the formation of TeCH and 2-chloro-1,4-benzenediol (DCBE) (Sharma and Thakur 2008). In gram-positive bacteria, genes have been identified that encode enzymes responsible for HCB dechlorination to PCP as well as those encoding for PCP-degrading enzymes. In these strains, PCP is dechlorinated to TeCH, which is converted to 2,3,5,6-tetrachloro-p-benzoquinone, subsequently dechlorinated to 2,5,6-trichloro-p-hydroquinone (Ito 2021).

**Table 3 | Overview of general HCB microbial degradation steps.** Table shows the general microbial HCB degradation steps with their respective enzyme types and examples of encoding genes.

Reaction type	Reaction step	Enzyme type	Gene examples
Anaerobic	Reductive dechlorination	Reductive dehalogenases	rdhA, cprA
Aerobic	Aerobic dechlorination	Reductase	hcbA
Aerobic	Hydroxylation	oxygenases or peroxidases	pcpB, pcpC, pcpD
(An)aerobic	Further downstream metabolisation	oxygenases	catA,

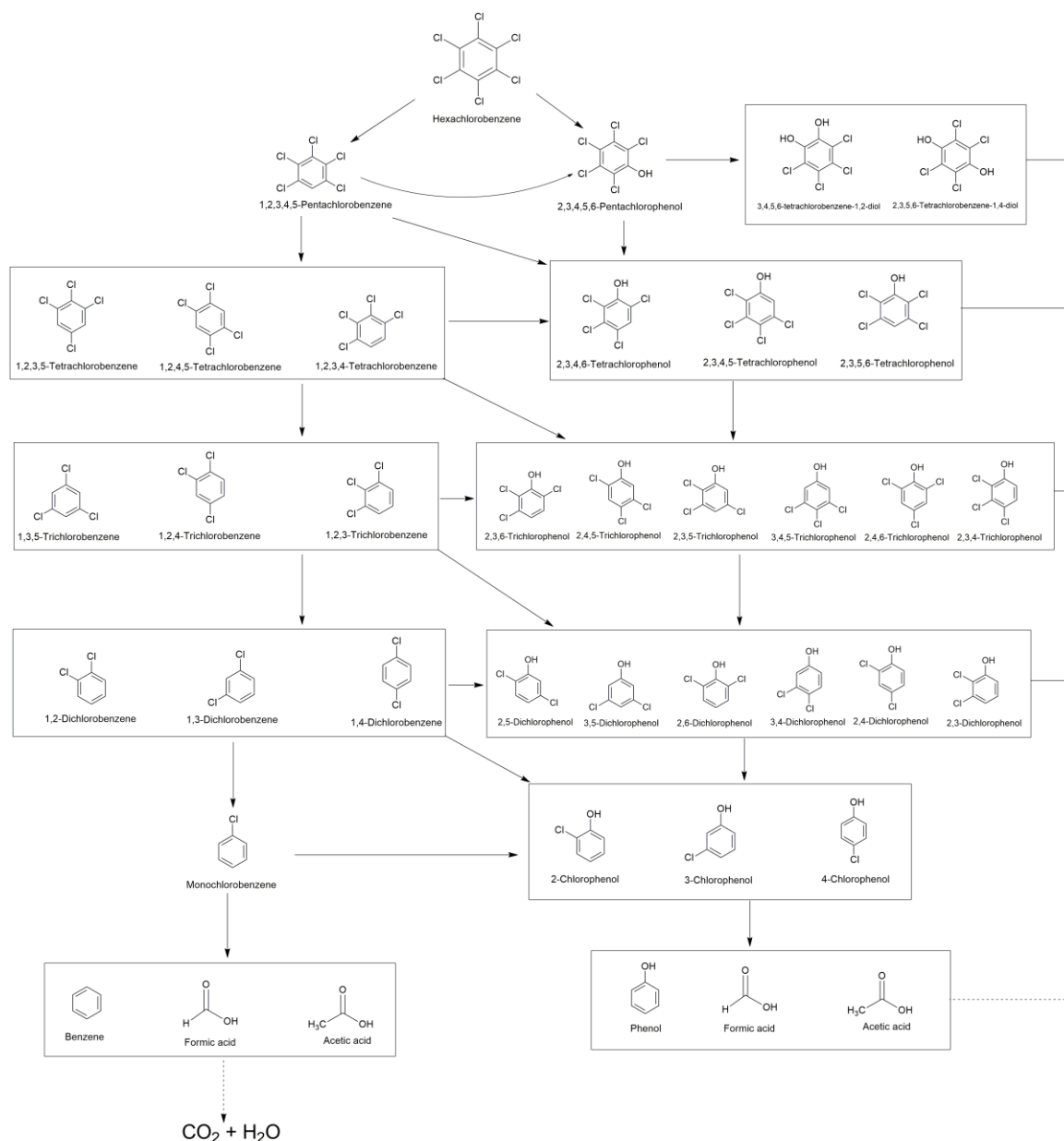


**Fig. 3 | Proposed microbial HCB microbial degradation pathways.** (Source: <http://mibpop.genome-mining.cn/>)

#### 2.3.6.4 Polybrominated diphenyl ethers (PBDE)

PBDEs are brominated flame retardants, which were used in various polymers to reduce combustibility (Alaee et al. 2003). They consist of two brominated benzene rings linked by an ether bond. High PBDEs are debrominated through dehalogenase activity to low PBDEs (Fig. 4) (Table 4) (Wu et al. 2018). *Shewanella oneidensis* has been revealed to degrade 4-monobromodiphenyl ether (BDE-3) by mediation of the Fenton reaction. Hydroxyl addition results in the production of both monobromophenol and hydroxylated BDE-3. In addition, certain microbial communities located in sludge samples can anaerobically debrominate BDE-3 resulting in the production of diphenyl ether and bromide ions (Shih, Chou, and Peng 2012).

**Table 4 | Overview of general PBDE microbial degradation steps.** Table shows the general microbial PBDE degradation steps with their respective enzyme types and examples of encoding genes.

Reaction type	Reaction step	Enzyme type	Gene examples
Anaerobic	Reductive debromination	Reductive dehalogenases	rdhA
Aerobic	Hydroxylation	Monoxygenases	bphA
Aerobic	Ring cleavage	Dioxygenases	bphC
Aerobic	Further downstream metabolization	Oxygenases	catA

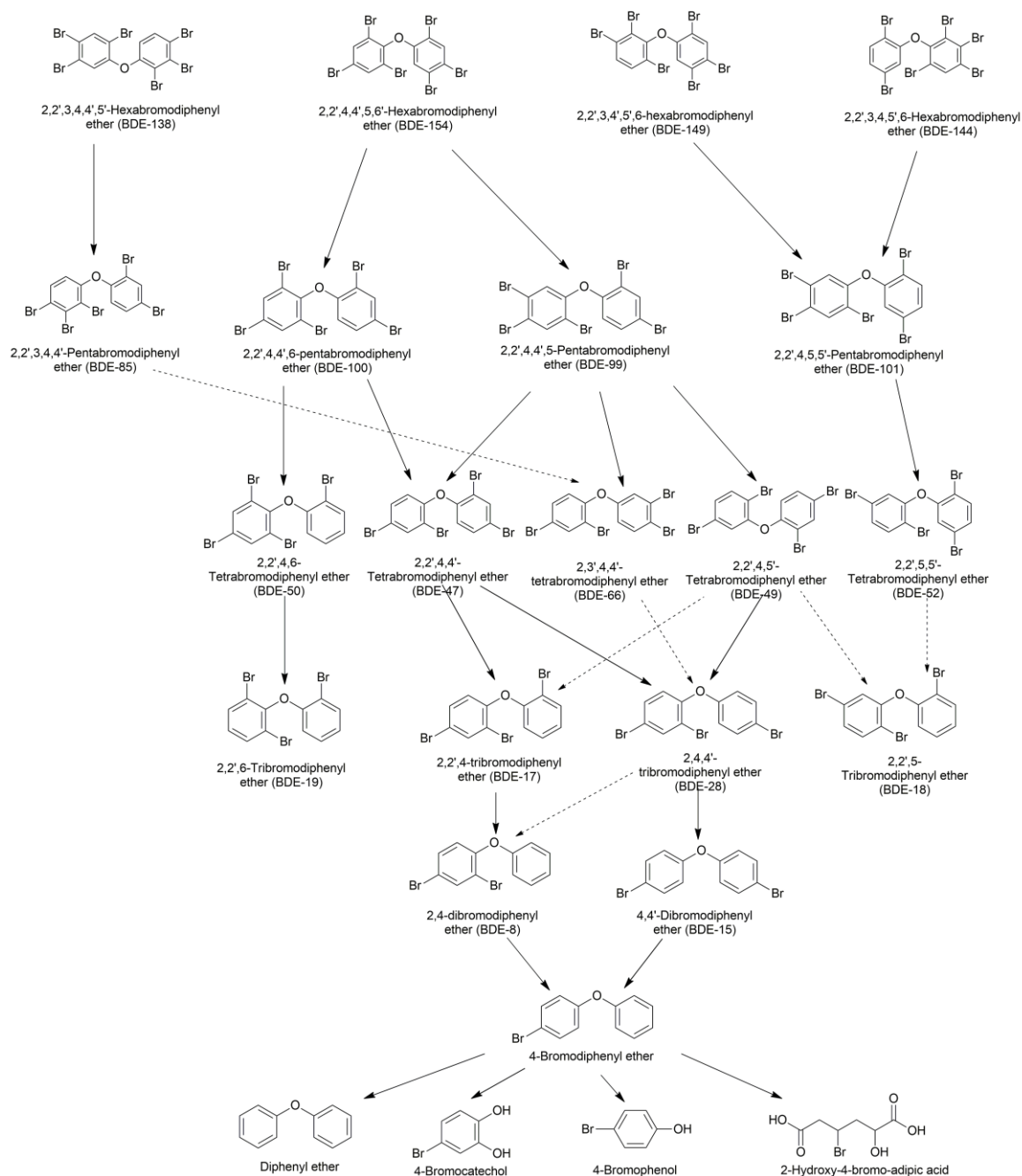


**Fig. 4 | Proposed microbial PBDE degradation pathway.** (Source: <http://mibpop.genome-mining.cn/>)

### 2.3.6.5. Hexachlorocyclohexane (HCH)

HCH is an organochlorine compound consisting of a cyclohexane ring with six chlorine atoms. It was widely used as an agricultural insecticide, particularly in its gamma-isomer form known as lindane, until it was listed under the Stockholm Convention as a persistent organic pollutant in 2009 (Xu et al. 2013). In aerobic conditions, HCH is dehydrochlorinated to 1,3,4,6-tetrachloro-1,4-cyclohexadiene (1,4-TCDN) by a dehydrochlorinase enzyme called LinA. Subsequently, a halohydrinase (LinB) converts 1,4-TCDN to 2,5-dichloro-2,5-cyclohexadiene-1,4-diol (2,5-DDOL) which is then converted to 2,5-dichlorohydroquinone (2,5-DCHQ) by a dehydrogenase (LinC). These consecutive steps are defined as the upstream pathway, which is followed by the downstream pathway (Zhang et al. 2020). 2,5-DCHQ is dechlorinated to  $\beta$ -keto adipate by a dechlorinase (LinD). It is then converted to acylchloride by a ring-cleavage dioxygenase (LinE). Subsequently, acylchloride is degraded to  $\beta$ -keto adipate by a maleylacetate reductase (LinF). Next,  $\beta$ -keto adipate can be converted to  $\beta$ -keto adipate CoA by CoA transferase (LinGH) activity which is broken down to succinyl-CoA and acetyl-CoA by  $\beta$ -keto adipyl CoA thiolase (LinJ) (Table 5). Finally these products are metabolized in the tricarboxylic acid (TCA) cycle (Fig. 5) (Endo et al. 2005).

In anoxic environments, HCHs are reductively dechlorinated with chlorobenzene and benzene as end products (Farrakh Mehboob et al. 2013). Liang et al. created microcosms in which they combined a culture capable of dechlorinating chlorobenzene and a culture capable of degrading benzene. This resulted in formation of CO<sub>2</sub> and CH<sub>4</sub> as end products (Liang et al. 2013).

**Table 5 | Overview of proposed HCH microbial degradation steps.** Table shows the general microbial HCH degradation steps with their respective enzyme types and examples of encoding genes.

Reaction Type	Reaction step	Enzyme type	Gene examples
Anaerobic	Reductive dechlorination	Reductive dehalogenases	rdhA
Aerobic	Dehydrochlorination	Dehydrochlorinases	linA
Aerobic	Dehalogenation	Dehalogenases	linB
Aerobic	Dehydrogenation	Dehydrogenases	linC
Aerobic	Ring cleavage	Reductive dechlorinases	linE
Aerobic	Reduction	Dioxygenases	linD
Aerobic	Further downstream metabolization	Maleylacetate reductases	linF, linG, linH, linJ

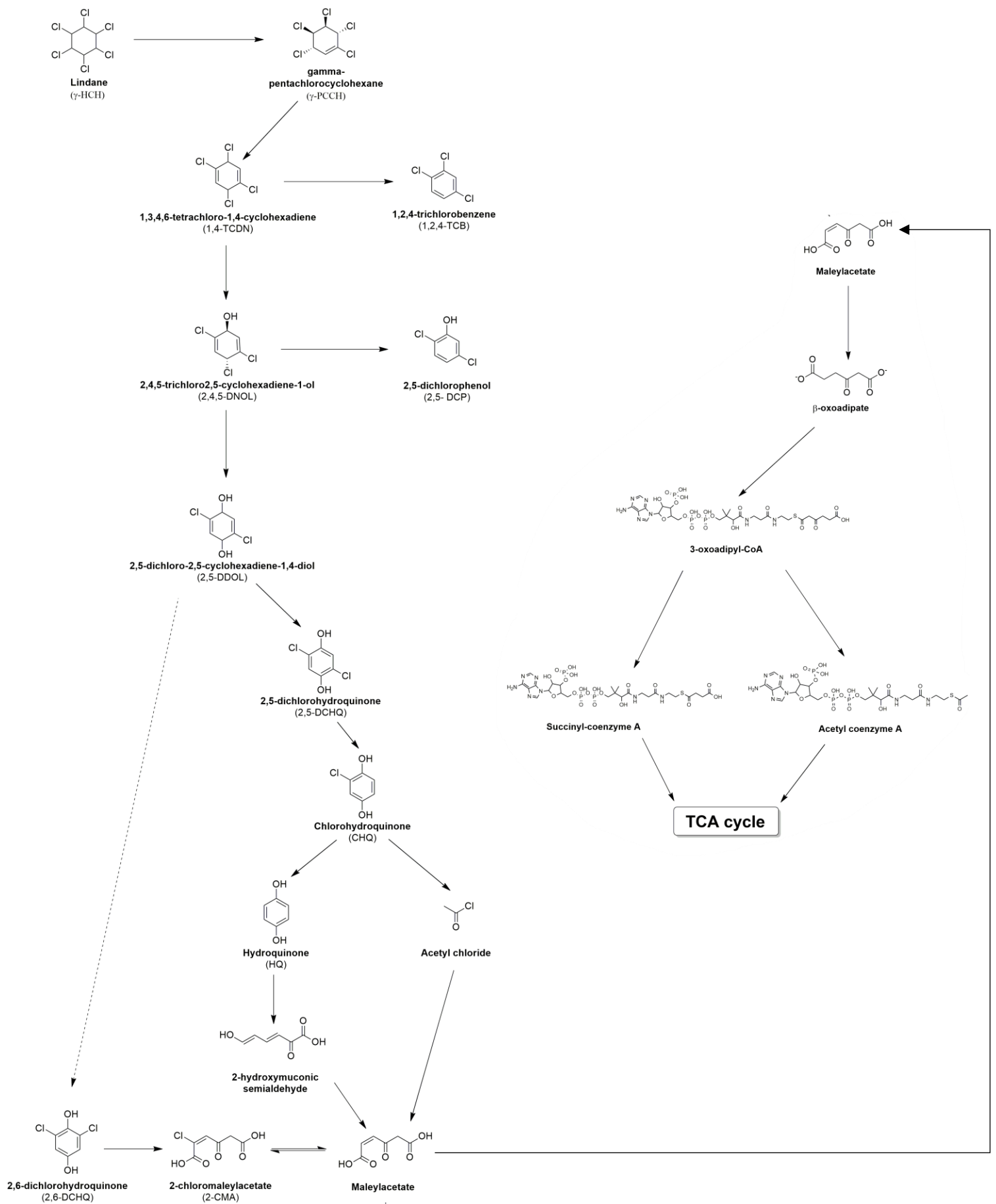


**Fig. 5 | Proposed aerobic microbial  $\gamma$ -HCH degradation.** (Source: <http://mibpop.genome-mining.cn/>)

### 2.3.6.6. Hexabromocyclododecane (HBCD)

HBCD is a brominated flame retardant, primarily used in polystyrene for the building industry, classified as an emergent POP and has been part of the Stockholm Convention on Persistent Organic Pollutants since 2013. Similar to most POPs, HBCD exposure has been linked to disruption of the hypothalamic-pituitary-thyroid axis (Marvin et al., 2011). Microbial HBCD degradation, primarily consists of anaerobic debromination to cyclododecatriene (CDT) (Fig. 6) (Peng et al. 2018). Subsequently, aerobic ring cleavage further degrades the metabolites (Table 6). In addition, HBCD can be aerobically debrominated to pentabromocyclododecene (PBCDE) and pentabromocyclododecanol (PBCDOH) (Chang et al. 2020).

**Table 6 | Overview of proposed HBCD microbial degradation steps.** Table shows the general microbial HBCD degradation steps with their respective enzyme types and examples of encoding genes.

Reaction type	Reaction step	Enzyme type	Gene examples
Anaerobic	Reductive debromination	Reductive dehalogenases	rdhA
Aerobic	Debromination	Haloalkane dehalogenases	linA, linB
aerobic	Hydroxylation	Oxygenases	/

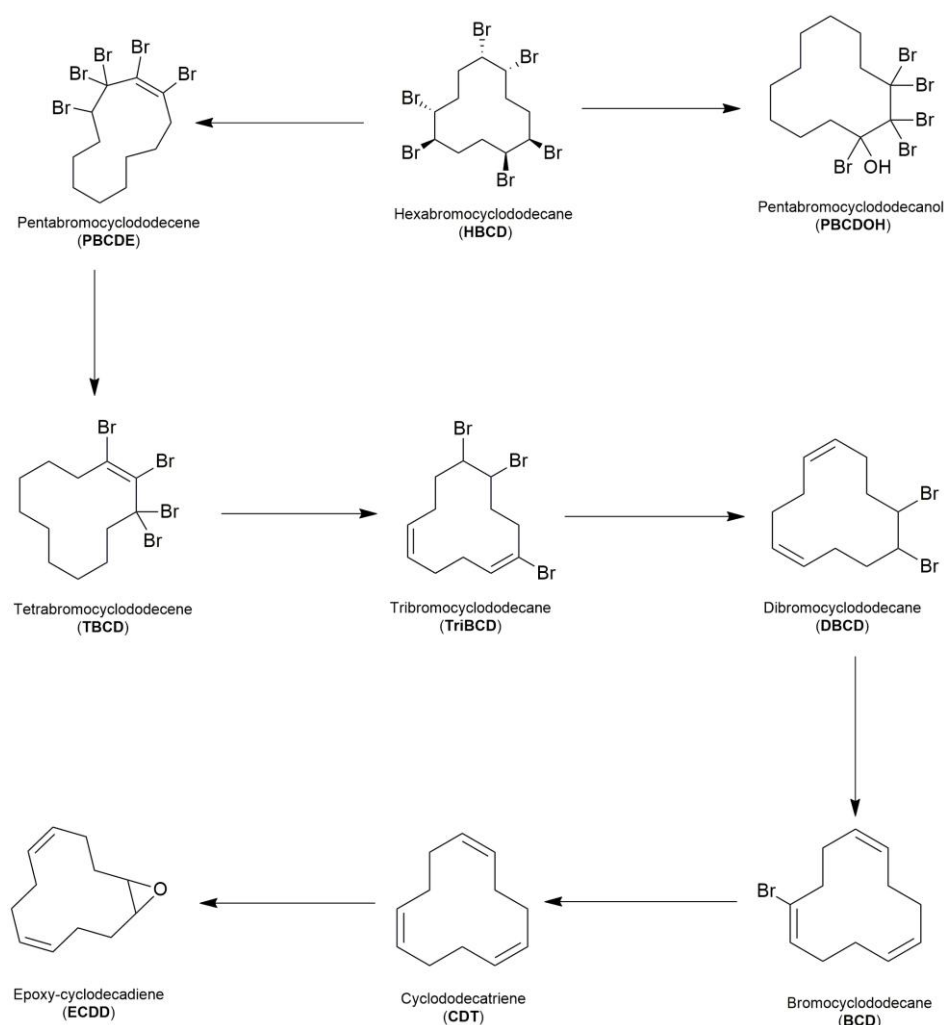


**Fig. 6 | Proposed microbial HBCD degradation pathway.** (Source: <http://mibpop.genome-mining.cn/>).

#### 2.3.6.7. POP metabolism by the gut microbiome

The majority of revealed microbial pollutant degrading pathways have been characterized in soil. Knowledge on the capacity of bacterial strains in the gut microbiome to degrade POPs remains limited although a few studies shed light on this phenomenon. The gut microbiome of rats has been revealed to be capable of degrading DDT, producing DDD (Claus, Guillou, and Ellero-Simatos 2016). However, as both compounds are considered endocrine disruptors, this might be an example of bioactivation. Furthermore, gut microbiota can mediate the degradation of PCBs to MeSO<sub>2</sub>-PCB which is excreted in the bile (Claus et al. 2016). A recent study revealed that the gut microbiome of a human population in Italy living in areas highly polluted with dioxins and PCBs was characterized by a higher abundance of microbial species capable of degrading POPs, such as *Asaccharobacter sp.*, *Eggerthella lenta*, *Gordonibacter urolithinifaciens*, and *G. pamelaee*. In addition, an increased prevalence of genes encoding for POP-degrading enzymes, i.e. dehalogenases and chlorobenzene dioxygenases, in the microbiome of individuals living in the highly contaminated areas was identified (De Filippis et al. 2024). This suggests that exposure to xenobiotic pollutants selects for pollutant degrading genes.

### 2.4. Cetacean gut microbiome

Whales, dolphins and porpoises are all classified as Cetacea. Among the closest terrestrial relatives of Cetacea are the Ungulates, such as cows (Gatesy et al. 2013). They share some anatomical similarities with these relatives, including a multichambered stomach (Horstmann 2017). Baleen whales, who exclusively feed on animals, demonstrate gut functions usually found in herbivorous species such as fermentation of chitin, structurally alike to cellulose (Sanders et al. 2015). This chitinolytic function is performed by bacteria in the non-glandular forestomach. These produce volatile fatty acids, which are readily available for absorption by the host although their role in host energy levels seems minimal (Olsen and Mathiesen 1996). The conserved similarities between the gut microbiota of terrestrial ruminants and baleen whales demonstrate host phylogeny as an important driver of gut microbiome functions. Moreover, cetacean gut microbiome structure has been shown to vary among fine-scale taxonomic levels. For example, microbiome structure between the two closely related kogiid whale species (pygmy and dwarf sperm whale) differed significantly (Denison et al. 2020b). Despite these first insights, significant knowledge gaps remain, especially regarding how pollution affects the microbiome of marine mammals, marking it a critical area for future investigation.

### 2.5. Techniques to study gut microbiome functions

#### 2.5.1. 16s rRNA amplicon sequencing

Characterization of microbiome composition is traditionally performed using 16S rRNA sequencing, a technique that targets the highly conserved 16S rRNA subunit gene found within bacteria. Primers designed to match this gene are employed for amplification using PCR. Afterwards, high-throughput sequencing of the amplified sequences allows for the identification of species present within the analysed microbiome by sequence matching with a reference database containing previously reported 16S rRNA sequences. A traditional limitation of 16S rRNA sequencing has been its relatively low taxonomic resolution, often restricting classification to the genus level and only occasionally to the species level. However, this limitation is being addressed by the use of newer long-read sequencing technologies, such as PacBio, which allow for full-length 16S rRNA gene sequencing and thus enable more accurate species- and even strain-level classification.

Despite these improvements, 16S rRNA sequencing remains limited to taxonomic profiling, as it targets only a single gene. Functional profiling of the microbiota is therefore not directly possible using this method. While functional capabilities can be inferred based on the known genomes of identified species, such predictions are imprecise because functional gene content can vary considerably between strains within the same species.

### 2.5.2. Metagenomic sequencing

In contrast to 16S rRNA sequencing, metagenomic sequencing enables comprehensive analysis of the entire genetic content of a microbiome, providing both taxonomic and functional insights. One widely used approach is shotgun metagenomic sequencing, which involves randomly fragmenting microbial DNA and sequencing these fragments individually. The resulting reads are then assembled *in silico* into contiguous sequences (contigs) or draft genomes. Because it captures the full genome rather than a single marker gene, shotgun metagenomics offers higher taxonomic resolution, often down to the species or strain level, and enables the identification of individual genes. Functional annotation can then be performed by matching these genes to reference databases, allowing for a more accurate and direct assessment of the microbiome's functional potential.

Another increasingly popular technique is long-read metagenomic sequencing, such as Oxford Nanopore sequencing, which can read extended DNA fragments in a single pass. This approach reduces the complexity of genome assembly and improves resolution across repetitive regions. While Nanopore sequencing historically suffered from high error rates, recent improvements in sequencing chemistry and base-calling algorithms have substantially increased its accuracy, making it a viable alternative for metagenomic analysis.

Additionally, hybrid assembly approaches, which combine short- and long-read data, can be employed to maximize the strengths of both platforms. Two main strategies exist: 1) scaffolding: Improving alignment of contigs by using long reads as a reference. 2) Polishing: Using the short reads to improve long read quality.

## 3. Objectives

Gut content samples of a stranded killer whale were sequenced for the 16S rRNA gene, using PacBio Revio sequencing. Subsequently, Amplicon Sequence Variants (ASVs) were annotated and employed to infer alpha-diversity, beta-diversity and microbiome composition across different intestinal regions: duodenum, jejunum, ileum, colon and rectum. To evaluate the gut microbiome's potential for degrading persistent organic pollutants (POPs), shotgun metagenomic sequencing was performed on samples from both wild and captive individuals using Illumina NovaSeq. In addition, long-read sequencing (Oxford Nanopore) was conducted on one wild individual to improve recovery of full-length degradation genes. Using the mibPOP database, we identified and compared the abundance and diversity of POP-degradation genes across habitats.

This dual approach allowed for mapping microbial diversity along the intestinal tract and investigating functional adaptations to environmental contaminant exposure.

The objectives of this master thesis are to answer the following research questions:

- ❖ What is the diversity and community composition of the killer whale gut microbiome?
- ❖ How does the microbiome differ among anatomical regions of the gut?
  - Hypothesis: Microbiome composition differs across gut regions due to region-specific physiological functions.
- ❖ What is the diversity of POP-degrading genes and pathways in the killer whale gut microbiome and how common are these genes in killer whales from different habitats (wild vs captive)?
  - Hypothesis 1: High and chronic exposure to POPs has selected for microbial strains with POP-degrading capabilities in the killer whale gut microbiome.
  - Hypothesis 2: Wild killer whales, exposed to higher environmental POP loads, will exhibit greater diversity and higher abundance of POP-degrading genes compared to captive individuals.

## 4. Materials & Methods

### 4.1. Sample collection

#### 4.1.1. Gut content sampling from wild killer whales

Three stranded killer whales were sampled: stranding Sognefjord December 2021 (female subadult), stranding Cadzand October 2022 (female adult) and stranding De Panne October 2023 (male juvenile). Since sampling was performed by different collaborating partners, the sampling procedure differed for each stranding.

##### 4.1.1.1. Stranded killer whale - De Panne, Belgium

The killer whale was stranded alive on 29 October 2023 at the De Panne beach in Belgium. Sampling was performed by Broos Van de Moortel 18.5 hours postmortem during the public necropsy performed on the De Panne beach at 30 October 2023 under the direction of Prof. Thierry Jauniaux (FARAH – Veterinary Public Health, Faculty of Veterinary Medicine, University of Liège). Three replicate samples of 50mL were taken from the rectum, colon and three equally spaced small intestine locations each by making a small incision in the gut wall and collecting the gut content into a sterile 50mL falcon tube. The equally spaced small intestine samples will hereon forth be referred to as duodenum, jejunum and ileum, respectively. However, compartmentalization in the cetacean small intestine is not as defined as in terrestrial mammals (Gerussi et al. 2024). Therefore these annotations might not be completely accurate. The samples were transported on ice (4°C) to the IRF Life Sciences facilities at Kulak and stored at -80°C for long term storage; except for one aliquot, containing gut content from the rectum. For this sample we immediately performed host DNA depletion and microbial DNA extraction using the HostZERO Microbial DNA kit.

##### 4.1.1.2. Stranded killer whale - Cadzand, The Netherlands

The killer whale was stranded alive at 15 October 2022 at the Cadzand beach in The Netherlands. Sampling was performed 9.5 hours postmortem by Lonneke IJsseldijk (Stranding Research – Faculty of Veterinary Medicine, University of Utrecht). The gut sample was taken from a random gut location during the necropsy at the facilities of the Faculty of Veterinary Medicine. The sample was stored at -80°C for long term storage.

#### 4.1.1.3. Stranded killer whale - Sognefjord, Norway

The killer whale stranding in Sognefjord took place most likely on 10 December 2021, at this date she was discovered. She was last seen alive on 5 December 2021. The necropsy and gut sampling took place at 11 December 2021. Therefore the killer whale might have been deceased for multiple days by the time of sampling. During the necropsy, a sample was taken from the rectum and stored at -80°C at Norwegian Orca Survey. For transport to Belgium, this sample was transferred into eNAT medium which preserves DNA and RNA integrity. Once arrived at the lab the sample was stored at -80°C.

#### 4.1.2. Gut content sampling from captive killer whales

Faecal samples were extracted by veterinarians at Loro Parque zoo and was coordinated by Dr. Nakita Câmara (Postdoc - University of Las Palmas de Gran Canaria), Marta Canchal (Conservation and research officer - Loro Parque) and Javier Almunia (Director - Loro Parque) using a tube and syringe which was inserted in the rectum. The samples were stored in RNALater medium, which preserves DNA and RNA integrity, for transport and kept at -80°C for long term storage.

### 4.2. Microbial DNA extraction and quantification

#### 4.2.1. Microbial DNA extraction | PowerFecal Pro kit

DNA extraction was performed on all samples – with the addition of three negative controls containing Vaseline, RNALater and eNAT to account for possible contamination introduced by these media during sampling – according to the *QIAamp PowerFecal Pro DNA kit handbook* experienced user protocol with a few modifications: usage of 300 µL stool per sample, vortexing for 3min followed by 2min of rest (repeated 3 times), transferring 900 µL at step 4, transferring 700 µL at step 6 and allowing evaporation at room temperature of the samples for 1 min before centrifugation at step 16. The final samples were eluted with 30µL C6 solution.

#### 4.2.2. Host DNA depletion and microbial DNA extraction | HostZero Microbial DNA kit

A fresh rectal sample from the stranded killer whale in De Panne was processed using the HostZERO™ Microbial DNA Kit protocol with an input volume of 200µL rectal content and elution volume of 20µL. This kit isolates only prokaryotic DNA through selective lysis of eukaryotic cells and subsequent application of DNases. This kit could only be used on the De Panne sample since all other samples had been frozen, causing all cells, including prokaryotic, to have been lysed by the time they arrived at the IRF lab in Belgium. As such the selective lysis principle of the HostZERO kit would be rendered ineffective for these other samples.

#### 4.2.3. DNA quantification | Qubit dsDNA High Sensitivity Assay kit

DNA quantification was performed using a Qubit™ fluorometer with samples prepared according to the Qubit dsDNA High Sensitivity Assay Kit protocol (Table 7).

**Table 7 | Qubit DNA concentrations of all gut samples and negative controls.**

Sample	Sample Code	category	Extraction Kit	Qubit DNA concentration (ng/ $\mu$ L)
Morgan	MO-FE	Captive	PowerFecal Pro	3.640
Tekoa	TE-FE	Captive	PowerFecal Pro	1.530
Keto	KE-FE	Captive	PowerFecal Pro	1.400
Adan	AD-FE	Captive	PowerFecal Pro	0.674
De Panne	DP-HZ	Stranded	HostZERO	34.9
Cadzand	CZ-GR	Stranded	PowerFecal Pro	0.29
Sognefjord	SO-FE	Stranded	PowerFecal Pro	91.8
Control Vaseline	VA-NC	Negative Control	PowerFecal Pro	$<0.50 \times 10^{-3}$
Control RNALater	RN-NC	Negative Control	PowerFecal Pro	$<0.50 \times 10^{-3}$
Control eNAT	EN-NC	Negative Control	PowerFecal Pro	$<0.50 \times 10^{-3}$
De Panne duodenum 1	DP-DU-A	Stranded	PowerFecal Pro	93.4
De Panne duodenum 2	DP-DU-B	Stranded	PowerFecal Pro	99.4
De Panne duodenum 3	DP-DU-C	Stranded	PowerFecal Pro	92.4
De Panne jejunum 1	DP-JE-A	Stranded	PowerFecal Pro	8.8
De Panne jejunum 2	DP-JE-B	Stranded	PowerFecal Pro	21.4
De Panne jejunum 3	DP-JE-C	Stranded	PowerFecal Pro	8.44
De Panne ileum 1	DP-IL-A	Stranded	PowerFecal Pro	94.4
De Panne ileum 2	DP-IL-B	Stranded	PowerFecal Pro	96.6
De Panne ileum 3	DP-IL-C	Stranded	PowerFecal Pro	100
De Panne colon 1	DP-CO-A	Stranded	PowerFecal Pro	31.4
De Panne colon 2	DP-CO-B	Stranded	PowerFecal Pro	37.2
De Panne colon 3	DP-CO-C	Stranded	PowerFecal Pro	26.2
De Panne rectum 1	DP-RE-A	Stranded	PowerFecal Pro	16.6
De Panne rectum 2	DP-RE-B	Stranded	PowerFecal Pro	18.2
De Panne rectum 3	DP-RE-C	Stranded	PowerFecal Pro	22.2

### 4.3. 16S amplicon sequencing

The extracted DNA was sequenced by Genomics Core for PacBio full-length 16s rRNA gene sequencing.

#### 4.3.1. Full-length 16S rRNA gene sequencing | PacBio Revio

All intestinal region (duodenum, jejunum, ileum, colon and rectum) sample replicates were sent to Genomics Core for 16S amplicon sequencing. A fragment analysis was performed to assess fragment lengths. A minimum fragment length of 1.5kbp was required, as this is the length of the 16S gene. DNA samples were 16S PCR amplified and subsequently library prepared according to the PacBio protocol: *Preparing Kinnex™ libraries from 16S*. Afterwards, another fragment analysis was performed on the 16S PCR amplicons to verify successful 16S amplification. Subsequently, PacBio Revio sequencing was performed

### 4.4. Metagenomic Sequencing

#### 4.4.1. Shotgun sequencing | Illumina NovaSeq

Seven samples, one rectum sample from each killer whale, was sent to Genomics Core for paired-end Illumina NovaSeq sequencing. Library preparation was performed using the

Nextera XT kit to amplify the DNA and ligate adapters. Samples were sequenced at a depth of 7500 Gbp.

#### 4.4.2. Long read sequencing | Oxford Nanopore

Oxford Nanopore sequencing was performed by Dr. Rakeshkumar Yadav (Postdoc - soil and water management unit, KULeuven). Nanopore sequencing was performed on the DP-HZ sample (extracted with the HostZERO DNA extraction kit) since this sample showed great potential for long read sequencing based on a fragment analysis with a peak size of 13060bp. Sequencing was performed according to the *Ligation sequencing gDNA - Native Barcoding Kit 96 V14 (SQK-NBD114.96)* protocol except for a few modifications. During the bead binding-DNA step, incubation was increased to 15-20 minutes. The elution step was performed at 37 degrees C. During the end-repair step, incubation was extended to 20 minutes at 20°C, followed by 5 minutes at 65°C. During the barcoding ligation step, incubation was extended to 25 minutes at 20°C, followed by 10 minutes at 65°C to inactivate ligase, and held at 12°C until cleanup.

### 4.5. Bioinformatics

#### 4.5.1. 16S amplicon sequencing

##### 4.5.1.1 DADA2 pipeline

PacBio HiFi reads were bioinformatically deconcatenated into segmented reads using *Skera* v1.4.0 (Pacific Biosciences, 2024). The segmented reads were then demultiplexed with *lima* v2.13.0 (Pacific Biosciences, 2024). Quality filtering, primer trimming, error correction, dereplication, denoising, chimera removal, and taxonomic assignment based on the Greengenes2 database (McDonald et al. 2024) were performed using the *DADA2* pipeline in R following an adjusted 16S PacBio workflow provided by Benjamin J. Callahan on [GitHub](#) (Callahan et al. 2019). This analysis utilized the *dada2* and *ShortRead* packages. The *DADA2* workflow inferred 1799 distinct Amplicon Sequence Variants (ASVs) from the segmented reads, providing single-nucleotide resolution of true biological sequences. Subsequently, a phylogenetic tree was constructed of the ASVs across all the samples using the *BioStrongs*, *phangorn* and *DECIPHER* packages. Finally, the ASVs, their assigned taxonomy, phylogenetic tree and sample metadata were merged into a *phyloseq* object for subsequent downstream data analysis, using the *phyloseq* package..

#### 4.5.2. Metagenomic sequencing

All bioinformatics were performed on the high performance computing (HPC) clusters of the Flemish Supercomputer Centre (VSC).

##### 4.5.2.1. Shotgun read assembly

Illumina short reads were quality-filtered using *fastp* v0.23.4 (Chen 2023) with default settings. Post-filtering, all samples exhibited a Phred score >30 in over 90% of their reads. Host-derived reads were removed by mapping against the killer whale reference genome (assembly mOrcOrc1.1, NCBI) using *bowtie2* v2.5.4 with default parameters. Bacterial read counts were assessed with *KRAKEN2* v2.1.2 (Wood, Lu, and Langmead 2019), revealing that two captive samples (Keto and Adan) and the stranded Cadzand sample had notably low bacterial sequencing output (Table 8). These samples were excluded from further analysis, which proceeded with four remaining samples: captive killer whales

Morgan and Tekoa, and stranded killer whales from Sognefjord and De Panne. To account for differences in sequencing depth, these samples were subsampled to a uniform depth of 428,551 bacterial reads, corresponding to the lowest bacterial read count observed (Sognefjord sample), using *KrakenTools* (commit hash: d4a2fbe) (Lu et al. 2022). Additionally, the DP-HZ sample was retained in its full sequencing depth (83,548,284 bacterial reads) to facilitate a focused, high-quality analysis, using hybrid assembly (see section 4.5.5.2.). Paired-end bacterial reads were assembled into contigs using *MEGAHIT* v1.2.9 (Li et al. 2015) with default parameters. Gene prediction on the assembled contigs was performed with *Prodigal* v2.6.3 (Hyatt et al. 2010), and resulting gene sequences were aligned against the mibPOP database via *DIAMOND* v2.1.8 (Buchfink, Reuter, and Drost 2021) BLASTp, limiting target sequences to one per query. Finally, the original quality-filtered reads were mapped back to the predicted open reading frames that matched against the reference database, using *BBMap* v39.06 (Bushnell, 2014) to generate read counts.

**Table 8 | Illumina sequencing statistics.** Total Illumina reads, killer whale genome reads and bacterial reads of all Illumina-NovaSeq samples.

Sample Code	Category	Total reads	Killer whale reads	Non-killer whale reads	Non-killer whale (%)	Bacterial reads
MO-FE	Captive	90,481,207	77,948,722	12,532,485	13.85	9,797,239
TE-FE	Captive	102,681,307	91,062,444	11,618,863	11.31	1,410,658
KE-FE	Captive	73,952,307	72,800,298	1,152,009	1.55	124,444
AD-FE	Captive	3,781,571	3,476,802	304,769	8.05	47,684
DP-HZ	Stranded	102,542,639	93,819	102,448,820	99.9	83,303,255
CZ-GR	Stranded	84,108,617	77,218,597	6,890,020	8.19	109,315
SO-FE	Stranded	94,945,081	93,922,024	1,023,057	1.07	428,551
VA-NC	Neg. control	230,244	3,577	226,667	98.44	161,387
RN-NC	Neg. control	3,682	164	3,518	95.54	853
EN-NC	Neg. control	86,682	20,483	66,199	76.36	13,987

#### 4.5.2.2. Hybrid assembly of shotgun and long reads

Nanopore reads were filtered for a minimum length of 1,000 bp and a minimum window Phred quality score of 10 using *Fillong* v0.2.1 (Wick, 2017). Adapter sequences were trimmed with *Porechop* v0.2.4 (Wick, 2017) using default settings. Hybrid scaffolding was performed with *OPERA-MS* v0.9.0 (Bertrand et al. 2019), integrating contigs from the prior short-read *MEGAHIT* assembly and the filtered Nanopore reads as input. Gene prediction was conducted on the resulting scaffolds using *Prodigal* v2.6.3. Predicted genes were then aligned to the MIBPOP database via *DIAMOND* v2.1.8 BLASTp. Consistent with the short-read workflow, gene abundances were estimated by mapping reads against the predicted open reading frames using *BBMap* v39.06, followed by TPM normalization.

## 4.6. Data Analysis

All data analysis was performed on R v. 4.4.3 and RStudio/2025.05.0+496

### 4.6.1. 16S amplicon sequencing data analysis

The previously created phyloseq object (see 4.5.1.) was used as the start for microbial community analysis. All samples were rarefied to 195088 reads, which was the lowest

sequencing depth among the samples, using the `phyloseq_mult_raref` function from the *metagMix* package to account for differences in sequencing depth (Table 9). Rarefaction curves for all replicates were close to flat at this sequencing depth (Fig. S1). After rarefaction, 1039 of the 1799 initial ASVs were retained. To investigate community composition, taxonomic bar plots (Fig. 9-11, S2-S5) were generated using *ggplot2* and enhanced with the *ggh4x* package. Beta diversity was assessed to examine compositional differences across the intestinal tract of the killer whale stranded in De Panne. This was performed using Principal Coordinates Analysis (PCoA) based on four distance metrics: Bray–Curtis, Jaccard, weighted UniFrac, and unweighted UniFrac (Fig. 8). For the visualization of beta diversity we utilized *ggplot2*, and *RcolorBrewer* packages. A permutational ANOVA with 999 permutations was performed on Bray-Curtis, Jaccard, weighted Unifrac and unweighted Unifrac distance metrics to test whether different intestinal regions had a significantly different microbiome composition using the `adonis2` function from the *vegan* package (Table 11). Multivariate homogeneity of group dispersions was checked by performing a PERMDISP test, using the `betadisper` function from the *vegan* package which evaluates the variability of distances from each sample to the group centroid in ordination space. Significance was assessed via a permutation-based ANOVA (Table S3), set to 999 permutations, using the `anova.betadisper` function from the *vegan* package. To test for pairwise differences between all five intestinal regions, a post hoc test was performed using the `pairwise.adonis` function from the *Pairwiseadonis* package, which also corrected the P-values for multiple testing using the false discovery rate method with the Benjamini-Hochberg (BH) procedure (Table S4). Alpha diversity metrics, including species richness, Shannon diversity, Inverse Simpson diversity and Faith’s phylogenetic diversity indices, were calculated using the *picante* and *vegan* packages and visualized using scatterplots with *ggplot2*, *dplyr*, *tidyr*, and *RcolorBrewer* packages (Fig. 7). To test for significant differences in alpha diversity across intestinal regions, generalized linear models (GLMs) were fitted for each diversity index and subsequently tested for overdispersion using the *stats* package and ANOVA tests were performed using the *car* package (Table 10). Pairwise comparisons between sites were conducted using estimated marginal means with Tukey adjustment for multiple testing using the `pairs` function from the *emmeans* package (Table S2).

**Table 9 | Sequencing depth after filtering.** Table showing the read count per sample after DADA2 pipeline filtering.

Intestinal region	replicate	Sample code	Sequencing depth (reads)
Duodenum	A	DP-DU-A	236,251
Duodenum	B	DP-DU-B	245,955
Duodenum	C	DP-DU-C	213,169
Jejunum	A	DP-JE-A	195,088
Jejunum	B	DP-JE-B	269,471
Jejunum	C	DP-JE-C	253,080
Ileum	A	DP-IL-A	298,076
Ileum	B	DP-IL-B	270,187
Ileum	C	DP-IL-C	248,654
Colon	A	DP-CO-A	531,908
Colon	B	DP-CO-B	252,035
Colon	C	DP-CO-C	248,758
Rectum	A	DP-RE-A	231,949
Rectum	B	DP-RE-B	259,562

#### 4.6.2. Short read assembly vs hybrid assembly

A comparative analysis was conducted between the short-read assembly and the hybrid assembly results. Assembly statistics were directly compared on the VSC Linux servers (Table 12), followed by the creation of comparative bar and box plots (Fig. 12-13) in R using the *ggplot2*, *patchwork*, and *Biostrings* packages. The assembly statistics demonstrated superior performance of the hybrid assembly, which was therefore selected for further investigation of the DP-HZ sample.

#### 4.6.3. Metagenomic data analysis

All DIAMOND hits (see section 4.5.2.2) were filtered, removing any hits with identity score < 30%, E-value > 1E<sup>-5</sup> and coverage < 40%. After filtering, DIAMOND hits of the same Enzymes\_ID (see mibPOP database) were merged by summing their abundance, and read counts were TPM normalized using following formula:

$$(1) \text{ RPK (reads per kilobase)} = \frac{\text{\#reads}}{\text{gene length (kb)}}$$

$$(2) \text{ per million scaling factor} = \frac{\text{summed RPK per sample}}{1\,000\,000}$$

$$(3) \text{ TPM (transcripts per million)} = \frac{\text{RPK}}{\text{per million scaling factor}}$$

##### 4.6.3.1. Killer whale De Panne data analysis

To assess the completeness of microbial POP degradation pathways, the detected genes were mapped onto their respective metabolic pathways (Fig. 14–18), allowing evaluation of whether the full set of enzymatic steps required for complete degradation of each POP was present. To analyse the most abundant POP-degrading enzymes, a bar plot was created using *ggplot2* to display the cumulative TPM abundances of all detected enzymes involved in POP degradation. Distinct colours were assigned to each compound using the *colorspace* package for clear differentiation (Fig. 19). Additionally, a bar plot was generated using the *ggplot2* package to visualize the top five most abundant genes encoding enzymes responsible for degrading DDT, PCBs, HCH, PBDEs, HCB, and HBC (Fig. 20). Prior to plotting, the abundances of individual enzymes were aggregated by gene, yielding total gene-level abundance.

##### 4.6.3.2. Data analysis of subsampled captive and stranded killer whale samples

To explore compositional differences in the presence of POP-degrading genes encoding for POP-degrading enzymes between samples, a bar plot was generated using *ggplot2*, displaying the cumulative TPM (transcripts per million) counts of genes for all POP compounds per sample (Fig. 21). To further investigate individual enzyme-level variation, a jitter plot was constructed based on raw read counts (Fig. 22). For this analysis, only enzymes detected in all four samples were included to account for potential sampling method variability affecting enzyme detection. Visualization annotation of this plot were performed using *ggplot*.

## 5. Results

### 5.1. 16S amplicon sequencing results

#### 5.1.1. Gut microbiome diversity along the intestinal tract of killer whale De Panne

Figure 7 reveals that the ileum, colon and rectum showed higher species richness, Shannon diversity and Simpson diversity values relative to the duodenum and jejunum intestinal regions. In contrast, Faith's phylogenetic diversity exhibited less variation between intestinal regions, although considerable variability was observed among colon samples; overall, the colon showed the highest Faith's PD values, while the ileum had the lowest. One-way ANOVA indicated significant differences in all alpha diversity metrics across intestinal regions (Table 10). Tukey's HSD tests revealed significant pairwise differences in Shannon and Simpson indices across all regions. Species richness differed significantly among most regional pairs (duodenum/ileum, duodenum/colon, duodenum/rectum, jejunum/ileum, jejunum/colon, jejunum/rectum), while Faith's PD differed only between the ileum and colon (Table S2). The fitted GLMs showed no sign of overdispersion (Table S1). Note that these  $\alpha$ -diversity indices reflect the diversity and richness of ASVs, which do not necessarily correspond to distinct species.

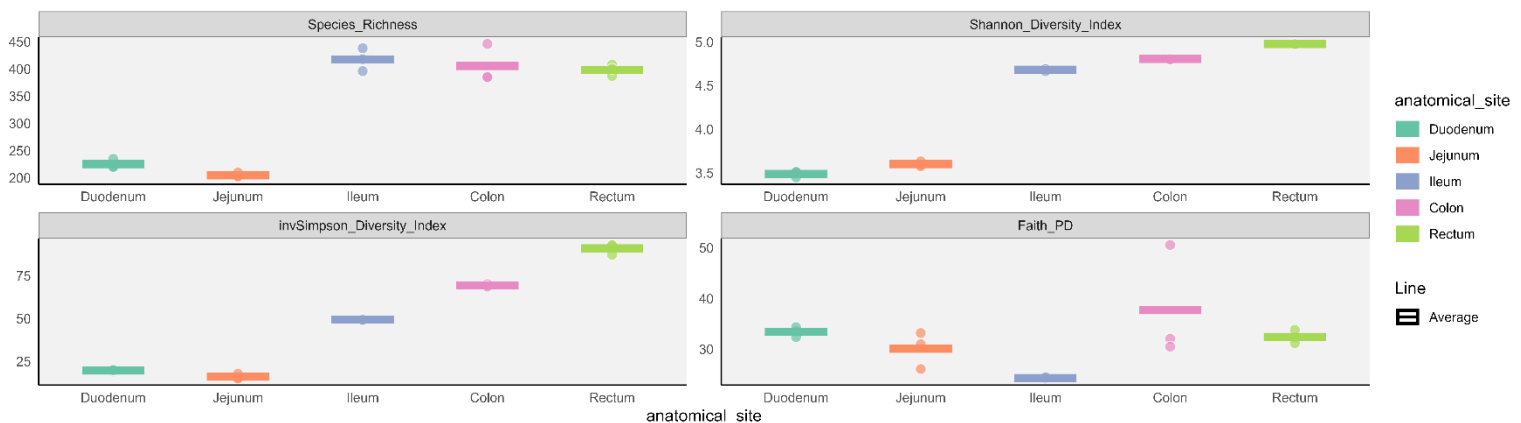


**Figure 7 | Diversity indices along the intestinal tract.** Scatterplots showing species richness, Shannon diversity, Inverse Simpson diversity and Faith's phylogenetic diversity indices values per intestinal region. Horizontal bars indicate averages across the replicates and dots indicate values of individual replicates.

**Table 10 | ANOVA  $\alpha$ -diversity statistics.** Results of one-way ANOVAs conducted to assess differences in alpha diversity across five intestinal regions: duodenum, jejunum, ileum, colon, and rectum. Four alpha diversity indices were evaluated: SR: species richness, SHD: Shannon diversity, SID: inverse Simpson diversity, and FPD: Faith's phylogenetic diversity. Statistically significant results are indicated in bold.

	Response	Chisq ( $\chi^2$ )	Df	p-value
<b>SR</b>	Intestinal region	429.34	4	<b>&lt; 2.2e-16 ***</b>
<b>SHD</b>	Intestinal region	9668.7	4	<b>&lt; 2.2e-16 ***</b>
<b>SID</b>	Intestinal region	2952.8	4	<b>&lt; 2.2e-16 ***</b>
<b>FPD</b>	Intestinal region	14.674	4	<b>0.005428 **</b>

#### 5.1.2. Gut microbiome composition along the intestinal tract of killer whale De Panne

All four permutational ANOVAs, performed on Bray-Curtis, Jaccard, Weighted Unifrac and Unweighted Unifrac distance metrics, revealed a significant difference in microbiome

community composition along the intestinal tract ( $F = 347.26$ ,  $p = 0.001$ ;  $F = 127.43$ ,  $p = 0.001$ ;  $F = 159.67$ ;  $p = 0.001$ ;  $F = 6.6816$ ,  $p = 0.001$ , respectively) (Table 11). None of the PERMANOVAs violated the assumption of homogeneous dispersion (Table S3). All intestinal regions showed defined clustering on all four PCoA plots, performed on Bray-Curtis, Jaccard, Weighthed Unifrac and Unweighted Unifrac distance metrics (Fig. 8), however, pairwise permutational ANOVAs revealed no significant differences in microbiome community composition between individual regions (Table S4).

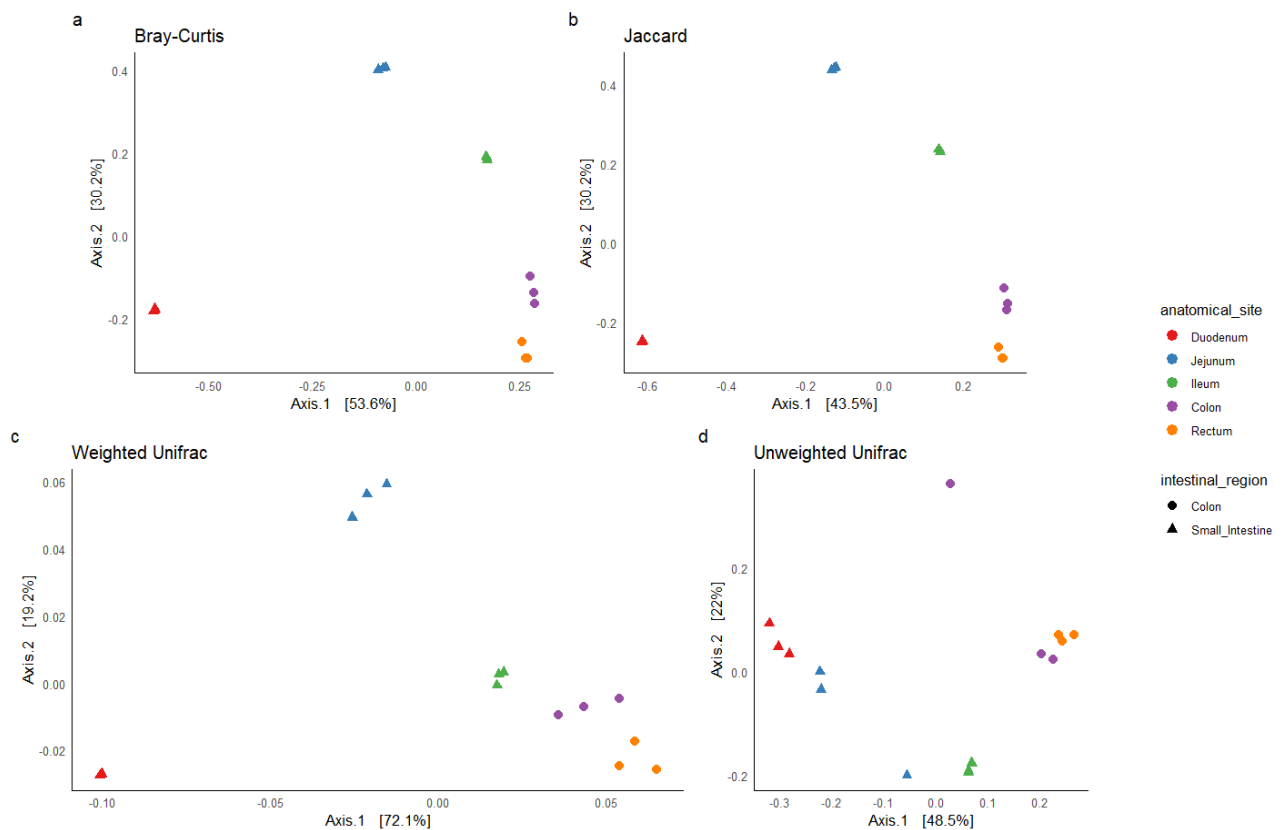
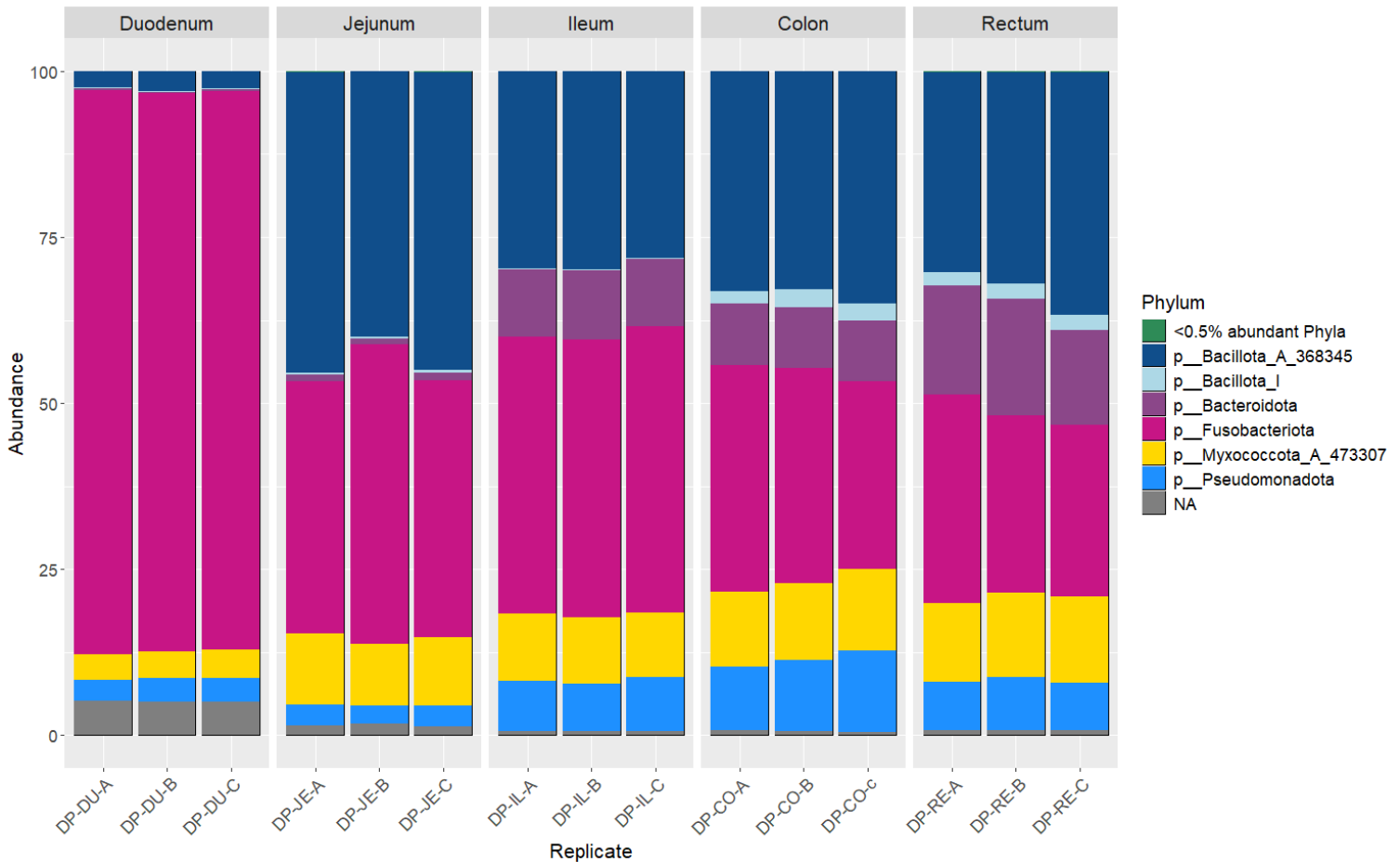


**Figure 8 | PCoA of microbiome composition along the intestinal tract using different distance metrics.** Principal Coordinates Analysis (PCoA) plots showing beta diversity based on four distance metrics: (a) Bray-Curtis, (b) Jaccard, (c) Weighted UniFrac, and (d) Unweighted UniFrac. Samples are coloured by anatomical site (Duodenum, Jejunum, Ileum, Colon and Rectum) and shaped by intestinal region (Small Intestine and Colon). Each plot shows the first two principal coordinates along with the percentage of variance they explain.

**Table 11 | PERMANOVA  $\beta$ -diversity statistics.** Results from the permutational ANOVA to test for differences in microbiome composition across 5 intestinal regions: duodenum, jejunum, ileum, colon and rectum; for all four dissimilarity matrices (BC: Bray-Curtis, JC: Jaccard, WUF: weighted UniFrac, UUF: unweighted UniFrac). Significant effects and p-values are in bold.

	Response	Df	Sum SQ	R <sup>2</sup>	F	p-value
<b>BC dissimilarity</b>	Intestinal region	4	3.237	0.992	347.26	<b>0.001***</b>
<b>JC dissimilarity</b>	Intestinal region	4	4.0371	0.98076	127.43	<b>0.001***</b>
<b>WUF dissimilarity</b>	Intestinal region	4	0.067075	0.98458	159.67	<b>0.001***</b>
<b>UUF dissimilarity</b>	Intestinal region	4	0.99955	0.72772	6.6816	<b>0.001***</b>

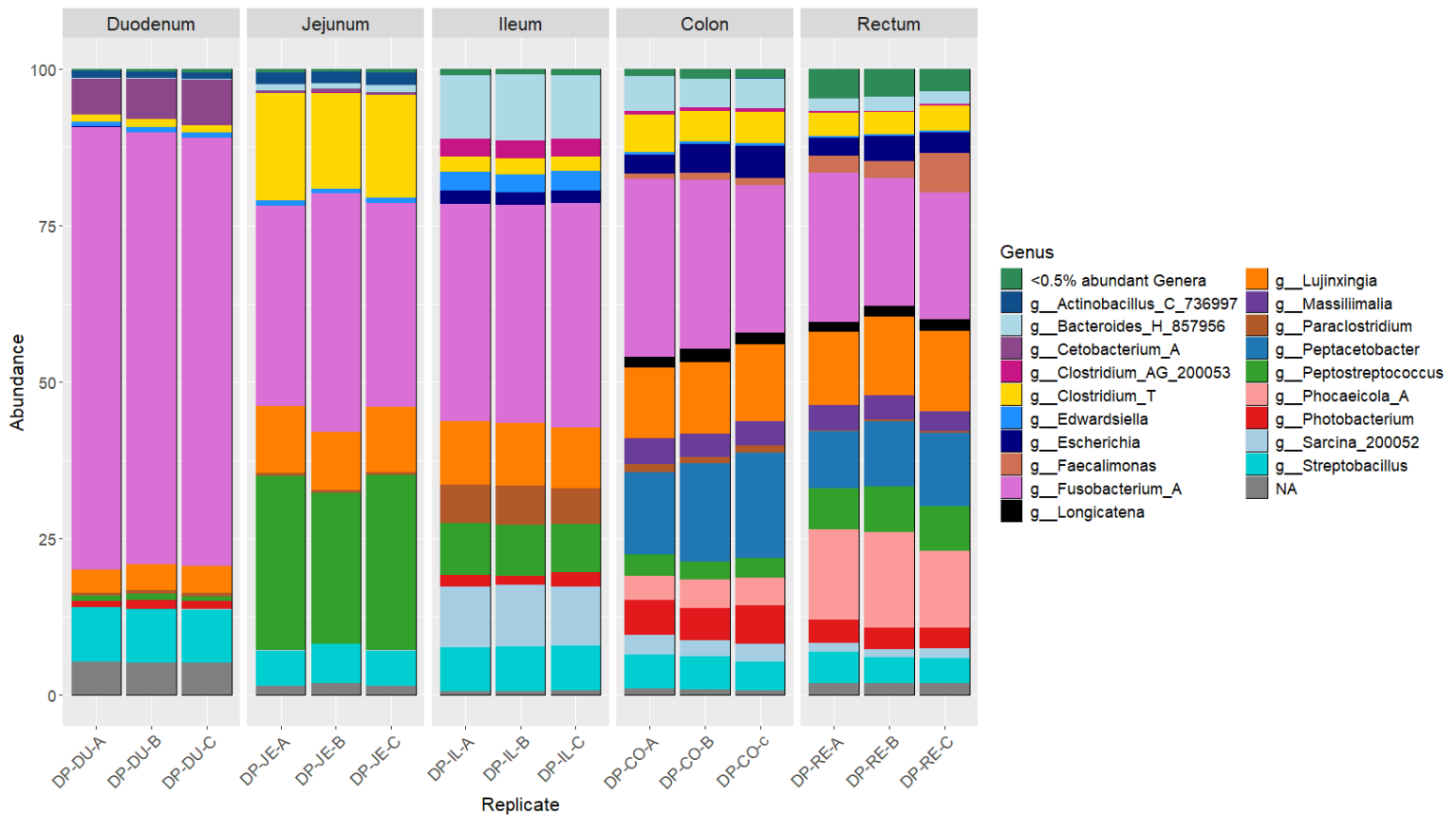
All intestinal regions were predominantly colonised by bacteria from the phyla Bacillota, Bacteroidota, Fusobacteriota, Myxococota, and Pseudomonadota (Fig. 9). Among these, Bacillota and Fusobacteriota exhibited the highest mean relative abundances across most intestinal regions (29% and 45%, respectively) with the exception of the duodenum, which was almost entirely dominated by Fusobacteriota. In fact, Fusobacteriota declined along the intestinal tract from 84.4% in duodenum (over 40.6% in jejunum, 42.2% in ileum and 31.6% in colon) to 28% in rectum. Whereas, Bacteroidota relative abundance increased along the intestinal tract from 0.2% in duodenum (over 1% in jejunum, 10.3% in ileum and 9.2% in colon) to 16% in rectum.



**Figure 9 | Microbiome composition of killer whale De Panne along its intestinal tract at phylum level.** Bar plots show the relative abundances (%) of bacterial phyla per replicate grouped by anatomical site: duodenum, jejunum, ileum, colon, and rectum for killer whale De Panne. Phyla with a relative abundance < 0.5% are pooled under the category “<0.5% abundant Phyla”.

The duodenum was predominantly colonised by members of the genus *Fusobacterium*, comprising 69.3% of the relative abundance, with limited representation of other bacterial genera (8.6% *Streptobacillus* and 6.4% *Cetobacterium*) (Fig. 10). The taxonomic composition at the genus level in the jejunum, ileum, colon, and rectum exhibited greater diversity than in the duodenum. The jejunum was characterized by high relative abundances of *Clostridium* and *Peptostreptococcus* (16.3% and 26.6%, respectively), whereas these genera were present at much lower levels in the ileum, colon, and rectum (5.3%/5.9%/4% and 8%/3.1%/7%, respectively). Notably, the ileum was the only region to show a significant relative abundance of *Paraclostridium* (6.1%), while the colon and

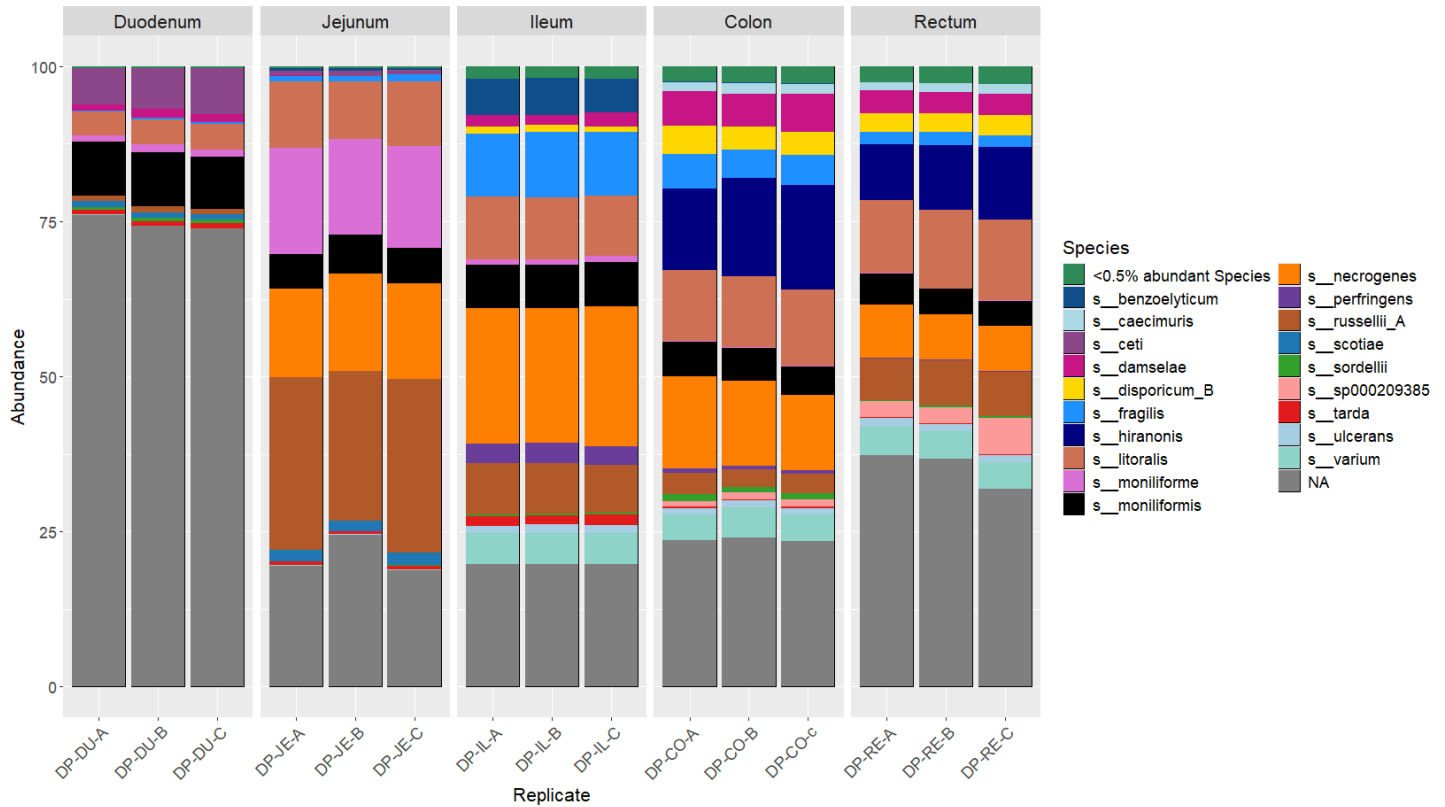
rectum were the only to show notable abundances of *Phocaeicola*, *Peptacetobacter*, *Masiliimalia*, and *Faecalimonas* (4.2%/14%, 15.3%/10.4%, 3.9%/3.7% and 1.1%/3.9%, respectively). The relative abundance of *Fusobacterium* exhibited a decreasing gradient along the intestinal tract from 69.3% in duodenum (over 34.2% in jejunum, 35.2% in ileum and 26.3% in colon) to 21.5% in rectum. In contrast, *Lujinxingia* displayed an increasing gradient in relative abundance from proximal to distal regions of the intestine from 4% in duodenum (over 10.1% in jejunum, 9.9% in ileum and 11.7% in colon) to 12.4% in rectum.



**Figure 10 | Microbiome composition of killer whale De Panne along its intestinal tract at genus level.** Bar plots show the relative abundances (%) of bacterial genera per replicate grouped by anatomical site: Duodenum, Jejunum, Ileum, Colon, and Rectum for killer whale De Panne. Genera with a relative abundance < 0.5% are pooled under the category “<0.5% abundant Genera”.

Overall, species-level annotations accounted for 65.1% of the total relative abundance (Fig. 11), although the duodenum yielded substantially fewer annotated species (25.3%) compared to the other regions (79.1% in jejunum, 80% in ileum, 76.3% in colon, 64.7% in rectum). *Streptobacillus moniliformes* and *Lujinxingia litoralis* were consistently present along the intestinal tract at similar relative abundances (8.6%/4% in duodenum, 5.9%/10.1% in jejunum, 7%/9.9% in colon and 4.3%/12.4% in rectum). *Fusobacterium necrogenes* displayed the highest overall relative abundance (11.7%), although its relative abundance in the duodenum was < 0.1%. The jejunum exhibited higher relative abundances of *Peptostreptococcus russellii* and *Clostridium monoliforme* (26.6%/16.3%, respectively) than the other intestinal regions (0.9%/1.1% in duodenum, 8%/0.9% in ileum, 3.1%/0.2% in colon and 7%/3.5% in rectum, respectively). Additionally, the ileum exclusively showed notable relative abundances of *Paraclostridium benzoelyticum* and

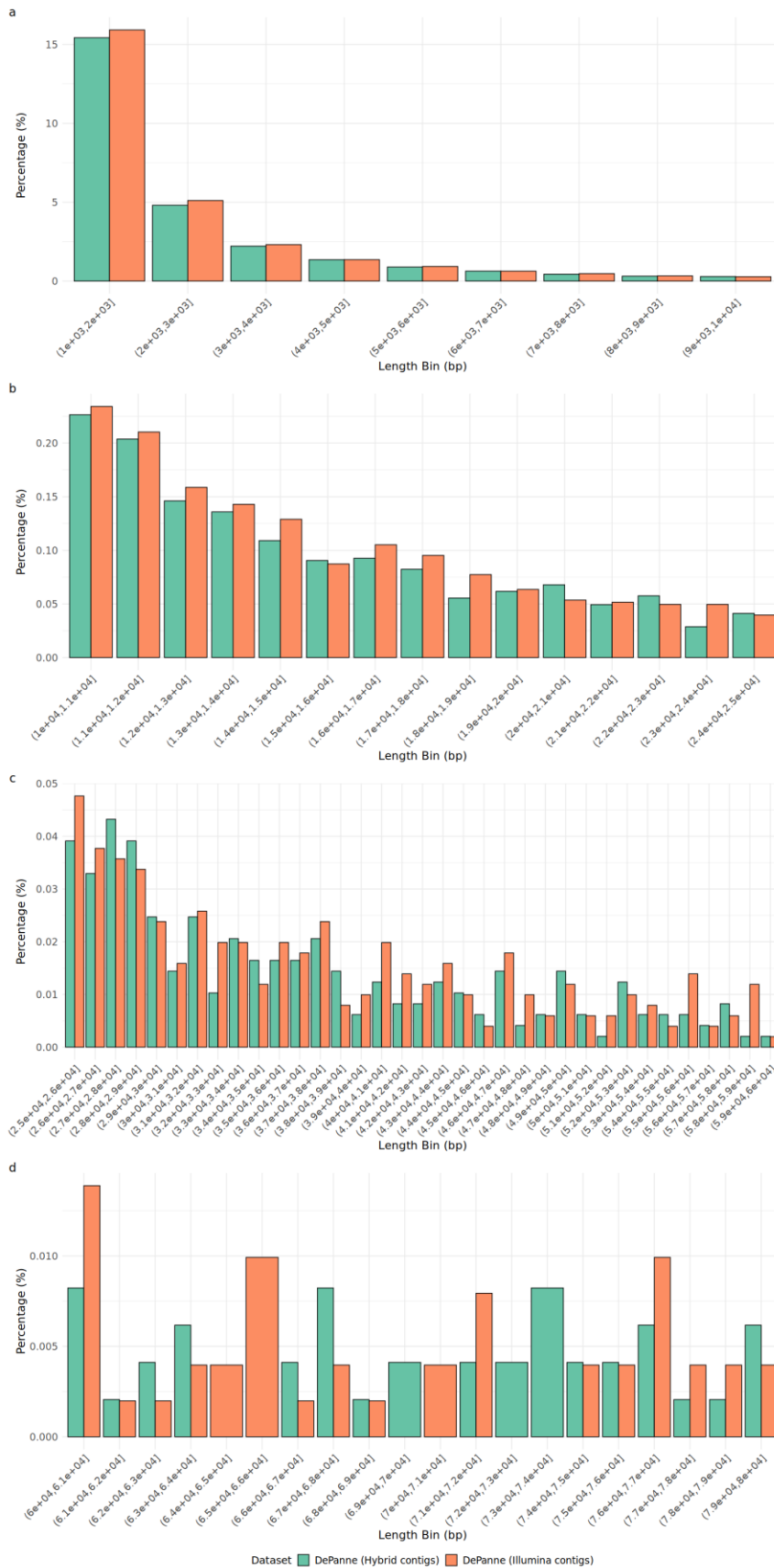
*Clostridium perfringens* (5.7%/3.1%, respectively), whereas *Peptacetobacter hiranonis* was uniquely abundant in the colon and rectum (15.3% in colon and 10.4% in rectum).



**Figure 11 | Microbiome composition of killer whale De Panne along its intestinal tract at species level.** Bar plots show the relative abundances (%) of bacterial species per replicate grouped by anatomical site: Duodenum, Jejunum, Ileum, Colon, and Rectum for killer whale De Panne. Species with a relative abundance < 0.5% are pooled under the category “<0.5% abundant Species”.

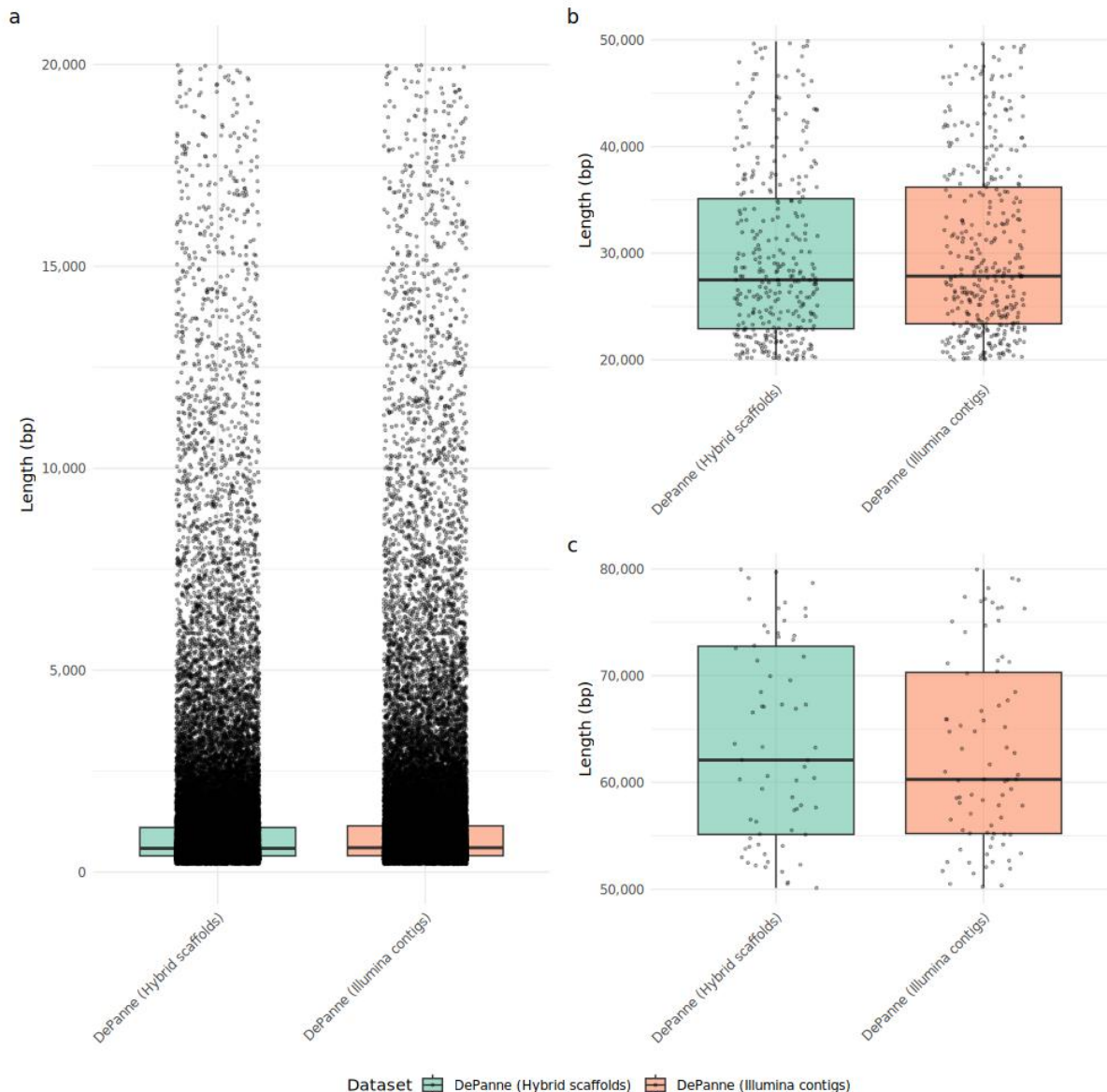
## 5.2.Short read assembly vs hybrid assembly

Figure 12 reveals that both assembly methods show a strong right-skewed distribution for contigs length. The Illumina-single assembly (of short reads) produced a higher number of short contigs (1-5kbp) compared to the Illumina-Nanopore hybrid assembly (Fig. 12a). From 20 kb onward, the proportionate contig counts were similar between assemblies, with some contig length bins starting to show a higher relative abundance in the hybrid assembly (Fig. 12b, c, d). However, no clear overall increase in the proportionate abundance of long contigs (>20 kb) in the hybrid assembly compared to the Illumina-single assembly was visible on the plot.



**Figure 12 | Contig/scaffold length distribution for Illumina-single and hybrid assemblies.** Bar plots display the relative abundance of contigs binned into 1000bp intervals and divided across four length ranges: a) 1,000-10,000bp, b) 10,000-25,000bp, c) 25,000-60,000bp and d) 60,000-80,000bp comparing an Illumina-single assembly with an Illumina-Nanopore hybrid assembly

Both assemblies showed little difference in distribution of short contigs lengths (<20.kbp), as both show a strong right-skewed distribution (Fig. 13a). The median short contig length values were 587bp, for the hybrid assembly, and 602, for the Illumina-single assembly, in this contig range (Fig.13a). In the 20,000–50,000 bp range, both assembly methods exhibited a slightly more symmetrical distribution of contig lengths. For this range, the median contig length for the Illumina-only assembly was marginally higher than that of the hybrid assembly, 27,847 bp and 27,495bp (Fig. 13b). The 50,000-80,000 bp range shows an even more symmetrical distribution for both assembly methods. Median values were 62,094bp and 60,281bp for the hybrid- and Illumina-single assembly respectively, thus revealing longer contig assembly in long contig length ranges for the hybrid assembly method (Fig. 13c).



**Figure 13 | Contig/scaffold length distribution of Illumina-single and hybrid assemblies for different contig length ranges.** Box plots showing median length values of contig/scaffold length ranges: (a) ≤ 20,000bp, (b) 20,000-50,000bp and (c) 50,000-80,000bp. Black dots = individual contigs/scaffolds, black line = median.

The Illumina-single assembly versus the hybrid assembly gave more contigs (50,389 vs 48,588) but shorter ones (N50: 5,509bp vs 6,820bp and mean contig length: 1,758.7 vs

1,838.4). The summed scaffold read length was higher for the hybrid assembly. The hybrid assembly resulted in only 9 more BLASTp hits (against POP-degrading gene mibPOP database) than the Illumina-single assembly (1151 vs 1142) with very similar mean identity scores (36.7% vs 36.8%), E-values ( $1.3 \times 10^{-5}$  vs  $1.3 \times 10^{-5}$ ) and coverage values (76.7% vs 76.7%). After filtering the BLASTp hits (on >30% identity score, E-value  $< 1 \times 10^{-5}$  and >40% coverage) both assembly methods retained 165 BLASTp hits, with the Illumina-single assembly counting more reads (2,337,193 vs 1,630,593) mapped against these retained hits than the hybrid assembly (Table 12).

**Table 12 | Illumina-single and hybrid assembly statistics.** Number of assembled contigs/scaffolds, N50, average length of contigs/scaffolds (bp), summed contig/scaffold read length (bp), number of BLASTp hits, mean identity score (%), mean E-value and mean coverage (%) of BLASTp hits, number of BLASTp hits after filtering on >30% identity score,  $< 1E^{-5}$  E-value and >40% coverage and the summed read counts of the remaining BLASTp hits after filtering for both the Illumina-single and hybrid assembly methods.

Method	# Contigs/scaffolds	N50 (bp)	Mean contig/scaffold read length (bp)	Summed contig/scaffold read length (bp)	#BLASTp hits
Illumina	50,389	5,509	1,758.7	88,618,268	1,142
Hybrid	48,588	6,820	1,838.4	89,325,338	1,151

Method	Mean identity score (%)	Mean E-value	Mean coverage (%)	#BLASTp hits after filtering	Summed read counts after filtering
Illumina	36.8	$1.3 \times 10^{-5}$	76.7	165	2,337,193
Hybrid	36.7	$1.3 \times 10^{-5}$	76.7	165	1,630,593

### 5.3. Metagenomics results

#### 5.3.2. POP-degrading gene diversity and pathway completeness in gut microbiome of Killer whale *De Panne*

##### 5.3.2.1. Polychlorobiphenyl (PCB) degradation pathway

The observed PCB-degrading genes formed a continuous degradation pathway up until the two metabolites 2-hydroxypenta-2,4-dienoic acid and chlorobenzoic acid (Fig. 14). In addition, bphX was detected, which cleaves 4-hydroxy-2-oxovalerate to pyruvate and acetylaldehyde. No gene was present to encode for BphH, which facilitates mineralization of 2-hydroxypenta-2,4-dienoic acid to 4-hydroxy-2-oxovalerate. Neither were any genes detected encoding for further degradation of chlorobenzoic acid.

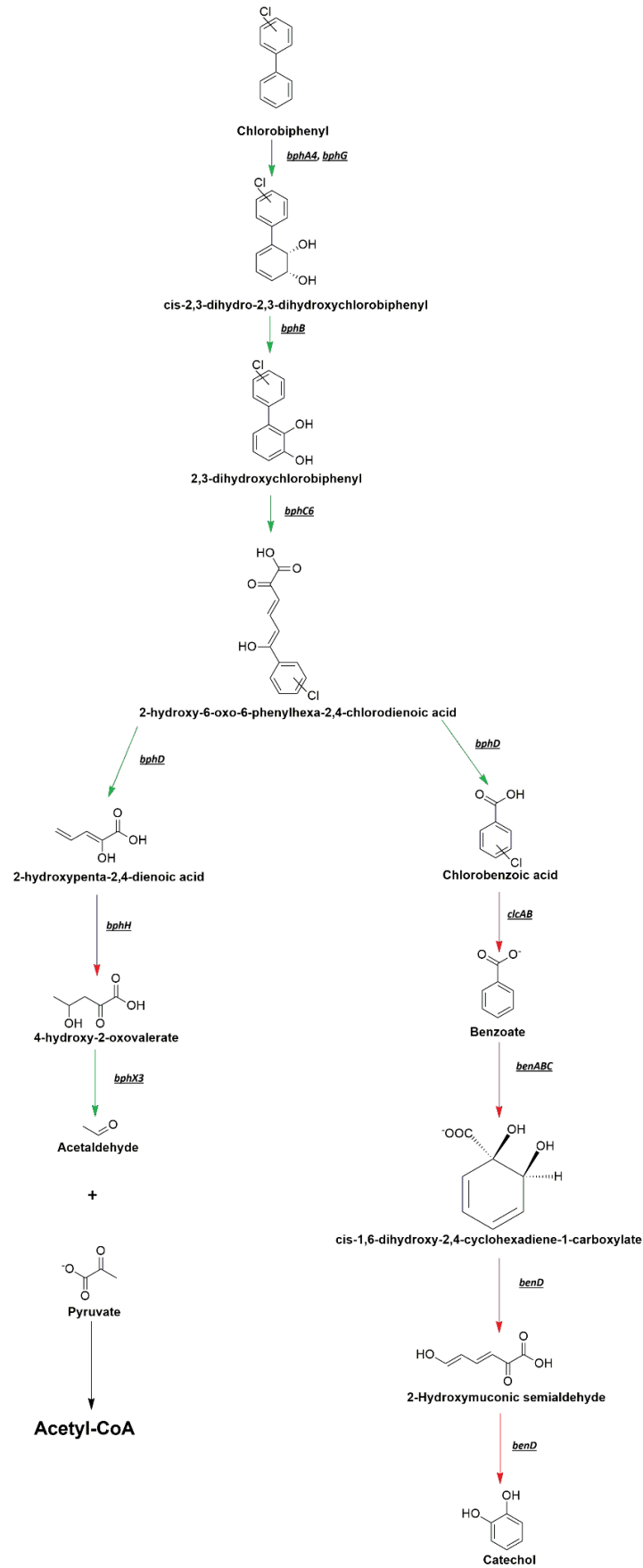


**Figure 14 | Detected aerobic PCB microbial degradation steps.** Suggested PCB degradation pathway with indicated presence of genes encoding for respective degradation steps. Green: detected gene, Red: undetected gene.

### 5.3.2.2. Dichlorodiphenyltrichloroethane (DDT) degradation pathway

Genes for complete microbial DDT degradation were detected, with the exception of *gstD1*, which facilitates aerobic DDT dehydrochlorination to DDE and *adh*, which facilitates the dehydrogenase of DDOH to DDA (Fig. 15). *Rdh* encodes for a reductive dehalogenase, which anaerobically catalyses the biotransformation DDT to DDD. *Dhc* encodes for a dehydrochlorinase which catalyses subsequent aerobic dichlorination. *Sds* encodes for a reductase which catalyses the biotransformation of DDMU to 2,2-bis(p-chlorophenyl)nitroethane (DDNU). *Hdt* encodes for a hydratase which degrades DDNU to DDOH. *Dcl* encodes for a decarboxylase which catalyses decarboxylase of DDA to DDM. OHCTT degradation is catalysed by a hydrolase, encoded by *hdl*.

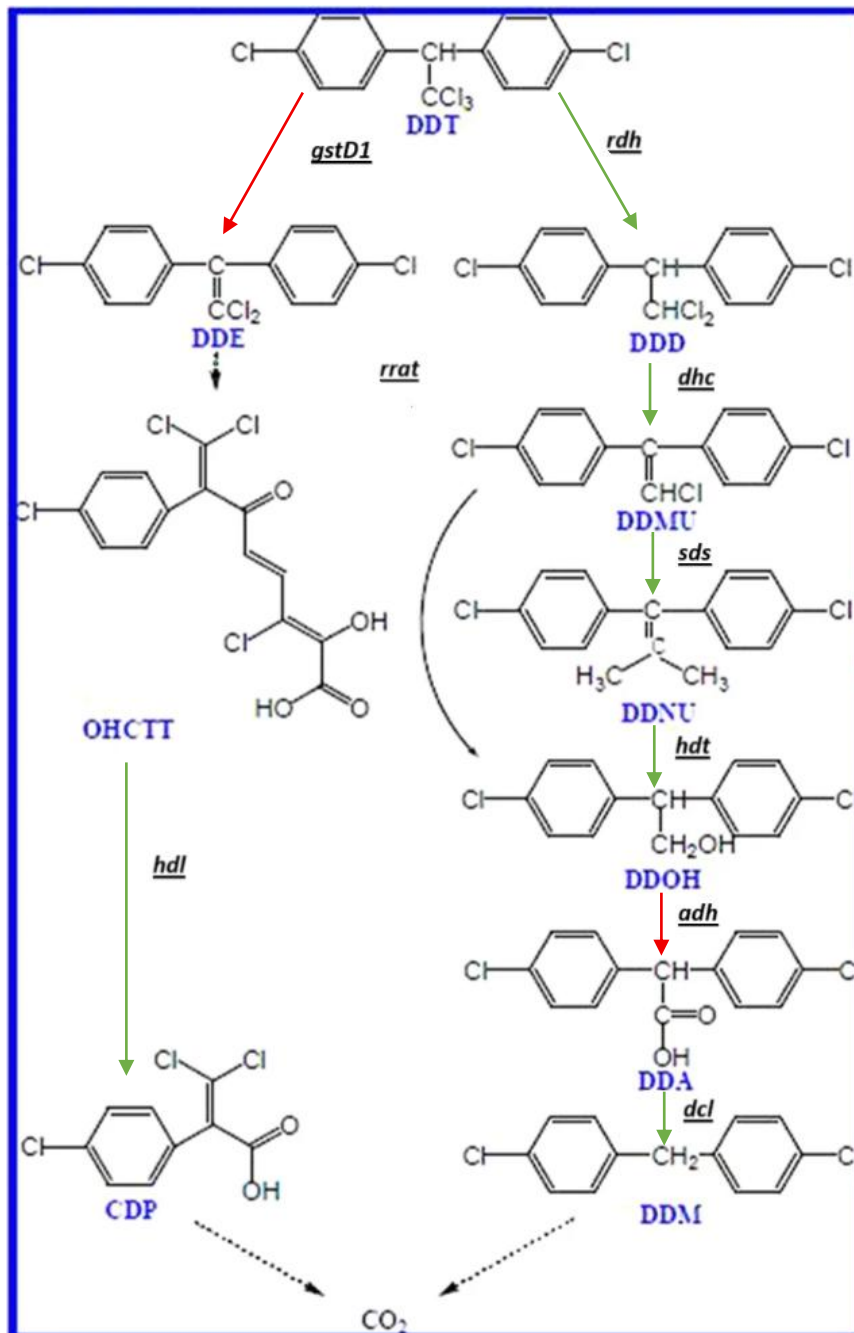


**Figure 15 | Detected DDT microbial degradation steps.** Suggested DDT degradation pathway with indicated presence of genes encoding for respective degradation steps. Green: detected gene, red: undetected gene.

### 5.3.2.3. Hexachlorobenzene (HCB) degradation pathway

Regarding the degradation of HCB, *hcbA2* was detected, which encodes an aerobic putative reductase component, allowing early HCB dichlorination to PCB and PCP. In addition, the reductive dehalogenases *cprA* and *rdhA* were detected. The microbial HCB degradation pathway is dominated by reductive dechlorination. Therefore these genes could possibly cover a wide range of the pathway but their exact sites of activity remain unclear due to limited functional and mechanistic studies of this pathway (Fig. 16). *cprD* and *cprE* were also detected. These two genes are part of the same gene cluster as *cprA* and encode for molecular chaperonins and thus aid in correct folding of proteins, such as CprA.

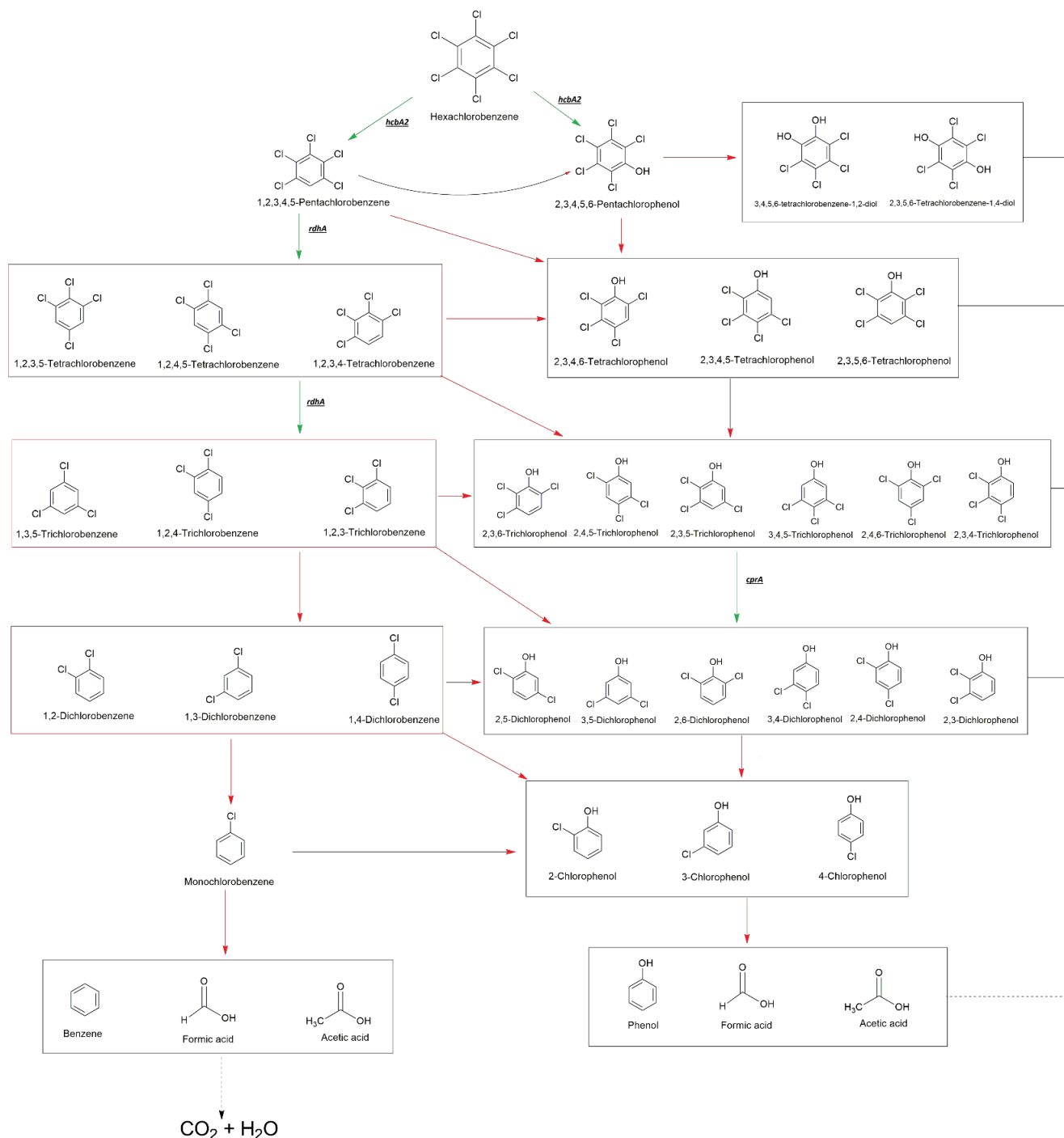


**Figure 16 | Detected HCB microbial degradation steps.** Suggested HCB degradation pathway with indicated presence of genes encoding for respective degradation steps. Green: detected gene, red: undetected gene.

#### 5.3.2.4. Polybrominated diphenyl ethers (PBDE) degrading genes

The only detected genes annotated to PBDE degradation were *CCR98\_02005* and *CCR98\_02495*, which encode a haloacid dehalogenase and dioxygenase enzyme respectively. Dehalogenases debrominate PBDE congeners and dioxygenases allow for aromatic ring cleavage. Similar to HCB, the microbial PBDE degradation pathway is dominated by dehalogenation. Yet, the specific enzymes, and encoding genes, responsible for catalysation of each individual debromination step remain uncertain. Consequently, mapping these genes to discrete steps within the pathway would be speculative. Therefore, no annotated pathway is presented here.

#### 5.3.2.5. Hexachlorocyclohexane (HCH) degradation pathway

The genes responsible for the early degradation of lindane *linA*, *linB*, *linC* and *linX*, were all detected. In addition, *linG*, *linH* and *linJ* were detected, which encode for enzymes catalysing the final degradation steps to TCA cycle intermediates. *LinD*, *linE* and *linF*, which encode for intermediary HCH degradation, were not detected (Fig. 17).



### 5.3.2.6. Hexabromocyclododecane (HBCD) degrading genes

The genes *linA* and *linB* were detected which respectively catalyse dehydrohalogenation of HBCDs to 1,5,6,9,10-pentabromocyclododecenes (PBCDEs) and the biotransformation of HBCDs to 2,5,6,9,10-pentabromocyclododecanols (PBCDOHs) (Fig. 18). The haloacid dehalogenase encoding genes *RPYSC3\_04710*, *RPYSC3\_16500*, *RPYSC3\_29420* and *RPYSC3\_43300* were detected. Since the exact enzymes responsible for each debromination step of HBCD degradation remain unclear, these steps have been given an orange colour in the pathway figure. The *gstA* gene was detected, encoding for a glutathione S-transferase which detoxifies the reactive brominated intermediates. The oxidoreductase encoding genes *RPYSC3\_18690* and *RPSYC3\_38300* were not detected.

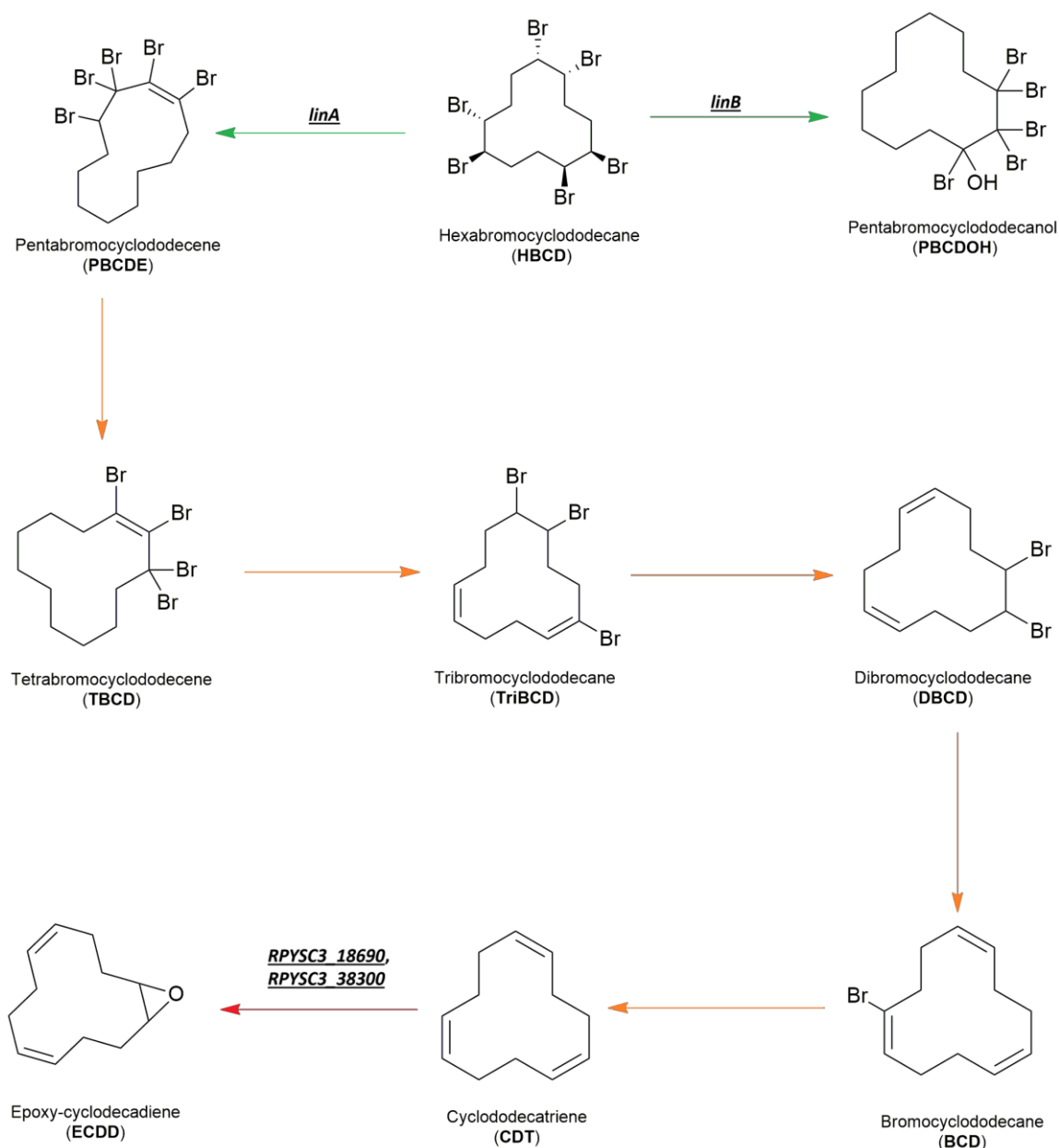


**Figure 18 | Detected HBCD microbial degradation steps.** Suggested HBCD degradation pathway with indicated presence of genes encoding for respective degradation steps. Green: detected gene, red: undetected gene, orange: gene possibly present.

### 5.3.2.7. POP-degrading gene diversity

DDT-degrading genes showed the highest cumulative TPM abundance (TPM= 289328.035), followed by genes encoding  $\alpha$ -HCH (TPM = 261664.189 ),  $\beta$ -HCH and  $\gamma$ -HCH/Lindane (TPM = 179481.749) and HBCD (TPM= 149600.597). PBDEs, PCBs and HCB showed a cumulative TPM count of 13718.929, 8416.783 and 87177.802 respectively (Fig. 19).

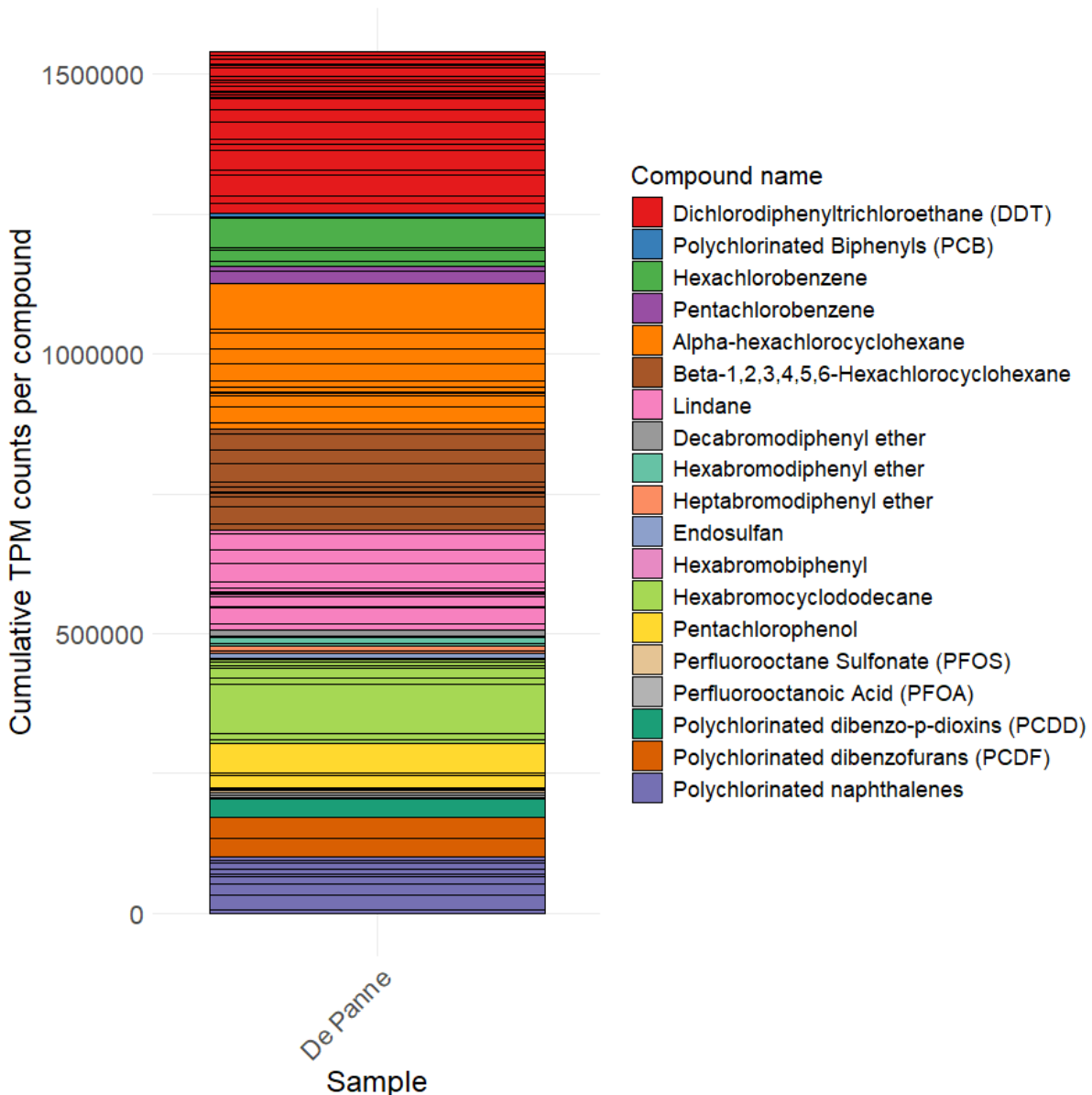


**Figure 19 | Cumulative TPM normalized read counts per POP compound for hybrid assembled killer whale De Panne (HostZERO DNA extraction) sample.** Bar plot showing the abundances of POP degrading enzymes, grouped per POP compound.

Figure 20 shows the TPM-normalized abundance in function of the top 5 abundant genes per POP compound. Note: the bar plot is constructed based on the enzyme annotation of the mibPOP database which was not always complete (e.g. *bphB* is annotated to DDT but also shows PCB degrading activity). The genes *linC*, *linJ* and *RPYSC3\_16500* showed the highest abundance, far exceeding the other genes (Fig. 20). DDT degrading genes showed the most consistent high abundance across its top 5 genes, while HCH and HBCD showed only 1 to 3 high abundant degrading genes. Overall, PCB and PBDE showed the lowest POP degrading gene abundance.

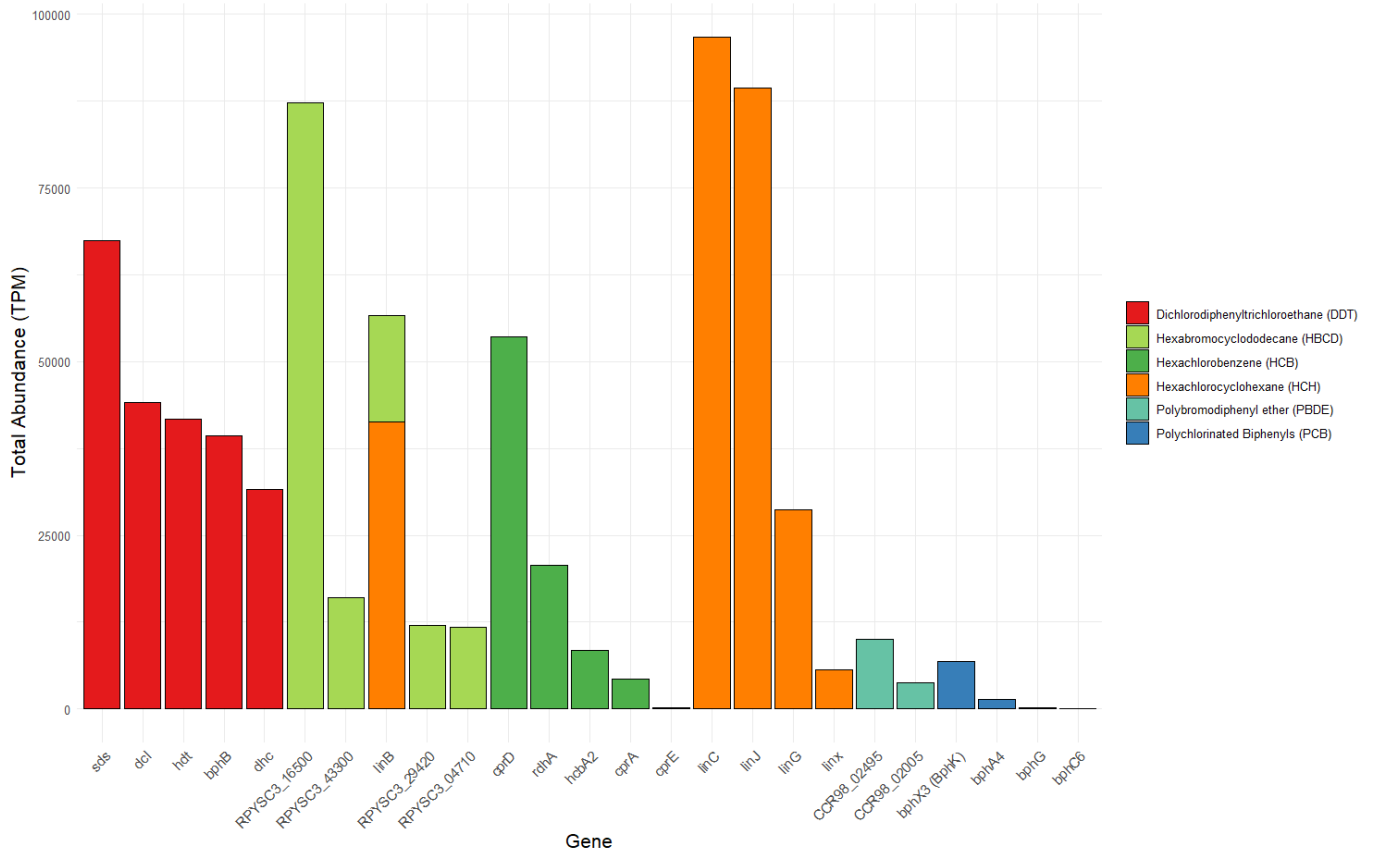


**Figure 20 | TPM-normalized abundance of the top 5 most abundant POP-degrading genes per POP class for killer whale De Panne (hybrid assembly on the HostZERO extracted sample).** The bar plot shows the total TPM normalized abundance of the top 5 most abundant genes for each POP class. The *linB* gene was annotated to both HBCD and HCH degradation in the mibPOP database and therefore has a two-coloured bar showing the total abundance for each class.

### 5.3.3. POP-degrading gene diversity in stranded vs captive killer whales

Only the DP-HZ sample showed presence of PCB-degrading enzymes (Fig. 21) DDT degrading enzymes showed the highest abundance for both groups with the captive samples showing a higher abundance (mean= 399,776) than the stranded samples (mean= 294,121) (Table 13). In addition to DDT, Hexabromocyclodecane, HCHs, HCB and pentachlorophenol showed the highest TPM abundances. No PBDE's (decabromodiphenyl ether, hexabromodiphenyl ether and heptabromodiphenyl ether) degrading enzymes were present in the captive samples whilst they were present in the stranded samples. HCHs degrading enzymes were present in both groups in similar abundances except for Alpha-Hexachlorocyclohexane, which had a higher abundance in stranded samples (Captive mean = 133,461, Stranded mean = 233,381).

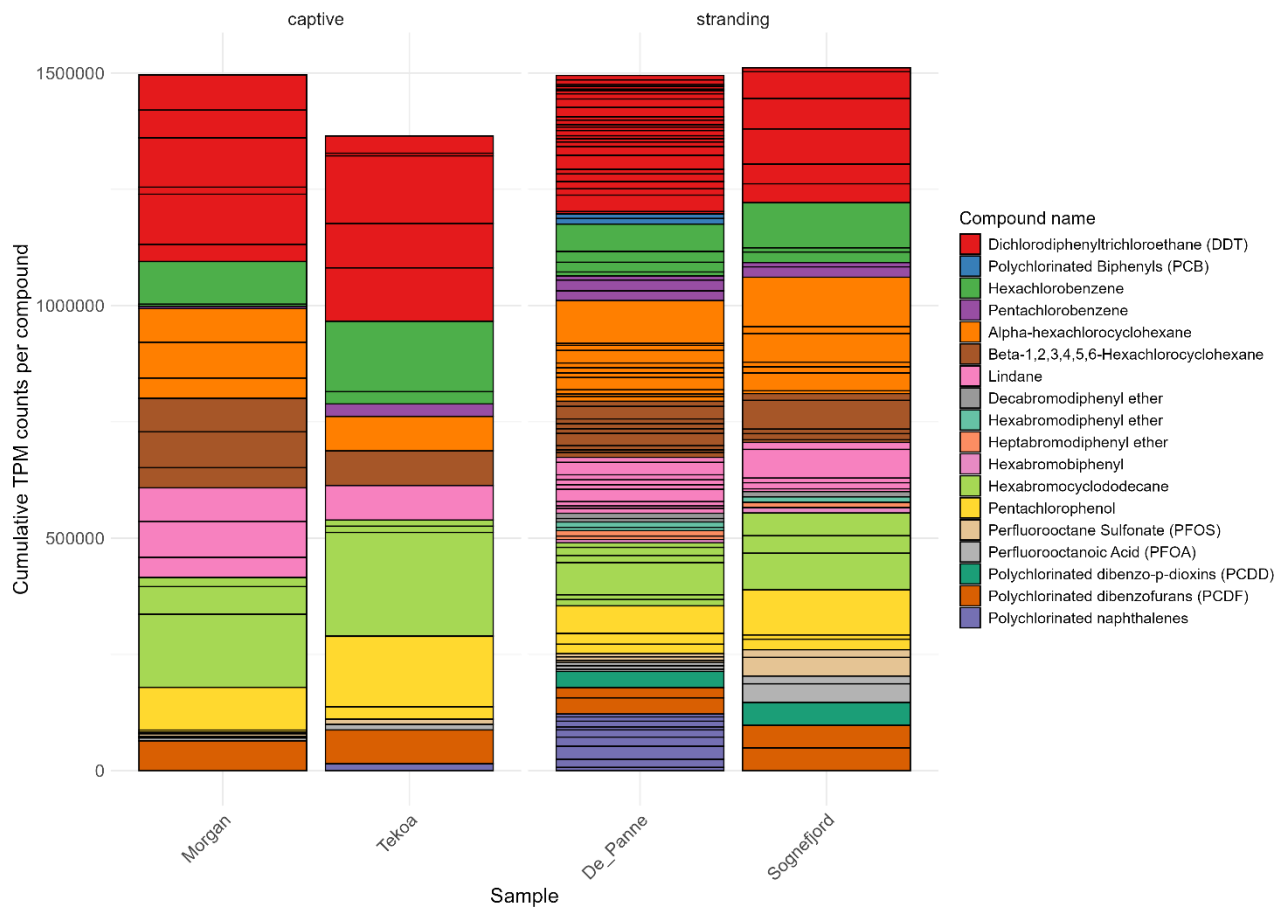


**Figure 21 | TPM-normalized abundance of POP-degrading genes in stranded vs captive killer whales.** Bar plot showing the TPM normalized abundances of POP-degrading genes grouped per POP compound for all the subsampled samples (samples which were subsampled due to sequencing depth differences).

**Table 13 | Mean cumulative TPM-normalized abundances of POP-degrading genes by group (captive vs stranded).**

POP compound	Captive	Stranded
Dichlorodiphenyltrichloroethane (DDT)	399 776	294 121
Polychlorinated Biphenyls (PCB)	0	10 853
Hexachlorobenzene (HCB)	137 177	120 153
Pentachlorobenzene	15 725	42 205
Alpha-hexachlorocyclohexane ( $\alpha$ -HCH)	133 461	233 381
Beta-Hexachlorocyclohexane ( $\beta$ -HCH)	133 461	112 807
Lindane ( $\gamma$ -HCH)	133 461	112 807
Decabromodiphenyl ether (PBDE)	0	15 178
Hexabromodiphenyl ether (PBDE)	0	15 178
Heptabromodiphenyl ether (PBDE)	0	15 178
Hexabromobiphenyl	0	9 463
Hexabromocyclododecane (HBCD)	243 369	150 429
Pentachlorophenol	137 177	115 750
Perfluorooctane Sulfonate (PFOS)	10 410	37 958
Perfluorooctanoic Acid (PFOA)	10 410	37 958
Polychlorinated dibenzo-p-dioxins (PCDD)	0	41 805

Polychlorinated dibenzofurans (PCDF)	68 388	77 007
Polychlorinated naphthalenes	7 418	60 922

Overall, the captive samples displayed a higher abundance of the enzymes present in all samples, with the exception of the putative reductive dehalogenase encoded by *rdhA* (Fig. 22). The haloacid dehalogenase encoded by *RPYSC3\_16500* showed the most significant abundance difference between captive and stranded.

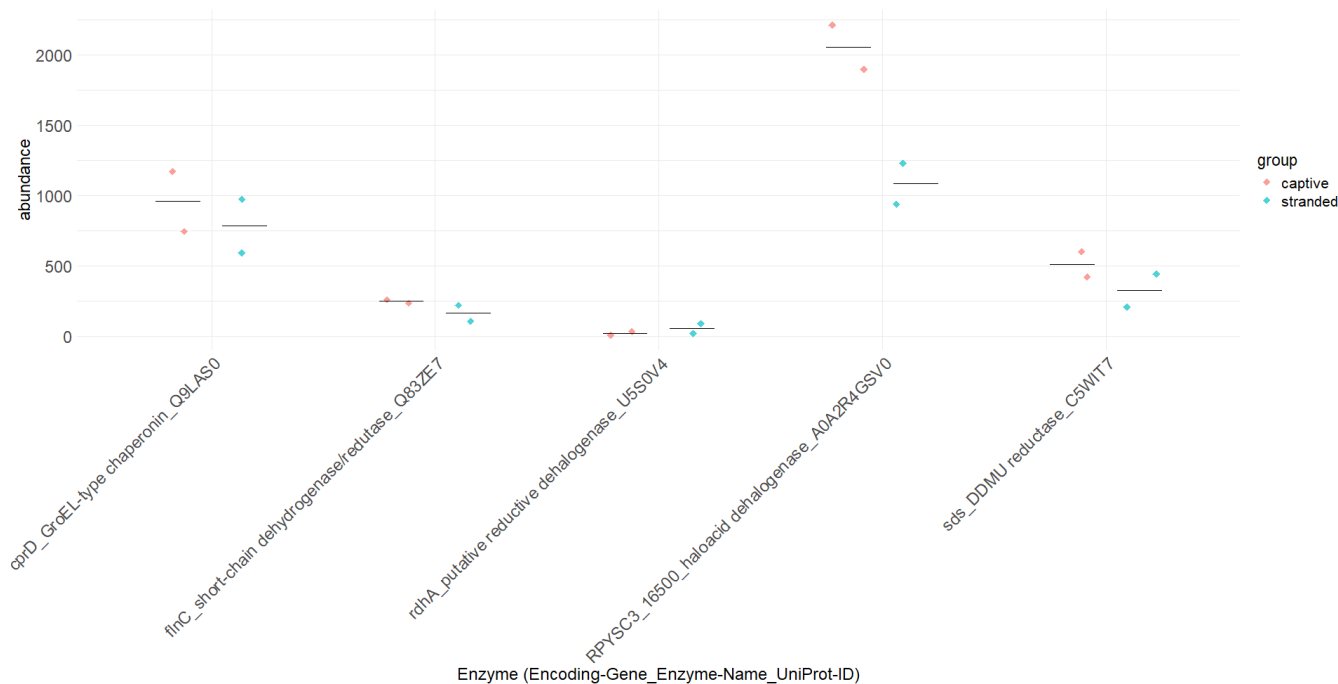


**Figure 22 | Abundances of POP-degrading genes detected in all retained captive and stranded samples (MO-FE, TE-FE, DP-HZ and SO-FE)** Plots showing the mapped read counts of POP-degrading genes that were detected in all killer whales. Black line = mean abundance per group.

## 6. Discussion

### 6.1. The gut microbiome of killer whale De Panne displays an increasing gradient in $\alpha$ -diversity along the intestinal tract

Species richness, Shannon diversity and inverse Simpson diversity displayed an increasing gradient along the intestinal tract (Fig. 7). Moreover, Shannon and inverse Simpson diversity displayed significant pairwise differences between all intestinal pair combinations (Table S2). Species richness showed significant pairwise differences between more distal (ileum, colon and rectum) and proximal (duodenum and jejunum) gut regions. Faith's phylogenetic diversity was only significantly different between ileum and colon. Increased microbial richness in the large intestine is attributed to a longer transit time, which allows microbes more time to colonise the gut environment (Asnicar et al. 2021). Interestingly, the ileum displayed similar  $\alpha$ -diversity values as the colon whilst its transit time is significantly shorter. A possible explanation for these similar values could be

that the ileum sample was actually sampled at the colon, as distinction of intestinal segments in cetaceans is poorly established. The colon exhibited the highest Faith's phylogenetic diversity, suggesting colonisation by taxa from more distantly related lineages. This elevated diversity is consistent with the extended transit time in the colon, which may facilitate the establishment of a broader range of microbial taxa (Asnicar et al. 2021). Interestingly, the duodenum also displayed relatively high phylogenetic diversity despite having low species richness, indicating colonisation by fewer but more distantly related microbial lineages. In contrast, the ileum exhibited high species richness but the lowest phylogenetic diversity, suggesting colonisation by a larger number of closely related taxa.

To date, no studies have applied ASV-based approaches to characterize gut microbiomes in marine mammals; prior studies have relied on operational taxonomic units (OTUs). As a result, making direct comparisons of absolute richness values with existing literature is not possible, because ASV-based methods typically yield higher taxonomic resolution and greater richness estimates than OTU-based methods. However, relative differences in richness between intestinal regions remain comparable across studies. The observed increasing gradient of  $\alpha$ -diversity is in line with the literature. For instance, Tian et al. revealed that the microbiome richness and diversity were significantly higher in the large intestines of a stranded dwarf mink whale compared to the duodenum and jejunum (Tian et al. 2020). Similar results were observed in bowhead whales, stranded short-finned pilot whales and a stranded pygmy sperm whale (Bai et al. 2021; Miller et al. 2020).

## 6.2. Microbiome composition varied along the intestinal tract of killer whale De Panne

The PERMANOVA results revealed that the microbiome composition differed significantly along the intestinal tract (Table 11). Pairwise comparisons between intestinal regions revealed no significant differences, likely due to low statistical power due to the small sample size (Table S4). However, PCoA analysis clearly clustered replicates of respective intestinal region for all distance metrics, Bray-Curtis, Jaccard, Weighted Unifrac and Unweighted Unifrac (Fig. 8), supporting regional differentiation in the microbiome community.

All intestinal regions were predominantly colonised by taxa of the Fusobacteriota and/or Bacillota phyla (mean = 45% and 29%, respectively) (Fig. 9). Previous studies have found similar dominance of Fusobacteriota and Bacillota in other cetacean species, such as finless porpoise (*Neophocaena phocaenoides*), Risso's dolphin (*Grampus griseus*), spotted dolphins (*Stenella attenuate*) and bowhead whales (*Balaena mysticetus*). In previously mentioned studies, in addition to Fusobacteriota and Bacillota, Pseudomonadota, formerly known as Proteobacteria, was another dominant bacterial phylum (Bai et al. 2024; Li et al. 2022; Miller et al. 2020; Wan et al. 2023). In contrast, Pseudomonadota only displayed a mean relative abundance of 6% across the entire intestinal tract of killer whale De Panne. Overall, the microbiome composition at the genus level was dominated by *Fusobacterium* (37%), *Streptobacillus* (6%) (Fusobacteriota); *Peptostreptococcus* (9%), *Clostridium* (7%), *Peptacetobacter* (5%) (Bacillota) and *Lujinxingia* (10%) (Myxococcota). These genera are all either strictly anaerobic or facultative anaerobic. *Fusobacterium*, *Peptostreptococcus*, and *Clostridium* were also found in high abundance throughout the digestive tract of bowhead whales (Miller et al. 2020). However, their distribution patterns varied. For example, *Peptostreptococcus* was

predominantly detected in the stomach and duodenum of bowhead whales, whereas in killer whale De Panne, it was primarily localized in the jejunum (27%) and was scarcely present in the duodenum (1%). Only 25% of 16S rRNA gene reads from the duodenum were successfully annotated at the species level, indicating that many of the taxa colonising the killer whale duodenum are poorly represented in the Greengenes2 database. This highlights a valuable opportunity for future research to improve taxonomic resolution and characterization of marine mammal gut microbiota. Among the identified taxa, *Fusobacterium necrogenes* exhibited the highest mean relative abundance in the intestinal samples (12%). Although little is currently known about the functional capabilities of *F. necrogenes*, it is reported to antagonize *Clostridium perfringens* – a species that was not detected (Yurdusev et al. 1989). *Streptobacillus moniliformis* was abundant along the entire intestinal tract. *S. moniliformis*, known as a pathogen causing rat bite fever in humans, has not yet been documented as part of the gut microbiome (Elliott 2007). *Paraclostridium benzoelyticum* and *Peptostreptococcus russellii*, which were most abundant in the jejunum and ileum, respectively, are known to be mucin, an important intestinal mucus component, degraders (Raimondi et al. 2021; Wlodarska et al. 2017). Furthermore, *P. russellii* has been revealed to produce the tryptophan metabolite indoleacrylic acid, which results in improvement of intestinal barrier function and suppression of inflammatory responses (Wlodarska et al. 2017). *Bacteroides fragilis*, which was primarily detected in the ileum and colon (10% and 5%, respectively), is a commensal gut bacterium that has been revealed to produce and secrete polysaccharide A (Round et al. 2011).

### 6.3. Comparison of short read and hybrid assembly

The hybrid assembly resulted in a higher N50 (6,820bp vs. 5,509bp) and average contig/scaffold length (1,838.4bp vs. 1,758.7bp) than the short read assembly (Table 12), which shows that inclusion of the long nanopore reads as scaffolds during the assembly helped to assemble more long contigs. However, this improvement was only of modest size, as previous studies reported a 2x-10x N50 improvement when performing hybrid assembly compared to Illumina-single assembly (Brown et al. 2021; Tan et al. 2018). Figure 12 and 13 confirm that the hybrid assembly scaffold length distribution was less right-skewed than the short read assembly. However, the hybrid assembly still showed a strong right skewed distribution. This indicates a significant degree of fragmentation for both assembly methods. The weak improvement of assembly results is likely due to low sequencing depth of the long reads. After adapter trimming and quality filtering, the Nanopore sequencing resulted in a sequencing depth of 296.4 Mbp, whilst, for metagenome assembly, a sequencing depth of > 5 Gbp is recommended in order to get a proper coverage of all bacterial species/strains present in the sample, including those with < 0.5% relative abundance (Jin et al. 2022). The insufficient depth likely allowed for effective scaffolding primarily of the most abundant taxa, while leaving low-abundance species and strains underrepresented and fragmented.

Interestingly, when assemblies were compared based on the number and quality of BLASTp hits, no clear improvement was observed with the hybrid assembly. Both the hybrid and short-read assemblies retained 165 hits, of which 125 were unique enzymes. Likely because POP-degrading genes – who typically range between 0bp and 1800bp – were already fully captured by short contigs, and the longer contigs in the hybrid assembly did not recover additional hits. On initial inspection, the short-read assembly appeared to perform better, as it had a higher number of mapped reads. However, this may be partly explained by the phenomenon of multimapping, where individual reads map equally well to multiple open reading frames (Canzar et al. 2016). This effect is more pronounced in

fragmented assemblies, such as those generated from short reads alone. It is possible that improved assembly results could have been achieved through alternative parameter settings, as optimal assembly configurations can vary substantially depending on the characteristics of the dataset.

To conclude, although hybrid metagenome assembly did not enhance the detection of POP-degrading genes in this study, it remains a promising approach for improving overall gene recovery. This is particularly relevant when investigating specific gene clusters, which often require longer contig lengths for accurate identification. POP-degrading genes are frequently organized within such clusters, including the biphenyl-degrading *bph* gene cluster and the chlorophenol-degrading *tfd* gene cluster (Laemmli et al. 2000; Yang et al. 2007).

#### 6.4. The gut microbiome of killer whale De Panne exhibits the ability to degrade a wide range of POPs, highlighting enhanced degradation potential for DDT, HBCD, and HCH compounds

Since the killer whale was stranded at De Panne beach in Belgium, I will assume it was part of an North-Eastern Atlantic population although the exact origin has yet to be confirmed. Overall, POP-degradation genes were abundantly represented over several pathways (Fig. 14-18). The PCB-degradation pathway, in fact, only lacked one step, encoded by the *bphH* gene (Fig. 14). However, since this was the only missing reaction, it seems possible that it was actually present but went undetected – possibly due to the limited sample size ( $n = 1$ ). The DDT degradation pathway lacked only two degradation steps, encoded by *gstD1* and *adh* (Fig. 15). Interestingly, DDT degradation showed a higher abundance for genes facilitating intermediary and late-phase degradation than those facilitating initial degradation of DDT (DDT  $\rightarrow$  DDD or DDE). This is in contradiction to the literature, which suggests microbial DDT degradation primarily involves its initial degradation (Chen et al. 2013). The PBDE, HCB and HBCD degradation pathways are dominated by debromination reactions. A multitude of dehalogenases were detected, both annotated and not annotated to PBDE, HCB and HBCD degradation. However, since it remains unclear which exact dehalogenases catalyse each dehalogenation step of PBDE, HCB and HBCD degradation, it is difficult to assess how complete their gut microbial degradation pathways were. Lindane, but also  $\alpha$ - and  $\beta$ -HCH, showed a near complete degradation pathway. The only steps lacking, required for full metabolization of lindane, were encoded by *linD*, *linE* and *linF*, which catalyse the ring cleavage of CHQ and its subsequent dehydrogenation.

Interestingly, the majority of detected genes were aerobic, whilst the majority of identified taxa were anaerobic (See section 6.2.). The most abundant genes (*linC*, *linJ*, *RPYSC3\_16500*, *sds*, *linB*, respectively) encoded dehydrogenases, a dehalogenase, an acetyltransferase and a reductase, degrading HCH, HBCD and DDT (Fig. 20). These three compounds were also the three compounds with the overall highest abundance of degrading genes (Fig 19). A recent study revealed HBCD and  $\alpha$ -HCH concentrations in North-Eastern Atlantic killer whales to average around 200 ng/g lw and 32 ng/g lw respectively, whereas some PCB congeners and DDT and its metabolites averaged around 9000-12000 ng/g lw and 376-26758 ng/g lw respectively. (Remili et al. 2023). Therefore, the high abundance of genes encoding for HBCD and  $\alpha$ -HCH degrading enzymes was unexpected. A possible explanation could be reduced intestinal absorption due to lower lipophilicity of HBCD and  $\alpha$ -HCH compared to other POPs, which would both explain their

low blubber concentrations and prevalence of HBCD and  $\alpha$ -HCH degrading enzymes in the microbiome since higher HBCD and  $\alpha$ -HCH concentration would pass by the gut microbiome, available for metabolism. The diet of North-Eastern Atlantic killer whales is dominated by herring (Remili et al. 2023; Similä, Holst, and Christensen 1996). Studies on the POP concentrations in Baltic herring and additional Baltic species revealed similar relative POP concentrations, where PCB and DDT concentrations far exceed those of HBCD and  $\alpha$ -HCH (Nyberg et al. 2015; de Wit et al. 2020). Assuming that dietary exposure reflects the contaminant concentrations found in prey species, the POP profiles observed in killer whale blubber tissue appear to mirror the relative abundances of POPs detected in Baltic herring and other prey species. Therefore, variation in intestinal absorption efficiency between different POPs is unlikely to fully explain the increased selection for HBCD- and  $\alpha$ -HCH-degrading genes.

According to existing literature, PCB and DDT are the most prominent POPs detected in killer whale blubber tissue (Andvik et al. 2021; Remili et al. 2023). This suggests high PCB and DDT exposure in killer whales and consequently, according to our hypothesis, a high abundance of microbial DDT and PCB degrading genes in the gut microbiome. This aligns with the high cumulative and individual abundances of DDT-degrading genes observed (Fig. 19- 20). In contrast, the abundances of genes and enzymes associated with PCB degradation were among the lowest, despite high PCB concentrations in blubber tissue (Fig. 19-20), suggesting a discrepancy between blubber pollutant levels and abundances of corresponding degradation genes. Overall, the abundances of degradation genes and enzymes did not consistently reflect the concentrations of the respective POPs in blubber or diet. The most plausible explanation for the difference in degradation gene abundance across POP classes lies in their structural and chemical. For example, HBCD and HCH lack aromatic rings, making them more susceptible to microbial degradation (Krygowski and Szatyłowicz 2015; Phale et al. 2007). Moreover, the carbon–bromine bond in HBCD has a lower average bond dissociation energy (276 kJ/mol) compared to the carbon–chlorine bond (339 kJ/mol), which may further reduce its chemical stability (Horrocks 2020). This could help explain the higher abundance of genes encoding HBCD-degrading enzymes. Although DDT contains two aromatic rings, it is less heavily chlorinated than PCBs and HCB, contributing to greater microbial degradability. Together, these structural characteristics may promote the selection and persistence of genes encoding enzymes that target more readily degradable POPs - such as DDT, HCH, and HBCD - over more recalcitrant compounds like PCBs, due to the lower energetic cost of degradation.

It should be noted that the annotation of POP-degrading enzymes to specific compound classes within the consulted mibPOP database may have limitations. For instance, bphB, bphC, and bphD were annotated solely to DDT degradation, although they are well-documented to also participate in PCB degradation (Hayase, Taira, and Furukawa 1990). This may have led to an underestimation of PCB-degrading gene abundances and raises questions about potential “under”-annotation affecting other compounds as well. Additionally, a bias in our current knowledge of POP-degrading genes may contribute to such inconsistencies. The mibPOP database, for instance, lists 1,638, 226, 831, 5, 191, and 61 distinct enzymes for DDT, PCB, HCB, PBDE, HCH, and HBCD, respectively. However, this biased distribution does not align proportionally to the observed gene abundances and therefore does not directly explain the discrepancy between observed gene counts and POP exposure. While the discrepancy is not directly explained by enzyme count alone, database bias likely influences the representation and apparent prevalence of degradation pathways.

## 6.5. The wild killer whale gut microbiome exhibits the ability to degrade a wider range of POPs, while the captive killer whale gut microbiome shows higher abundances of specific POP-degrading genes

The captive killer whales were exclusively fed fish sourced from various regions across the Northeast Atlantic, including the Norwegian Sea, Baltic Sea, Porcupine Bank, the coast of Spain, and the Eastern English Channel. Whereas the stranded individuals – assuming they come from the North-Eastern Atlantic population – primarily feed on fish and occasionally consume marine mammals such as harbour seals. Marine mammals are known to exhibit higher POP concentrations as a result of biomagnification and bioaccumulation (see section 2.1.2). Consequently, due to lower POP concentrations in their diet, the POP exposure of captive killer whales was expected to be lower than that of the stranded killer whales. We hypothesized that elevated POP exposure in wild killer whales may exert selective pressure favouring the proliferation of bacteria capable of degrading these compounds, similar to findings in the human gut microbiome by De Filippis et al. (2024), who reported that individuals living in highly polluted areas exhibited an increase in gut microbial genes involved in pollutant degradation. In line with this, the gut microbiome of the stranded killer whales encoded enzymes targeting the degradation of a wider variety of POPs compared to that of the captive killer whales. This might suggest that wild killer whales are exposed to a wider range of POP compounds than captive killer whales due to their more varied diet. However, the absence of PCB exposure – and of exposure to other POPs for which no corresponding degrading enzymes were detected – in captive killer whales is difficult to explain, given that fish from the Northeast Atlantic (the primary diet of the captive killer whales) are known to be contaminated with a broad spectrum of POPs, including those for which no corresponding degrading enzymes were detected in our captive samples. For instance, a study by Ho et al. (2023) showed that fish from the Northeast Atlantic ocean are contaminated with various PCB and PBDE congeners (Ho et al. 2023). Yet, in our results, degrading genes for both were absent in captive killer whales. This discrepancy raises questions about the detectability of these genes. One possible explanation is that the absence of specific POP-degrading genes in the captive killer whales may reflect methodological differences in sampling or sequencing depth, rather than true biological absence. Therefore, no definitive conclusions can be drawn regarding differences in the range of degradable POPs between wild and captive killer whales. Nevertheless, the overall pattern of the most abundantly targeted POPs was consistent with observations from the hybrid-assembled DP-HZ sample. DDT-degrading genes were the most abundant, followed by those targeting HBCD and HCH (Fig. 21) (Table 13). In contrast to the DP-HZ sample, however, the abundance of enzymes degrading HCB in the killer whale gut microbiomes was comparable to that of HCH-degrading enzymes. Interestingly, captive killer whales showed a higher abundance of DDT, HCB,  $\alpha$ -HCH, lindane and HBCD degrading enzymes (Table 13). According to our working hypothesis, that POP-degrading enzyme abundance reflects POP exposure, this pattern would suggest higher exposure levels to DDT, HCB, and HBCD in captive killer whales, which contrasts with our initial expectations.

## 6.6. Limitations of the study

This study faced a few limitations, the most prominent being an inconsistency in gut content sampling methods and DNA storage media. Because killer whale strandings are infrequent and typically occur in geographically distant locations, it is often not possible for the same personnel to carry out sample collection, making consistency in sampling execution difficult to maintain. Furthermore, as sampling of the killer whales stranded at Cadzand and

Sognefjord occurred prior and independent of the initiation of this study, no consistent sampling method was applied. Therefore, gut content of samples from different killer whales might vary. Consequently, possibility for comparisons are limited. Another limitation of this study is its low sample size. Only three stranded killer whales and four captive killer whales were sampled. Furthermore, only two samples of both stranded and captive killer whales were retained due to low microbial content of the other samples. The low sample size decreases statistical power and as a result, limits the possibility to draw robust conclusions.

This study generalized the gut microbiome to that of wild orcas. However, as samples were derived from stranded, deceased orcas, the microbial profiles may be influenced by post-mortem changes or the animals' health status at the time of death, potentially limiting the generalizability of our findings to healthy, free-ranging populations.

Marine mammals are phylogenetically related to ruminants and have been shown to possess multi-chambered stomachs that harbour distinct microbial communities. Although the harsh physicochemical conditions of the stomach limit the colonisation by diverse microbial taxa, its resident microbiome remains a compelling subject for investigating microbial degradation of POPs, as toxicant degrading bacteria have been observed in the stomach of *Artiodactyla*. Furthermore, since ingested pollutants transit through the stomach prior to intestinal absorption, the stomach is exposed to higher concentrations than the intestines, further selecting for pollutant-degrading genes. However, this study only analysed the microbial communities and its POP-degrading potential along the intestinal tract. In addition, this study looked at the genetic potential of the gut microbiome to degrade POPs. However, actual expression patterns remain undetermined. Therefore, actual microbial POP degradation activity remains speculative. Further studies characterising the metatranscriptomics and metaproteomics of the killer whale gut microbiome could confirm whether the observed genes are expressed and whether POP-degrading enzymes are present.

The presence of POP-degrading enzymes was assessed by aligning gene sequences against a reference database containing established POP-degrading gene sequences, based on sequence homology. However, sequence similarity alone does not guarantee conservation of enzymatic function. Therefore, further research is required to confirm the functional homology of the identified genes. A promising direction is to complement pairwise sequence alignments with structural comparisons using tools like FoldMason, which superimpose enzyme structures – predicted from the DNA sequences with ESMFold or Alphafold – and quantify structural similarity via local distance difference test scores. This structure-based approach provides stronger evidence for functional conservation than sequence similarity alone. Additionally, the mibPOP database exhibited a marked bias, containing reference sequences for 1,638, 226, 831, 5, 191, and 61 distinct enzymes associated with the degradation of DDT, PCB, HCB, PBDE, HCH, and HBCD, respectively. Consequently, the detection of POP-degrading genes is also subject to bias.

## 7. Conclusions and future perspectives

The killer whale gut microbiome was largely similar to that of other cetacean species, yet exhibited notable distinctions, such as a low relative abundance of Pseudomonadota. Microbiome composition varied significantly across the intestinal tract, although no significant pairwise differences were found between intestinal regions. Alpha diversity

exhibited a significant increase along the tract, with significant pairwise differences detected. The gut microbiome of both captive and stranded killer whales exhibited the genetic capacity to degrade a wide range of POPs, with an apparent selection for genes involved in degradation of DDT, HBCD and HCH. The captive killer whale gut microbiome exhibited higher abundances of POP-degrading genes, whereas the stranded killer whale gut microbiome displayed the presence of genes degrading a wider range of POPs. The hybrid metagenome assembly yielded longer contigs compared to Illumina-single assembly. However, the improvement in contig length was modest, likely due to the relatively low sequencing depth of the Nanopore data. Ultimately, the hybrid assembly did not lead to the identification of any additional POP-degrading genes.

These findings highlight the killer whale gut microbiome as a promising system for studying microbial POP degradation. However, the study is limited by its small sample size. Future research incorporating more individuals (larger population size) is necessary to robustly assess microbiome differences between captive and wild individuals, as well as among intestinal regions. Moreover, investigating the POP-degrading potential of the stomach microbiome could be particularly valuable, given that related Artiodactyla species have demonstrated microbial toxicant degradation in the stomach.

## 8. References

- Alaee, Mehran, Pedro Arias, Andreas Sjödin, and Åke Bergman. 2003. 'An Overview of Commercially Used Brominated Flame Retardants, Their Applications, Their Use Patterns in Different Countries/Regions and Possible Modes of Release'. *Environment International* 29(6):683–89. doi:10.1016/S0160-4120(03)00121-1.
- Amutova, Farida, Matthieu Delannoy, Almagul Baubekova, Gaukhar Konuspayeva, and Stefan Jurjanz. 2021. 'Transfer of Persistent Organic Pollutants in Food of Animal Origin – Meta-Analysis of Published Data'. *Chemosphere* 262.
- Andvik, Clare, Eve Jourdain, Jan L. Lyche, Richard Karoliussen, and Katrine Borgå. 2021. 'High Levels of Legacy and Emerging Contaminants in Killer Whales (*Orcinus Orca*) from Norway, 2015 to 2017'. *Environmental Toxicology and Chemistry* 40(7):1850–60. doi:10.1002/etc.5064.
- Andvik, Clare, Eve Jourdain, Anders Ruus, Jan L. Lyche, Richard Karoliussen, and Katrine Borgå. 2020. 'Preying on Seals Pushes Killer Whales from Norway above Pollution Effects Thresholds'. *Scientific Reports* 10(1). doi:10.1038/s41598-020-68659-y.
- Arrieta, Marie-Claire, Leah T. Stiemsma, Pedro A. Dimitriu, Lisa Thorson, Shannon Russell, Sophie Yurist-Doutsch, Boris Kuzeljevic, Matthew J. Gold, Heidi M. Britton, Diana L. Lefebvre, Padmaja Subbarao, Piush Mandhane, Allan Becker, Kelly M. McNagny, William W. Mohn, Stuart E. Turvey, and B. Brett Finlay. n.d. 'Early Infancy Microbial and Metabolic Alterations Affect Risk of Childhood Asthma'.
- Asano, Yasunari, Tetsuya Hiramoto, Ryo Nishino, Yuji Aiba, Tae Kimura, Kazufumi Yoshihara, Yasuhiro Koga, and Nobuyuki Sudo. 2012. 'Critical Role of Gut Microbiota in the Production of Biologically Active, Free Catecholamines in the Gut Lumen of Mice'. *Am J Physiol Gastrointest Liver Physiol* 303:1288–95. doi:10.1152/ajpgi.00341.2012.-There.
- Ascoli, Mario, Francesca Fanelli, and Deborah L. Segaloff. 2002. *The Lutropin/Choriogonadotropin Receptor, A 2002 Perspective*.
- Asnicar, Francesco, Emily R. Leeming, Eirini Dimidi, Mohsen Mazidi, Paul W. Franks, Haya Al Khatib, Ana M. Valdes, Richard Davies, Elco Bakker, Lucy Francis, Andrew Chan, Rachel Gibson, George Hadjigeorgiou, Jonathan Wolf, Timothy D. Spector, Nicola Segata, and Sarah E. Berry. 2021. 'Blue Poo: Impact of Gut Transit Time on the Gut Microbiome Using a Novel Marker'. *Gut* 70(9):1665–74. doi:10.1136/gutjnl-2020-323877.

- ATSDR. 2024. *Toxicological Profile for Hexachlorocyclohexane (HCH)*.
- Bai, Shijie, Peijun Zhang, Mingli Lin, Wenzhi Lin, Zixin Yang, and L. I. Songhai. 2021. 'Microbial Diversity and Structure in the Gastrointestinal Tracts of Two Stranded Short-Finned Pilot Whales (*Globicephala Macrorhynchus*) and a Pygmy Sperm Whale (*Kogia Breviceps*)'. *Integrative Zoology* 16(3):324–35. doi:10.1111/1749-4877.12502.
- Bai, Shijie, Peijun Zhang, Xiaoxue Qi, Jun Liu, Dongjiao Liu, Guangmou Wang, Lei Pang, and Songhai Li. 2024. 'Similarities and Differences in Gastrointestinal Microbiomes between Wild and Human-Cared Spotted Dolphins (*Stenella Attenuata*) in Natural Waters'. *Water Biology and Security*. doi:10.1016/j.watbs.2024.100288.
- Bauer, Heinz, Richard E. Horowitz, Stanley M. Levenson, and Hans Popper. 1963. 'THE RESPONSE OF THE LYMPHATIC TISSUE TO THE MICROBIAL FLORA. STUDIES ON GERM-FREE MICE'. *The American Journal of Pathology* 42(4):471–83.
- Belkaid, Yasmine, and Timothy W. Hand. 2014. 'Role of the Microbiota in Immunity and Inflammation'. *Cell* 157(1):121–41.
- Bertrand, Denis, Jim Shaw, Manesh Kalathiyappan, Amanda Hui Qi Ng, M. Senthil Kumar, Chenhao Li, Mirta Dvornic, Janja Paliska Soldo, Jia Yu Koh, Chengxuan Tong, Oon Tek Ng, Timothy Barkham, Barnaby Young, Kalisvar Marimuthu, Kern Rei Chng, Mile Sikic, and Niranjana Nagarajan. 2019. 'Hybrid Metagenomic Assembly Enables High-Resolution Analysis of Resistance Determinants and Mobile Elements in Human Microbiomes'. *Nature Biotechnology* 37(8):937–44. doi:10.1038/s41587-019-0191-2.
- Bik, Elisabeth M., Elizabeth K. Costello, Alexandra D. Switzer, Benjamin J. Callahan, Susan P. Holmes, Randall S. Wells, Kevin P. Carlin, Eric D. Jensen, Stephanie Venn-Watson, and David A. Relman. 2016. 'Marine Mammals Harbor Unique Microbiotas Shaped by and yet Distinct from the Sea'. *Nature Communications* 7. doi:10.1038/ncomms10516.
- Borja, Josephine, Donna Marie Taleon, Joseph Auresenia, and Susan Gallardo. 2005. 'Polychlorinated Biphenyls and Their Biodegradation'. *Process Biochemistry* 40(6):1999–2013.
- Bravo, Javier A., Paul Forsythe, Marianne V. Chew, Emily Escaravage, Hélène M. Savignac, Timothy G. Dinan, John Bienenstock, and John F. Cryan. 2011. 'Ingestion of *Lactobacillus* Strain Regulates Emotional Behavior and Central GABA Receptor Expression in a Mouse via the Vagus Nerve'. *Proceedings of the National Academy of Sciences of the United States of America* 108(38):16050–55. doi:10.1073/pnas.1102999108.
- Bredhult, Carolina, Britt Marie Bäcklin, Anders Bignert, and Matts Olovsson. 2008. 'Study of the Relation between the Incidence of Uterine Leiomyomas and the Concentrations of PCB and DDT in Baltic Gray Seals'. *Reproductive Toxicology* 25(2):247–55. doi:10.1016/j.reprotox.2007.11.008.
- Brown, Connor L., Ishi M. Keenum, Dongjuan Dai, Liqing Zhang, Peter J. Vikesland, and Amy Pruden. 2021. 'Critical Evaluation of Short, Long, and Hybrid Assembly for Contextual Analysis of Antibiotic Resistance Genes in Complex Environmental Metagenomes'. *Scientific Reports* 11(1). doi:10.1038/s41598-021-83081-8.
- Buchfink, Benjamin, Klaus Reuter, and Hajk Georg Drost. 2021. 'Sensitive Protein Alignments at Tree-of-Life Scale Using DIAMOND'. *Nature Methods* 18(4):366–68. doi:10.1038/s41592-021-01101-x.
- Bushnell B. BMap: a fast, accurate, splice-aware aligner. 2014. [Software]. Available from: <https://sourceforge.net/projects/bbmap/>
- Callahan, Benjamin J., Joan Wong, Cheryl Heiner, Steve Oh, Casey M. Theriot, Ajay S. Gulati, Sarah K. McGill, and Michael K. Dougherty. 2019. 'High-Throughput Amplicon Sequencing of the Full-Length 16S rRNA Gene with Single-Nucleotide Resolution'. *Nucleic Acids Research* 47(18):E103. doi:10.1093/NAR/GKZ569.

- Canzar, Stefan, Khaled Elbassioni, Mitchell Jones, and Julián Mestre. 2016. 'Resolving Conflicting Predictions from Multimapping Reads'. *Journal of Computational Biology* 23(3):203–17. doi:10.1089/cmb.2015.0164.
- Carabotti, Marilia, Annunziata Scirocco, Maria Antonietta Maselli, and Carola Severi. 2015. *The Gut-Brain Axis: Interactions between Enteric Microbiota, Central and Enteric Nervous Systems*. Vol. 28.
- Ceja-Navarro, Javier A., Fernando E. Vega, Ulas Karaoz, Zhao Hao, Stefan Jenkins, Hsiao Chien Lim, Petr Kosina, Francisco Infante, Trent R. Northen, and Eoin L. Brodie. 2015. 'Gut Microbiota Mediate Caffeine Detoxification in the Primary Insect Pest of Coffee'. *Nature Communications* 6. doi:10.1038/ncomms8618.
- Chairatana, Phoom, and Elizabeth M. Nolan. 2017. 'Defensins, Lectins, Mucins, and Secretory Immunoglobulin A: Microbe-Binding Biomolecules That Contribute to Mucosal Immunity in the Human Gut'. *Critical Reviews in Biochemistry and Molecular Biology* 52(1):45–56.
- Chang, Tse Hao, Reuben Wang, Yu Huei Peng, Tzu Ho Chou, Yi Jie Li, and Yang hsin Shih. 2020. 'Biodegradation of Hexabromocyclododecane by Rhodopseudomonas Palustris YSC3 Strain: A Free-Living Nitrogen-Fixing Bacterium Isolated in Taiwan'. *Chemosphere* 246. doi:10.1016/j.chemosphere.2019.125621.
- Charbonneau, Michel. 1992. *Sex-Related Difference in Hepatic Glutathione Conjugation of Hexachlorobenzene in the Rat*. Vol. 112.
- Chen, Manjia, Fang Cao, Fangbai Li, Chengshuai Liu, Hui Tong, Weijian Wu, and Min Hu. 2013. 'Anaerobic Transformation of DDT Related to Iron(III) Reduction and Microbial Community Structure in Paddy Soils'. *Journal of Agricultural and Food Chemistry* 61(9):2224–33. doi:10.1021/jf305029p.
- Chen, Shifu. 2023. 'Ultrafast One-Pass FASTQ Data Preprocessing, Quality Control, and Deduplication Using Fastp'. *IMeta* 2(2). doi:10.1002/imt2.107.
- Claus, Sandrine P., Hervé Guillou, and Sandrine Ellero-Simatos. 2016. 'The Gut Microbiota: A Major Player in the Toxicity of Environmental Pollutants?' *Npj Biofilms and Microbiomes* 2.
- Dabrowska, Krystyna, and Wojciech Witkiewicz. 2016. 'Correlations of Host Genetics and Gut Microbiome Composition'. *Frontiers in Microbiology* 7(AUG).
- Daniel, Volker, Wolfgang Huber, Klausdieter Bauer, Caner Suesal, Christian Conradt, and Gerhard Opelz. 2001. *Associations of Blood Levels of PCB, HCHs, and HCB with Numbers of Lymphocyte Subpopulations, in Vitro Lymphocyte Response, Plasma Cytokine Levels, and Immunoglobulin Autoantibodies*. Vol. 109.
- Davenport, Emily R., Darren A. Cusanovich, Katelyn Michelini, Luis B. Barreiro, Carole Ober, and Yoav Gilad. 2015. 'Genome-Wide Association Studies of the Human Gut Microbiota'. *PLoS ONE* 10(11). doi:10.1371/journal.pone.0140301.
- Davila, Anne Marie, François Blachier, Martin Gotteland, Mireille Andriamihaja, Pierre Henri Benetti, Yolanda Sanz, and Daniel Tomé. 2013. 'Intestinal Luminal Nitrogen Metabolism: Role of the Gut Microbiota and Consequences for the Host'. *Pharmacological Research* 68(1):95–107.
- Debier, Cathy, Gina M. Ylitalo, Michael Weise, Frances Gulland, Daniel P. Costa, Burney J. Le Boeuf, Tanguy De Tillesse, and Yvan Larondelle. 2005. 'PCBs and DDT in the Serum of Juvenile California Sea Lions: Associations with Vitamins a and e and Thyroid Hormones'. *Environmental Pollution* 134(2):323–32. doi:10.1016/j.envpol.2004.07.012.
- Denison, Elizabeth R., Ryan G. Rhodes, William A. McLellan, D. Ann Pabst, and Patrick M. Erwin. 2020a. 'Host Phylogeny and Life History Stage Shape the Gut Microbiome in Dwarf (Kogia Sima) and Pygmy (Kogia Breviceps) Sperm Whales'. *Scientific Reports* 10(1). doi:10.1038/s41598-020-72032-4.
- Denison, Elizabeth R., Ryan G. Rhodes, William A. McLellan, D. Ann Pabst, and Patrick M. Erwin. 2020b. 'Host Phylogeny and Life History Stage Shape the Gut Microbiome in Dwarf (Kogia

- Sima) and Pygmy (Kogia Breviceps) Sperm Whales'. *Scientific Reports* 10(1). doi:10.1038/s41598-020-72032-4.
- Desforges, Jean Pierre, Steven H. Ferguson, Anaïs Remili, Melissa A. McKinney, Courtney A. Watt, and Cory J. D. Matthews. 2024. 'Assessment of Persistent Organic Pollutants in Killer Whales (Orcinus Orca) of the Canadian Arctic: Implications for Subsistence Consumption and Conservation Strategies'. *Environmental Research* 244. doi:10.1016/j.envres.2023.117992.
- Desforges, Jean Pierre W., Christian Sonne, Milton Levin, Ursula Siebert, Sylvain De Guise, and Rune Dietz. 2016. 'Immunotoxic Effects of Environmental Pollutants in Marine Mammals'. *Environment International* 86:126–39.
- Desforges, Jean-Pierre, Ailsa Hall, Bernie Mcconnell, Aqqalu Rosing-Asvid, Jonathan L. Barber, Andrew Brownlow, Sylvain De Guise, Igor Eulaers, Paul D. Jepson, Robert J. Letcher, Milton Levin, Peter S. Ross, Filipa Samarra, Gísli Víkingsson, Christian Sonne, and Rune Dietz. 2018. 'Predicting Global Killer Whale Population Collapse from PCB Pollution'. *Science* 361(6409):1373–76.
- Diniz Pinto Coelho, Gabriela, Lilian Fernandes Arial Ayres, Daniela Sezilio Barreto, Bruno David Henriques, Mara Rúbia Maciel Cardoso Prado, and Camila Mendes Dos Passos. 2021. 'Acquisition of Microbiota According to the Type of Birth: An Integrative Review'. *Revista Latino-Americana de Enfermagem*. doi:10.1590/1518-8345.4466.3446.
- Dulfer, Wiegert J., Harrie A. J. Govers, and John P. Groten. 1998. 'Kinetics and Conductivity Parameters of Uptake and Transport of Polychlorinated Biphenyls in the Caco-2 Intestinal Cell Line Model'. *Environmental Toxicology and Chemistry* 17(3):493–501. doi:10.1002/etc.5620170321.
- Duncan, Sylvia H., Grietje Holtrop, Gerald E. Loble, A. Graham Calder, Colin S. Stewart, and Harry J. Flint. 2004. 'Contribution of Acetate to Butyrate Formation by Human Faecal Bacteria'. *British Journal of Nutrition* 91(6):915–23. doi:10.1079/bjn20041150.
- Eigeland, Karen A., Janet M. Lanyon, Darren J. Trott, Diane Ouwerkerk, Wendy Blanshard, Gabriel J. Milinovich, Lisa Maree Gulino, Emilio Martinez, Samuel Merson, and Athol V. Klieve. 2012. 'Bacterial Community Structure in the Hindgut of Wild and Captive Dugongs (Dugong Dugon)'. *Aquatic Mammals* 38(4):402–11. doi:10.1578/AM.38.4.2012.402.
- Elliott, Sean P. 2007. 'Rat Bite Fever, Streptobacillus Moniliformis'. *Clinical Microbiology Reviews* 20(1):13–22.
- Endo, Ryo, Mayuko Kamakura, Keisuke Miyauchi, Masao Fukuda, Yoshiyuki Ohtsubo, Masataka Tsuda, and Yuji Nagata. 2005. 'Identification and Characterization of Genes Involved in the Downstream Degradation Pathway of  $\gamma$ -Hexachlorocyclohexane in *Sphingomonas Paucimobilis* UT26'. *Journal of Bacteriology* 187(3):847–53. doi:10.1128/JB.187.3.847-853.2005.
- Erickson, Mitchell D., and Robert G. Kaley. 2011. 'Applications of Polychlorinated Biphenyls'. *Environmental Science and Pollution Research* 18(2):135–51. doi:10.1007/s11356-010-0392-1.
- Farrakh Mehboob, Alette A. M. Langenhoff, Gosse Schraa, and Alfons J. M. Stams. 2013. 'Anaerobic Degradation of Lindane and Other HCH Isomers'. Pp. 495–521 in *Management of Microbial Resources in the Environment*. Springer.
- De Filippis, Francesca, Vincenzo Valentino, Giuseppina Sequino, Giorgia Borriello, Marita Georgia Riccardi, Biancamaria Pierri, Pellegrino Cerino, Antonio Pizzolante, Edoardo Pasolli, Mauro Esposito, Antonio Limone, and Danilo Ercolini. 2024. 'Exposure to Environmental Pollutants Selects for Xenobiotic-Degrading Functions in the Human Gut Microbiome'. *Nature Communications* 15(1). doi:10.1038/s41467-024-48739-7.
- Frick, P. G., G. Riedler, H. Brggli, and H. Br~gli. 1967. *Dose Response and Minimal Daily Requirement for Vitamin K in Man*. Vol. 23.

- Frouin, Héloïse, Michel Lebeuf, Mike Hammill, and Michel Fournier. 2012. 'Transfer of PBDEs and Chlorinated POPs from Mother to Pup during Lactation in Harp Seals *Phoca Groenlandica*'. *Science of the Total Environment* 417–418:98–107. doi:10.1016/j.scitotenv.2011.11.084.
- Gatesy, John, Jonathan H. Geisler, Joseph Chang, Carl Buell, Annalisa Berta, Robert W. Meredith, Mark S. Springer, and Michael R. McGowen. 2013. 'A Phylogenetic Blueprint for a Modern Whale'. *Molecular Phylogenetics and Evolution* 66(2):479–506. doi:10.1016/j.ympev.2012.10.012.
- Gerussi, Tommaso, Jean Marie Grač, Ksenia Orekhova, Bruno Cozzi, and Annamaria Grandis. 2024. 'Vascularization of the Gastrointestinal Tract of the Bottlenose Dolphin (*Tursiops Truncatus*, Montagu 1821)'. *Journal of Anatomy* 244(4):628–38. doi:10.1111/joa.13989.
- Gouin, T., D. MacKay, K. C. Jones, T. Harner, and S. N. Meijer. 2004. 'Evidence for the "Grasshopper" Effect and Fractionation during Long-Range Atmospheric Transport of Organic Contaminants'. *Environmental Pollution* 128(1–2):139–48. doi:10.1016/j.envpol.2003.08.025.
- Greig, Denise J., Gina M. Ylitalo, Ailsa J. Hall, Deborah A. Fauquier, and Frances M. D. Gulland. 2007. 'Transplacental Transfer of Organochlorines in California Sea Lions (*Zalophus Californianus*)'. *Environmental Toxicology and Chemistry* 26(1):37–44. doi:10.1897/05-609R.1.
- Guo, Wenjing, Bohu Pan, Sugunadevi Sakkiah, Gokhan Yavas, Weigong Ge, Wen Zou, Weida Tong, and Huixiao Hong. 2019. 'Persistent Organic Pollutants in Food: Contamination Sources, Health Effects and Detection Methods'. *International Journal of Environmental Research and Public Health* 16(22).
- Hapfelmeier, Siegfried, Melissa A. E. Lawson, Emma Slack, Jorum K. Kirundi, Maaïke Stoel, Mathias Heikenwalder, Julia Cahenzli, Yuliya Velykoredko, Maria L. Balmer, Kathrin Endt, Markus B. Geuking, Roy Curtiss, Kathy D. McCoy, and Andrew J. Macpherson. 2010. 'Reversible Microbial Colonization of Germ-Free Mice Reveals the Dynamics of IgA Immune Responses'. *Science* 328(5986):1705–9. doi:10.1126/science.1188454.
- Hayase, Nobuki, Kazunari Taira, and Kensuke Furukawa. 1990. *Pseudomonas Putida KF715 BphABCD Operon Encoding Biphenyl and Polychlorinated Biphenyl Degradation: Cloning, Analysis, and Expression in Soil Bacteria*. Vol. 172.
- Heijtz, Rochellys Diaz, Shugui Wang, Farhana Anuar, Yu Qian, Britta Björkholm, Annika Samuelsson, Martin L. Hibberd, Hans Forssberg, and Sven Pettersson. 2011. 'Normal Gut Microbiota Modulates Brain Development and Behavior'. *Proceedings of the National Academy of Sciences of the United States of America* 108(7):3047–52. doi:10.1073/pnas.1010529108.
- Herman, D. P., D. G. Burrows, P. R. Wade, J. W. Durban, C. O. Matkin, R. G. Leduc, L. G. Barrett-Lennard, and M. M. Krahn. 2005. 'Feeding Ecology of Eastern North Pacific Killer Whales *Orcinus Orca* from Fatty Acid, Stable Isotope, and Organochlorine Analyses of Blubber Biopsies'. *Marine Ecology Progress Series* 302:275–91. doi:10.3354/meps302275.
- Hirokane, Hisako, Mayuko Nakahara, Shizuko Tachibana, Makoto Shimizu, and Ryuichiro Sato. 2004. 'Bile Acid Reduces the Secretion of Very Low Density Lipoprotein by Repressing Microsomal Triglyceride Transfer Protein Gene Expression Mediated by Hepatocyte Nuclear Factor-4'. *Journal of Biological Chemistry* 279(44):45685–92. doi:10.1074/jbc.M404255200.
- Ho, Quang Tri, Sylvia Frantzen, Bente M. Nilsen, Ole Jakob Nøstbakken, Atabak M. Azad, Arne Duinker, Lise Madsen, and Michael S. Bank. 2023. 'Congener-Specific Accumulation of Persistent Organic Pollutants in Marine Fish from the Northeast Atlantic Ocean'. *Journal of Hazardous Materials* 457. doi:10.1016/j.jhazmat.2023.131758.
- Hoban, A. E., R. M. Stilling, F. J. Ryan, F. Shanahan, T. G. Dinan, M. J. Claesson, G. Clarke, and J. F. Cryan. 2016. 'Regulation of Prefrontal Cortex Myelination by the Microbiota'. *Translational Psychiatry* 6. doi:10.1038/tp.2016.42.
- Horrocks, A. Richard. 2020. 'The Potential for Bio-Sustainable Organobromine-Containing Flame Retardant Formulations for Textile Applications-a Review'. *Polymers* 12(9).

- Horrocks, Victoria, Olivia G. King, Alexander Y. G. Yip, Inês Melo Marques, and Julie A. K. McDonald. 2023. 'Role of the Gut Microbiota in Nutrient Competition and Protection against Intestinal Pathogen Colonization'. *Microbiology (United Kingdom)* 169(8).
- Horstmann, Lara. 2017. 'Gastrointestinal Tract'. Pp. 397–400 in *Encyclopedia of Marine Mammals, Third Edition*. Elsevier.
- Hyatt, Doug, Gwo-Liang Chen, Philip F. Locascio, Miriam L. Land, Frank W. Larimer, and Loren J. Hauser. 2010. *Prodigal: Prokaryotic Gene Recognition and Translation Initiation Site Identification*.
- IARC Working Group on the Evaluation of Carcinogenic Risks to Humans. 2018. '4.1. Toxicokinetic Data'. Pp. 179–84 in *DDT, Lindane, and 2,4-D*.
- Ilyina, T., T. Pohlmann, G. Lammel, and J. Sündermann. 2006. 'A Fate and Transport Ocean Model for Persistent Organic Pollutants and Its Application to the North Sea'. *Journal of Marine Systems* 63(1–2):1–19. doi:10.1016/j.jmarsys.2006.04.007.
- Ito, Koji. 2021. 'Mechanisms of Aerobic Dechlorination of Hexachlorobenzene and Pentachlorophenol by *Nocardioides* Sp. PD653'. *Journal of Pesticide Science* 46(4):373–81. doi:10.1584/JPESTICS.J21-04.
- Ito, Koji, Kazuhiro Takagi, Akio Iwasaki, Naoto Tanaka, Yu Kanasaki, Fabrice Martin-Laurent, and Shizunobu Igimi. 2017. 'Identification of the Hcb Gene Operon Involved in Catalyzing Aerobic Hexachlorobenzene Dechlorination in *Nocardioides* Sp. Strain PD653'. *Applied and Environmental Microbiology* 83(19). doi:10.1128/AEM.00824-17.
- Ivanov, Ivaylo I., Koji Atarashi, Nicolas Manel, Eoin L. Brodie, Tatsuichiro Shima, Ulas Karaoz, Dongguang Wei, Katherine C. Goldfarb, Clark A. Santee, Susan V. Lynch, Takeshi Tanoue, Akemi Imaoka, Kikuji Itoh, Kiyoshi Takeda, Yoshinori Umesaki, Kenya Honda, and Dan R. Littman. 2009. 'Induction of Intestinal Th17 Cells by Segmented Filamentous Bacteria'. *Cell* 139(3):485–98. doi:10.1016/j.cell.2009.09.033.
- Jin, Hao, Lijun You, Feiyan Zhao, Shenghui Li, Teng Ma, Lai Yu Kwok, Haiyan Xu, and Zhihong Sun. 2022. 'Hybrid, Ultra-Deep Metagenomic Sequencing Enables Genomic and Functional Characterization of Low-Abundance Species in the Human Gut Microbiome'. *Gut Microbes* 14(1). doi:10.1080/19490976.2021.2021790.
- Kaji, Izumi, and Atsukazu Kuwahara. 2008. *Roles of Short-Chain Fatty Acids Receptors, GPR41 and GPR43 on Colonic Functions*.
- Kelly, Barry C., Frank Apc Gobas, and Michael S. McLachlan. 2004. 'Special Issue Honoring Don Mackay INTestinal Absorption and Biomagnification of Organic Contaminants in Fish, Wildlife, and Humans'. *Environmental Toxicology and Chemistry* 23(10).
- Kim, Gun Ha, and Jung Ok Shim. 2023. 'Gut Microbiota Affects Brain Development and Behavior'. *Clinical and Experimental Pediatrics* 66(7):274–80.
- Koopman-Esseboom, Corine, Nynke Weisglas-Kuperus, Maria A. J. De Ridde, and Pieter J. J. Sauer. 1996. *Effects of Polychlorinated Biphenyl/Dioxin Exposure and Feeding Type on Infants' Mental and Psychomotor Development MScll*. Vol. 97.
- Kowalski, Karol, and Agata Mulak. 2019. 'Brain-Gut-Microbiota Axis in Alzheimer's Disease'. *Journal of Neurogastroenterology and Motility* 25(1):48–60. doi:10.5056/jnm18087.
- Krygowski, T. M., and H. Szatyłowicz. 2015. 'Aromaticity: What Does It Mean?'. *ChemTexts* 1(3). doi:10.1007/s40828-015-0012-2.
- Kumar, Mukesh, Dinesh Kumar, and Puthupalayam Thangavelu Kalaichelvan. 2013. *HEXACHLOROBENZENE-SOURCES, REMEDIATION AND FUTURE PROSPECTS*.
- Laemmli, Caroline M., Johan H. J. Leveau, Alexander J. B. Zehnder, and Jan Roelof Van Der Meer. 2000. *Characterization of a Second Tfd Gene Cluster for Chlorophenol and Chlorocatechol Metabolism on Plasmid PJP4 in *Ralstonia Eutropha* JMP134(PJP4)*. Vol. 182.

- Lans, Martine C., Cecile Spiertz, Abraham Brouwer, and Jan H. Koeman. 1994. *Different Competition of Thyroxine Binding to Transthyretin and Thyroxine-Binding Globulin by Hydroxy-PCBs, PCDDs and PCDFs*. Vol. 270.
- Levin, Milton, Brenda Morsey, Chiharu Mori, Prashant R. Nambiar, and Sylvain De Guise. 2005. 'PCBs and TCDD, Alone and in Mixtures, Modulate Marine Mammal but Not B6C3F1 Mouse Leukocyte Phagocytosis'. *Journal of Toxicology and Environmental Health - Part A* 68(8):635–56. doi:10.1080/15287390590921766.
- Li, Chengzhang, Huiying Xie, Yajing Sun, Ying Zeng, Ziyao Tian, Xiaohan Chen, Edmond Sanganyado, Jianqing Lin, Liangliang Yang, Ping Li, Bo Liang, and Wenhua Liu. 2022. 'Insights on Gut and Skin Wound Microbiome in Stranded Indo-Pacific Finless Porpoise (*Neophocaena phocaenoides*)'. *Microorganisms* 10(7). doi:10.3390/microorganisms10071295.
- Li, Dinghua, Chi Man Liu, Ruibang Luo, Kunihiko Sadakane, and Tak Wah Lam. 2015. 'MEGAHIT: An Ultra-Fast Single-Node Solution for Large and Complex Metagenomics Assembly via Succinct de Bruijn Graph'. *Bioinformatics* 31(10):1674–76. doi:10.1093/bioinformatics/btv033.
- Liang, Xiaoming, Cheryl E. Devine, Jennifer Nelson, Barbara Sherwood Lollar, Stephen Zinder, and Elizabeth A. Edwards. 2013. 'Anaerobic Conversion of Chlorobenzene and Benzene to CH<sub>4</sub> and CO<sub>2</sub> in Bioaugmented Microcosms'. *Environmental Science and Technology* 47(5):2378–85. doi:10.1021/es3043092.
- Liu, Jing, Meirong Zhao, Shulin Zhuang, Yan Yang, Ye Yang, and Weiping Liu. 2012. 'Low Concentrations of o,p'-DDT Inhibit Gene Expression and Prostaglandin Synthesis by Estrogen Receptor-Independent Mechanism in Rat Ovarian Cells'. *PLoS ONE* 7(11). doi:10.1371/journal.pone.0049916.
- Liu, Simeng, Enyao Li, Zhenyu Sun, Dongjun Fu, Guiqin Duan, Miaomiao Jiang, Yong Yu, Lu Mei, Pingchang Yang, Youcai Tang, and Pengyuan Zheng. 2019. 'Altered Gut Microbiota and Short Chain Fatty Acids in Chinese Children with Autism Spectrum Disorder'. *Scientific Reports* 9(1). doi:10.1038/s41598-018-36430-z.
- Lora V. Hooper, Melissa H. Wong, Anders Thelin, Lennart Hansson, Per G. Falk, and Jeffrey I. Gordon. 2001. 'Molecular Analysis Of Commensal Host-Microbial Relationships in the Intestine'. *Science* 291(5505):881–84.
- Lu, Jennifer, Natalia Rincon, Derrick E. Wood, Florian P. Breitwieser, Christopher Pockrandt, Ben Langmead, Steven L. Salzberg, and Martin Steinegger. 2022. 'Metagenome Analysis Using the Kraken Software Suite'. *Nature Protocols* 17(12):2815–39. doi:10.1038/s41596-022-00738-y.
- Lyons, Katriona E., C. Anthony Ryan, Eugene M. Dempsey, R. Paul Ross, and Catherine Stanton. 2020. 'Breast Milk, a Source of Beneficial Microbes and Associated Benefits for Infant Health'. *Nutrients* 12(4).
- Marinescu, Mariana, M. Dumitru, and Anca Lăcătușu. 2009. 'BIODEGRADATION OF PETROLEUM HYDROCARBONS IN AN ARTIFICIAL POLLUTED SOIL'. *Research Journal of Agricultural Science* 41(2).
- Markle, Janet G. M., Daniel N. Frank, Steven Mortin-Toth, Charles E. Robertson, Leah M. Feazel, Ulrike Rolle-Kampczyk, Martin Von Bergen, Kathy D. McCoy, Andrew J. Macpherson, and Jayne S. Danska. 2013. 'Sex Differences in the Gut Microbiome Drive Hormone-Dependent Regulation of Autoimmunity'. *Science* 339(6123):1084–88. doi:10.1126/science.1233521.
- Matcovitch-Natan, Orit, Deborah R. Winter, Amir Giladi, Stephanie Vargas Aguilar, Amit Spinrad, Sandrine Sarrazin, Hila Ben-Yehuda, Eyal David, Fabiola Zelada González, Pierre Perrin, Hadas Keren-Shaul, Meital Gury, David Lara-Astaiso, Christoph A. Thaiss, Merav Cohen, Keren Bahar Halpern, Kuti Baruch, Aleksandra Deczkowska, Erika Lorenzo-Vivas, Shalev Itzkovitz, Eran Elinav, Michael H. Sieweke, Michal Schwartz, and Ido Amit. 2016. 'Microglia Development Follows a Stepwise Program to Regulate Brain Homeostasis'. *Science* 353(6301). doi:10.1126/science.aad8670.

- Mazmanian, Sarkis K., June L. Round, and Dennis L. Kasper. 2008. 'A Microbial Symbiosis Factor Prevents Intestinal Inflammatory Disease'. *Nature* 453(7195):620–25. doi:10.1038/nature07008.
- McDonald, Daniel, Yueyu Jiang, Metin Balaban, Kalen Cantrell, Qiyun Zhu, Antonio Gonzalez, James T. Morton, Giorgia Nicolaou, Donovan H. Parks, Søren M. Karst, Mads Albertsen, Philip Hugenholtz, Todd DeSantis, Se Jin Song, Andrew Bartko, Aki S. Havulinna, Pekka Jousilahti, Susan Cheng, Michael Inouye, Teemu Niiranen, Mohit Jain, Veikko Salomaa, Leo Lahti, Siavash Mirarab, and Rob Knight. 2024. 'Greengenes2 Unifies Microbial Data in a Single Reference Tree'. *Nature Biotechnology* 42(5):715–18. doi:10.1038/s41587-023-01845-1.
- Merson, Samuel D., Diane Ouwerkerk, Lisa Maree Gulino, Athol Klieve, Robert K. Bonde, Elizabeth A. Burgess, and Janet M. Lanyon. 2014. 'Variation in the Hindgut Microbial Communities of the Florida Manatee, *Trichechus Manatus Latiostris* over Winter in Crystal River, Florida'. *FEMS Microbiology Ecology* 87(3):601–15. doi:10.1111/1574-6941.12248.
- Miller, Carolyn A., Henry C. Holm, Lara Horstmann, John C. George, Helen F. Fredricks, Benjamin A. S. Van Mooy, and Amy Apprill. 2020. 'Coordinated Transformation of the Gut Microbiome and Lipidome of Bowhead Whales Provides Novel Insights into Digestion'. *ISME Journal* 14(3):688–701. doi:10.1038/s41396-019-0549-y.
- Miller, Corrie, Kayti Luu, Brandi Mikami, Jonathan Riel, Yujia Qin, Vedbar Khadka, and Men-Jean Lee. 2024. 'Temporal Investigation of the Maternal Origins of Fetal Gut Microbiota'. *Microorganisms* 12(9):1865. doi:10.3390/microorganisms12091865.
- Moore, John A. 2000. *Institute for Evaluating Health Risks REASSESSMENT OF LIVER FINDINGS in FIVE PCB STUDIES IN RATS*.
- Mori, Chiharu, Brenda Morsey, Milton Levin, Prashant R. Nambiar, and Sylvain De Guise. 2006. 'Immunomodulatory Effects of in Vitro Exposure to Organochlorines on T-Cell Proliferation in Marine Mammals and Mice'. *Journal of Toxicology and Environmental Health - Part A* 69(4):283–302. doi:10.1080/15287390500227472.
- Mos, Lizzy, Brenda Morsey, Steven J. Jeffries, Mark B. Yunker, Stephen Raverty, Sylvain De Guise, and Peter S. Ross. 2006. 'Chemical and Biological Pollution Contribute to the Immunological Profiles of Free-Ranging Harbor Seals'. *Environmental Toxicology and Chemistry* 25(12):3110–17. doi:10.1897/06-027R.1.
- Munier, Mathilde, Mohammed Ayoub, Valentine Suteau, Louis Gourdin, Daniel Henrion, Eric Reiter, and Patrice Rodien. 2021. 'In Vitro Effects of the Endocrine Disruptor p,p'DDT on Human Choriogonadotropin/Luteinizing Hormone Receptor Signalling'. *Archives of Toxicology* 95(5):1671–81. doi:10.1007/s00204-021-03007-1.
- Murphy, Sinéad, Jonathan L. Barber, Jennifer A. Learmonth, Fiona L. Read, Robert Deaville, Matthew W. Perkins, Andrew Brownlow, Nick Davison, Rod Penrose, Graham J. Pierce, Robin J. Law, and Paul D. Jepson. 2015. 'Reproductive Failure in UK Harbour Porpoises *Phocoena Phocoena*: Legacy of Pollutant Exposure?' *PLoS ONE* 10(7). doi:10.1371/journal.pone.0131085.
- Neerja, Jasneet Grewal, Amrik Bhattacharya, Sumit Kumar, Dileep K. Singh, and Sunil K. Khare. 2016. 'Biodegradation of 1,1,1-Trichloro-2,2-Bis(4-Chlorophenyl) Ethane (DDT) by Using *Serratia Marcescens* NCIM 2919'. *Journal of Environmental Science and Health - Part B Pesticides, Food Contaminants, and Agricultural Wastes* 51(12):809–16. doi:10.1080/03601234.2016.1208455.
- Nelson, Tiffanie M., Tracey L. Rogers, Alejandro R. Carlini, and Mark V. Brown. 2013. 'Diet and Phylogeny Shape the Gut Microbiota of Antarctic Seals: A Comparison of Wild and Captive Animals'. *Environmental Microbiology* 15(4):1132–45. doi:10.1111/1462-2920.12022.
- Nicholson An, Jean L., and Joseph Altman. 1972. *THE EFFECTS OF EARLY HYPO-AND HYPERTHYROIDISM ON THE DEVELOPMENT OF RAT CEREBELLAR CORTEX. I. CELL PRO-LIFERATION AND DIFFERENTIATION*.

- Nyberg, Elisabeth, Suzanne Faxneld, Sara Danielsson, Ulla Eriksson, Aroha Miller, and Anders Bignert. 2015. 'Temporal and Spatial Trends of PCBs, DDTs, HCHs, and HCB in Swedish Marine Biota 1969–2012'. *Ambio* 44:484–97. doi:10.1007/s13280-015-0673-5.
- Odamaki, Toshitaka, Kumiko Kato, Hirosuke Sugahara, Nanami Hashikura, Sachiko Takahashi, Jin Zhong Xiao, Fumiaki Abe, and Ro Osawa. 2016. 'Age-Related Changes in Gut Microbiota Composition from Newborn to Centenarian: A Cross-Sectional Study'. *BMC Microbiology* 16(1). doi:10.1186/s12866-016-0708-5.
- Ogbonnaya, Ebere S., Gerard Clarke, Fergus Shanahan, Timothy G. Dinan, John F. Cryan, and Olivia F. O'Leary. 2015. 'Adult Hippocampal Neurogenesis Is Regulated by the Microbiome'. *Biological Psychiatry* 78(4):e7–9. doi:10.1016/J.BIOPSYCH.2014.12.023.
- Olsen, Monica Alterskjær, and Svein Disch Mathiesen. 1996. 'Production Rates of Volatile Fatty Acids in the Minke Whale( *Balaenoptera Acutorostrata* ) Forestomach '. *British Journal of Nutrition* 75(1):21–31. doi:10.1079/bjn19960107.
- Van Ommen, Ben, Willem Hendriks, Jos G. M Bessems, Geert Geesink, Peter J. Van Bladeren, J. G. M Geesink, G. Moller, and Van Bladeren. 1989. *The Relation between the Oxidative Biotransformation of Hexachlorobenzene and Its Porphyrinogenic Activity The Relation between the Oxidative Biotransformation of Hexachlorobenzene and Its Por-Phyrinogenic Activity*. VAN OMMEN. Vol. 5.
- Osawa, R., F. Rainey!, T. Fujisawa, E. Lang, H. J. Busse", T. P. Walsh, and E. Stackebrandt. 1995. *Lonepinella Koalarum Gen. Nov., Sp. Nov., a New Tannin-Protein Complex Degrading Bacterium*. Vol. 18.
- Oseph, J., L. J. Acobson, and Andra W. J. Acobson. 1996. *INTELLECTUAL IMPAIRMENT IN CHILDREN EXPOSED TO POLYCHLORINATED BIPHENYLS IN UTERO INTELLECTUAL IMPAIRMENT IN CHILDREN EXPOSED TO POLYCHLORINATED BIPHENYLS IN UTERO A BSTRACT Background In Utero Exposure to Polychlorinated*.
- O'sullivan, Gwen, and David Megson. 2014. 'Brief Overview: Discovery, Regulation, Properties, and Fate of POPs'. Pp. 1–20 in *Environmental Forensics for Persistent Organic Pollutants*.
- Pacific Biosciences. (2023). SMRT Link Software v12.0 [Computer software]. Pacific Biosciences. Available from: <https://www.pacb.com/support/software-downloads/>
- Pacific Biosciences. (2024). SKERA v1.4.0 [Computer software]. Pacific Biosciences. Available from: <https://github.com/PacificBiosciences/skera>
- Pacheco-Sandoval, A., A. Lago-Lestón, A. Abadía-Cardoso, E. Solana-Arellano, and Y. Schramm. 2022. 'Age as a Primary Driver of the Gut Microbial Composition and Function in Wild Harbor Seals'. *Scientific Reports* 12(1). doi:10.1038/s41598-022-18565-2.
- Pan, Xiong, Dunli Lin, Yuan Zheng, Qian Zhang, Yuanming Yin, Lin Cai, Hua Fang, and Yunlong Yu. 2016. 'Biodegradation of DDT by *Stenotrophomonas* Sp. DDT-1: Characterization and Genome Functional Analysis'. *Scientific Reports* 6. doi:10.1038/srep21332.
- Peng, Xingxing, Dongyang Wei, Qiyuan Huang, and Xiaoshan Jia. 2018. 'Debromination of Hexabromocyclododecane by Anaerobic Consortium and Characterization of Functional Bacteria'. *Frontiers in Microbiology* 9(JUL). doi:10.3389/fmicb.2018.01515.
- Perez-Muñoz, Maria Elisa, Marie Claire Arrieta, Amanda E. Ramer-Tait, and Jens Walter. 2017. 'A Critical Assessment of the "Sterile Womb" and "in Utero Colonization" Hypotheses: Implications for Research on the Pioneer Infant Microbiome'. *Microbiome* 5(1).
- Phale, Prashant S., Aditya Basu, Prabin D. Majhi, Jaigeeth Deveryshetty, C. Vamsee-Krishna, and Rahul Shrivastava. 2007. 'Metabolic Diversity in Bacterial Degradation of Aromatic Compounds'. *OMICS A Journal of Integrative Biology* 11(3):252–79.
- Pircher, Parinaz C., Jennifer L. Kitto, Mary L. Petrowski, Rajendra K. Tangirala, Eric D. Bischoff, Ira G. Schulman, and Stefan K. Westin. 2003. 'Farnesoid X Receptor Regulates Bile Acid-Amino Acid Conjugation'. *Journal of Biological Chemistry* 278(30):27703–11. doi:10.1074/jbc.M302128200.

- Qi, Jinfeng, Fangjie Xiao, Xingxing Liu, Jing Li, Haocai Wang, Shu Li, Hongwei Yu, Yuxing Xu, and Hang Wang. 2024. 'The Fall Armyworm Converts Maize Endophytes into Its Own Probiotics to Detoxify Benzoxazinoids and Promote Caterpillar Growth'. *Microbiome* 12(1). doi:10.1186/s40168-024-01957-z.
- Raimondi, Stefano, Eliana Musmeci, Francesco Candelieri, Alberto Amaretti, and Maddalena Rossi. 2021. 'Identification of Mucin Degradors of the Human Gut Microbiota'. *Scientific Reports* 11(1). doi:10.1038/s41598-021-90553-4.
- Rayne, Sierra, Michael G. Ikonomou, Peter S. Ross, Graeme M. Ellis, and Lance G. Barrett-Lennard. 2004. 'PBDEs, PBBs, and PCNs in Three Communities of Free-Ranging Killer Whales (*Orcinus Orca*) from the Northeastern Pacific Ocean'. *Environmental Science and Technology* 38(16):4293–99. doi:10.1021/es0495011.
- Remili, Anaïs, Rune Dietz, Christian Sonne, Filipa I. P. Samarra, Robert J. Letcher, Audun H. Rikardsen, Steven H. Ferguson, Cortney A. Watt, Cory J. D. Matthews, Jeremy J. Kiszka, Aqqalu Rosing-Asvid, and Melissa A. McKinney. 2023. 'Varying Diet Composition Causes Striking Differences in Legacy and Emerging Contaminant Concentrations in Killer Whales across the North Atlantic'. *Environmental Science and Technology* 57(42):16109–20. doi:10.1021/acs.est.3c05516.
- Rosenberg, Eugene, and Ilana Zilber-Rosenberg. 2022. 'Reconstitution and Transmission of Gut Microbiomes and Their Genes between Generations'. *Microorganisms* 10(1).
- Round, June L., S. Melanie Lee, Jennifer Li, Gloria Tran, Bana Jabri, Talal A. Chatila, and Sarkis K. Mazmanian. 2011. 'The Toll-Like Receptor 2 Pathway Colonization by a Commensal of the Human Microbiota'. *Science* 332(6032):970–74. doi:10.1126/science.1198719.
- Routti, Heli, Robert J. Letcher, Augustine Arukwe, Bert Van Bavel, Nigel G. Yoccoz, Shaogang Chu, and Geir W. Gabrielsen. 2008. 'Biotransformation of PCBs in Relation to Phase I and II Xenobiotic-Metabolizing Enzyme Activities in Ringed Seals (*Phoca hispida*) from Svalbard and the Baltic Sea'. *Environmental Science and Technology* 42(23):8952–58. doi:10.1021/es801682f.
- Rowland, Ian, Glenn Gibson, Almut Heinken, Karen Scott, Jonathan Swann, Ines Thiele, and Kieran Tuohy. 2018. 'Gut Microbiota Functions: Metabolism of Nutrients and Other Food Components'. *European Journal of Nutrition* 57(1).
- Sanders, Jon G., Annabel C. Beichman, Joe Roman, Jarrod J. Scott, David Emerson, James J. McCarthy, and Peter R. Girguis. 2015. 'Baleen Whales Host a Unique Gut Microbiome with Similarities to Both Carnivores and Herbivores'. *Nature Communications* 6. doi:10.1038/ncomms9285.
- Schwacke, Lori H., Eric S. Zolman, Brian C. Balmer, Sylvain de Guise, R. Clay George, Jennifer Hogue, Aleta A. Hohn, John R. Kucklick, Steve Lamb, Milton Levin, Jenny A. Litz, Wayne E. Mcfee, Ned J. Place, Forrest I. Townsend, Randall S. Wells, and Teresa K. Rowles. 2011. 'Anaemia, Hypothyroidism and Immune Suppression Associated with Polychlorinated Biphenyl Exposure in Bottlenose Dolphins (*Tursiops truncatus*)'. *Proceedings of the Royal Society B: Biological Sciences* 279(1726):48–57. doi:10.1098/rspb.2011.0665.
- Sevelsted, Astrid, Jakob Stokholm, Klaus Bønnelykke, and Hans Bisgaard. 2015. 'Cesarean Section Chronic Immune Disorders'. *Pediatrics* 135(1):e92–98. doi:10.1542/peds.2014-0596.
- Sharma, Ashwani, and Indu Shekhar Thakur. 2008. 'Characterization of Pentachlorophenol Degrading Bacterial Consortium from Chemostat'. *Bulletin of Environmental Contamination and Toxicology* 81(1):12–18. doi:10.1007/s00128-008-9437-2.
- Sharon, Gil, Nikki Jamie Cruz, Dae Wook Kang, Michael J. Gandal, Bo Wang, Young Mo Kim, Erika M. Zink, Cameron P. Casey, Bryn C. Taylor, Christianne J. Lane, Lisa M. Bramer, Nancy G. Isern, David W. Hoyt, Cecilia Noecker, Michael J. Sweredoski, Annie Moradian, Elhanan Borenstein, Janet K. Jansson, Rob Knight, Thomas O. Metz, Carlos Lois, Daniel H. Geschwind, Rosa Krajmalnik-Brown, and Sarkis K. Mazmanian. 2019. 'Human Gut Microbiota

- from Autism Spectrum Disorder Promote Behavioral Symptoms in Mice'. *Cell* 177(6):1600-1618.e17. doi:10.1016/j.cell.2019.05.004.
- Sharon, Itai, Narciso Martín Quijada, Edoardo Pasolli, Marco Fabbrini, Francesco Vitali, Valeria Agamennone, Andreas Dötsch, Evelyne Selberherr, José Horacio Grau, Martin Meixner, Karsten Liere, Danilo Ercolini, Carlotta de Filippo, Giovanna Caderni, Patrizia Brigidi, and Silvia Turrone. 2022. 'The Core Human Microbiome: Does It Exist and How Can We Find It? A Critical Review of the Concept'. *Nutrients* 14(14).
- Shih, Yang Hsin, Hsi Ling Chou, and Yu Huei Peng. 2012. 'Microbial Degradation of 4-Monobrominated Diphenyl Ether with Anaerobic Sludge'. *Journal of Hazardous Materials* 213–214:341–46. doi:10.1016/j.jhazmat.2012.02.009.
- Similä, Tiu, Jens Christian Holst, and Ivar Christensen. 1996. *Occurrence and Diet of Killer Whales in Northern Norway: Seasonal Patterns Relative to the Distribution and Abundance of Norwegian Spring-Spawning Herring*.
- Song, Se Jin, Christian Lauber, Elizabeth K. Costello, Catherine A. Lozupone, Gregory Humphrey, Donna Berg-Lyons, J. Gregory Caporaso, Dan Knights, Jose C. Clemente, Sara Nakielny, Jeffrey I. Gordon, Noah Fierer, and Rob Knight. 2013. 'Cohabiting Family Members Share Microbiota with One Another and with Their Dogs'. *ELife* 2013(2). doi:10.7554/eLife.00458.
- Sorbara, Matthew T., Krista Dubin, Eric R. Littmann, Thomas U. Moody, Emily Fontana, Ruth Seok, Ingrid M. Leiner, Ying Taur, Jonathan U. Peled, Marcel R. M. Van Den Brink, Yael Litvak, Andreas J. Bäuml, Jean Luc Chaubard, Amanda J. Pickard, Justin R. Cross, and Eric G. Pamer. 2019. 'Inhibiting Antibiotic-Resistant Enterobacteriaceae by Microbiota-Mediated Intracellular Acidification'. *Journal of Experimental Medicine* 216(1):84–98. doi:10.1084/jem.20181639.
- Stapleton, Heather M., Shannon M. Kelly, Ruoting Pei, Robert J. Letcher, and Claudia Gunsch. 2009. 'Metabolism of Polybrominated Diphenyl Ethers (PBDEs) by Human Hepatocytes in Vitro'. *Environmental Health Perspectives* 117(2):197–202. doi:10.1289/ehp.11807.
- Stayrook, Keith R., Kelli S. Bramlett, Rajesh S. Savkur, James Ficorilli, Todd Cook, Michael E. Christie, Laura F. Michael, and Thomas P. Burris. 2005. 'Regulation of Carbohydrate Metabolism by the Farnesoid X Receptor'. *Endocrinology* 146(3):984–91. doi:10.1210/en.2004-0965.
- Suman, Sonal, and Tanuja. 2021. 'Isolation and Characterization of a Bacterial Strain Enterobacter Cloacae (Accession No. KX438060.1) Capable of Degrading DDTs Under Aerobic Conditions and Its Use in Bioremediation of Contaminated Soil'. *Microbiology Insights* 14:117863612110242. doi:10.1177/11786361211024289.
- Sun, Yuepeng, Daniel Snow, Harkamal Walia, and Xu Li. 2021. 'Transmission Routes of the Microbiome and Resistome from Manure to Soil and Lettuce'. *Environmental Science and Technology* 55(16):11102–12. doi:10.1021/acs.est.1c02985.
- Suzuki, Taichi A., and Michael Worobey. 2014. 'Geographical Variation of Human Gut Microbial Composition'. *Biology Letters* 10(2). doi:10.1098/rsbl.2013.1037.
- Swart, Rik De L., Peters Ross, Lies J. Vedder, Helga H. Timmerman, Siem Heisterkamp, Henk Van Loveren, Joseph G. V Os, Peter J. H. Reijnders, and Albert D. M. E. Osterhaus. 1994. 'Impairment of Immune Function in Harbor Seals (Phoca Vitulina) Feeding on Fish from Polluted Waters'. *AMBIO A Journal of the Human Environment* 23(2):155–59.
- Tan, Ai Huey, Shen Yang Lim, and Anthony E. Lang. 2022. 'The Microbiome–Gut–Brain Axis in Parkinson Disease — from Basic Research to the Clinic'. *Nature Reviews Neurology* 18(8):476–95.
- Tan, Eddie T. T., Rafat Al Jassim, Bruce R. D'Arcy, and Mary T. Fletcher. 2017. 'In Vitro Biodegradation of Hepatotoxic Indospicine in Indigofera Spicata and Its Degradation Derivatives by Camel Foregut and Cattle Rumen Fluids'. *Journal of Agricultural and Food Chemistry* 65(34):7528–34. doi:10.1021/acs.jafc.7b02492.

- Tan, Mun Hua, Christopher M. Austin, Michael P. Hammer, Yin Peng Lee, Laurence J. Croft, and Han Ming Gan. 2018. 'Finding Nemo: Hybrid Assembly with Oxford Nanopore and Illumina Reads Greatly Improves the Clownfish (*Amphiprion Ocellaris*) Genome Assembly'. *GigaScience* 7(3):1–6.
- Taş, Neslihan, Miriam H. A. van Eekert, Anke Wagner, Gosse Schraa, Willem M. de Vos, and Hauke Smidt. 2011. 'Role of "Dehalococcoides" Spp. in the Anaerobic Transformation of Hexachlorobenzene in European Rivers'. *Applied and Environmental Microbiology* 77(13):4437–45. doi:10.1128/AEM.01940-10.
- Tasiemski, Aurélie, François Massol, Virginie Cuvillier-Hot, Céline Boidin-Wichlacz, Emmanuel Roger, Franck Rodet, Isabelle Fournier, Frédéric Thomas, and Michel Salzet. 2015. 'Reciprocal Immune Benefit Based on Complementary Production of Antibiotics by the Leech *Hirudo Verbana* and Its Gut Symbiont *Aeromonas Veronii*'. *Scientific Reports* 5. doi:10.1038/srep17498.
- Tian, Jiashen, Jing Du, Zhichuang Lu, Jiabo Han, Zhen Wang, Duohui Li, Xiaoyan Guan, and Zhaohui Wang. 2020. 'Distribution of Microbiota across Different Intestinal Tract Segments of a Stranded Dwarf Minke Whale, *Balaenoptera Acutorostrata*'. *MicrobiologyOpen* 9(10). doi:10.1002/mbo3.1108.
- De Vadder, Filipe, Petia Kovatcheva-Datchary, Daisy Goncalves, Jennifer Vinera, Carine Zitoun, Adeline Duchamp, Fredrik Bäckhed, and Gilles Mithieux. 2014. 'Microbiota-Generated Metabolites Promote Metabolic Benefits via Gut-Brain Neural Circuits'. *Cell* 156(1–2):84–96. doi:10.1016/j.cell.2013.12.016.
- Vandenplas, Yvan, V. P. Carnielli, J. Ksiazek, M. Sanchez Luna, N. Migacheva, J. M. Mosselmans, J. C. Picaud, M. Possner, A. Singhal, and M. Wabitsch. 2020. 'Factors Affecting Early-Life Intestinal Microbiota Development'. *Nutrition* 78.
- Wan, Xiaoling, Jia Li, Mengxue Ao, Richard William McLaughlin, Fei Fan, Ding Wang, and Jinsong Zheng. 2023. 'The Intestinal Microbiota of a Risso's Dolphin (*Grampus Griseus*): Possible Relationships with Starvation Raised by Macro-Plastic Ingestion'. *International Microbiology* 26(4):1001–7. doi:10.1007/s10123-023-00355-z.
- de Wit, Cynthia A., Rossana Bossi, Rune Dietz, Annekatrin Dreyer, Suzanne Faxneld, Svend Erik Garbus, Peter Hellström, Jan Koschorreck, Nina Lohmann, Anna Roos, Ulla Sellström, Christian Sonne, Gabriele Treu, Katrin Vorkamp, Bo Yuan, and Igor Eulaers. 2020. 'Organohalogen Compounds of Emerging Concern in Baltic Sea Biota: Levels, Biomagnification Potential and Comparisons with Legacy Contaminants'. *Environment International* 144. doi:10.1016/j.envint.2020.106037.
- Wick, R. R. (2017). FilTlong: quality filtering tool for long reads. GitHub repository. Available from: <https://github.com/rrwick/FilTlong>
- Wick, R. R. (2017). Porechop: adapter trimming tool for Oxford Nanopore reads. GitHub repository. Available from: <https://github.com/rrwick/Porechop>
- Wlodarska, Marta, Chengwei Luo, Raivo Kolde, Eva d'Hennezel, John W. Annand, Courtney E. Heim, Philipp Krastel, Esther K. Schmitt, Abdifatah S. Omar, Elizabeth A. Creasey, Ashley L. Garner, Sina Mohammadi, Daniel J. O'Connell, Sahar Abubucker, Timothy D. Arthur, Eric A. Franzosa, Curtis Huttenhower, Leon O. Murphy, Henry J. Haiser, Hera Vlamakis, Jeffrey A. Porter, and Ramnik J. Xavier. 2017. 'Indoleacrylic Acid Produced by Commensal *Peptostreptococcus* Species Suppresses Inflammation'. *Cell Host and Microbe* 22(1):25-37.e6. doi:10.1016/j.chom.2017.06.007.
- Wójcik, Aneta, Paulina Perczyk, Paweł Wydro, and Marcin Broniatowski. 2020. 'Dichlorobiphenyls and Chlorinated Benzoic Acids – Emergent Soil Pollutants in Model Bacterial Membranes. Langmuir Monolayer and Grazing Incidence X-Ray Diffraction Studies'. *Journal of Molecular Liquids* 307. doi:10.1016/j.molliq.2020.112997.
- Wood, Derrick E., Jennifer Lu, and Ben Langmead. 2019. 'Improved Metagenomic Analysis with Kraken 2'. *Genome Biology* 20(1). doi:10.1186/s13059-019-1891-0.

- Wrobel, Michal, Jaroslaw Mlynarczuk, and Jan Kotwica. 2009. 'The Adverse Effect of Dichlorodiphenyltrichloroethane (DDT) and Its Metabolite (DDE) on the Secretion of Prostaglandins and Oxytocin in Bovine Cultured Ovarian and Endometrial Cells'. *Reproductive Toxicology* 27(1):72–78. doi:10.1016/j.reprotox.2008.10.008.
- Wu, Zhineng, Miaomiao Xie, Yao Li, Guanghai Gao, Mark Bartlam, and Yingying Wang. 2018. 'Biodegradation of Decabromodiphenyl Ether (BDE 209) by a Newly Isolated Bacterium from an e-Waste Recycling Area'. *AMB Express* 8(1). doi:10.1186/s13568-018-0560-0.
- Xiang, Yun, Ziyu Xing, Juan Liu, Wei Qin, and Xing Huang. 2020. 'Recent Advances in the Biodegradation of Polychlorinated Biphenyls'. *World Journal of Microbiology and Biotechnology* 36(10). doi:10.1007/s11274-020-02922-2.
- Xu, Weiguang, Xian Wang, and Zongwei Cai. 2013. 'Analytical Chemistry of the Persistent Organic Pollutants Identified in the Stockholm Convention: A Review'. *Analytica Chimica Acta* 790:1–13.
- Yang, X., X. Liu, L. Song, F. Xie, G. Zhang, and S. Qian. 2007. 'Characterization and Functional Analysis of a Novel Gene Cluster Involved in Biphenyl Degradation in *Rhodococcus* Sp. Strain R04'. *Journal of Applied Microbiology* 103(6):2214–24. doi:10.1111/j.1365-2672.2007.03461.x.
- Yurdusev, N., M. Ladire, R. Ducluzeau, and P. Raibaud. 1989. *Antagonism Exerted by an Association of a Bacteroides Thetaiotaomicron Strain and a Fusobacterium Necrogenes Strain against Clostridium Perfringens in Gnotobiotic Mice and in Fecal Suspensions Incubated In Vitro*. Vol. 57.
- Zhang, Ping. 2022. 'Influence of Foods and Nutrition on the Gut Microbiome and Implications for Intestinal Health'. *International Journal of Molecular Sciences* 23(17).
- Zhang, Ruiming, Pengfei Li, Ruiying Zhang, Xiangli Shi, Yanwei Li, Qingzhu Zhang, and Wenxing Wang. 2021. 'Computational Study on the Detoxifying Mechanism of DDT Metabolized by Cytochrome P450 Enzymes'. *Journal of Hazardous Materials* 414. doi:10.1016/j.jhazmat.2021.125457.
- Zhang, Wenping, Ziqiu Lin, Shimei Pang, Pankaj Bhatt, and Shaohua Chen. 2020. 'Insights Into the Biodegradation of Lindane ( $\gamma$ -Hexachlorocyclohexane) Using a Microbial System'. *Frontiers in Microbiology* 11.
- Zhang, Xue, Li Li, Zhiyong Xie, Jianmin Ma, Yi-Fan Li, Minghong Cai, Nan-Qi Ren, Roland Kallenborn, Zi-Feng Zhang, Xianming Zhang, and Derek C. G. Muir. 2024a. *ENVIRONMENT Exploring Global Oceanic Persistence and Ecological Effects of Legacy Persistent Organic Pollutants across Five Decades*. Vol. 10.
- Zhang, Xue, Li Li, Zhiyong Xie, Jianmin Ma, Yi-Fan Li, Minghong Cai, Nan-Qi Ren, Roland Kallenborn, Zi-Feng Zhang, Xianming Zhang, and Derek C. G. Muir. 2024b. *ENVIRONMENT Exploring Global Oceanic Persistence and Ecological Effects of Legacy Persistent Organic Pollutants across Five Decades*. Vol. 10.

## A. Addendum

### Risk Assessment

#### General safety

According to standard laboratory safety measurements, a lab coat and a fresh pair of gloves were worn during all lab procedures.

#### Chemical risks

Laboratory utensils and gloves were disinfected using 70% ethanol. As ethanol is a highly flammable liquid (H225), appropriate safety precautions were strictly followed. Ethanol was stored away from heat sources, open flames, and other potential ignition points, and smoking was strictly prohibited (P210). Containers were kept tightly closed when not in use (P233), and precautions were taken to avoid the buildup of static electricity (P243). Personnel wore suitable protective gloves during handling (P280). In the event of skin contact, contaminated clothing was to be removed immediately and affected skin rinsed thoroughly with water (P303 + P361 + P353). In the case of fire, suitable extinguishing media such as CO<sub>2</sub> or foam was to be used (P370 + P378). Ethanol was stored in a cool, well-ventilated area to reduce vapor accumulation and fire risk (P403 + P235).

The exact chemical composition of the reagents in the HostZERO and PowerFecal kits is proprietary and has not been publicly disclosed. As a result, a targeted risk assessment based on specific components could not be performed. However, based on their intended function – which involves cell lysis and nucleic acid purification – it is highly likely that these kits contain DNA-binding agents and chaotropic substances, which may pose potential hazards such as skin and eye irritation (H315, H319), respiratory irritation (H335), or suspected mutagenicity (H341). Accordingly, appropriate precautions were taken to mitigate these risks. Suitable personal protective equipment, including gloves and lab coats was worn at all times (P280). In the event of skin or eye contact, the affected area was to be rinsed thoroughly with water (P302 + P352, P305 + P351 + P338). Reagents were stored in tightly sealed containers in a well-ventilated, temperature-controlled environment (P403 + P233 + P235). Spills were cleaned up immediately using appropriate absorbent material, avoiding direct contact (P273, P370)

#### Physical risks

Samples were stored at -80 °C. Due to the risk of frostbite from prolonged exposure to sub-zero temperatures, insulated gloves were worn when accessing the -80 °C freezer. All handling was conducted swiftly and with appropriate protective measures to ensure safety.

#### Environmental

All chemicals and contaminated lab utensils were disposed of according to local regulations.

## B.Supplementary content

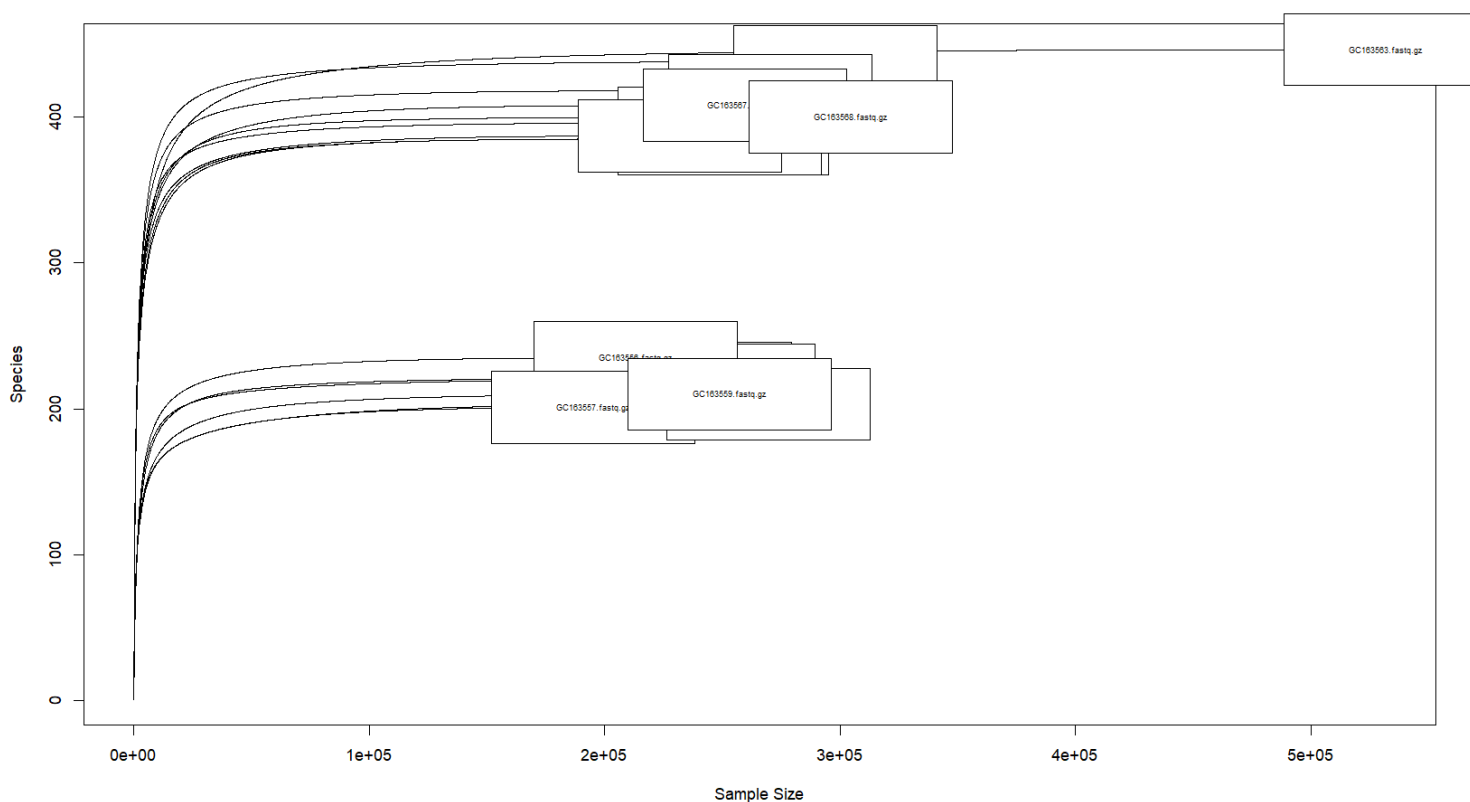


**Figure S1 | Rarefaction curves of DADA2 filtered 16S rRNA sequences for all samples.** Samples were rarified to  $1.9e^{+05}$  reads.

**Table S1 | Estimated dispersions for fitted generalized linear models.** Results showing the estimated dispersion parameter of the generalized linear models for all four  $\alpha$ -diversity indices: SR: species richness, SHD: Shannond diversity, SID: Simpson diversity, FPD: Faiths phylogenetic diversity.

	Estimated dispersion parameter
SR	0.9641619
SHD	3.515316e-05
SID	0.002178904
FPD	0.02087133

**Table S2 | Pairwise post hoc Tukey-adjusted comparisons of estimated marginal means statistics.** Results of post hoc pairwise tests conducted to assess differences in alpha diversity between individual intestinal regions: duodenum, jejunum, ileum, colon, and rectum. Four alpha diversity indices were evaluated: SR: species richness, SHD: Shannon diversity, SID: Simpson diversity, and FPD: Faith's phylogenetic diversity. Statistically significant results are indicated in bold. Significant results are indicated in bold.

Diversity index	contrast	ratio	SE	df	null	z.ratio/t-ratio	p.value
SR	Duodenum / Jejunum	1.100977	0.061378	Inf	1	1.725557	0.418103
	Duodenum / Ileum	0.539936	0.02577	Inf	1	-12.9127	<b>&lt; .0001 ***</b>

	Duodenum / Colon	0.555921	0.026671	Inf	1	-12.2381	< .0001 ***
	Duodenum / Rectum	0.56569	0.027224	Inf	1	-11.8379	< .0001 ***
	Jejunum / Ileum	0.490415	0.024162	Inf	1	-14.4616	< .0001 ***
	Jejunum / Colon	0.504934	0.024998	Inf	1	-13.8024	< .0001 ***
	Jejunum / Rectum	0.513808	0.025512	Inf	1	-13.411	< .0001 ***
	Ileum / Colon	1.029605	0.041455	Inf	1	0.724628	0.950878
	Ileum / Rectum	1.047699	0.042371	Inf	1	1.152175	0.778538
	Colon / Rectum	1.017573	0.041449	Inf	1	0.427677	0.993037
SHD	Duodenum / Jejunum	0.968782	0.00469	10	1	-6.5514	<b>0.000479</b> ***
	Duodenum / Ileum	0.744995	0.003607	10	1	-60.8092	< .0001 ***
	Duodenum / Colon	0.725856	0.003514	10	1	-66.1852	< .0001 ***
	Duodenum / Rectum	0.700926	0.003393	10	1	-73.4047	< .0001 ***
	Jejunum / Ileum	0.769001	0.003723	10	1	-54.2578	< .0001 ***
	Jejunum / Colon	0.749246	0.003627	10	1	-59.6338	< .0001 ***
	Jejunum / Rectum	0.723512	0.003503	10	1	-66.8533	< .0001 ***
	Ileum / Colon	0.97431	0.004717	10	1	-5.37605	<b>0.002238</b> ***
	Ileum / Rectum	0.940847	0.004555	10	1	-12.5955	< .0001 ***
	Colon / Rectum	0.965654	0.004675	10	1	-7.21947	<b>0.000215</b> ***
SID	Duodenum / Jejunum	1.22567	0.046714	10	1	5.339049	<b>0.002355</b> ***
	Duodenum / Ileum	0.396298	0.015104	10	1	-24.2854	< .0001 ***
	Duodenum / Colon	0.282015	0.010748	10	1	-33.2116	< .0001 ***
	Duodenum / Rectum	0.214657	0.008181	10	1	-40.3723	< .0001 ***
	Jejunum / Ileum	0.323331	0.012323	10	1	-29.6244	< .0001 ***
	Jejunum / Colon	0.230091	0.008769	10	1	-38.5507	< .0001 ***
	Jejunum / Rectum	0.175135	0.006675	10	1	-45.7114	< .0001 ***
	Ileum / Colon	0.711624	0.027122	10	1	-8.92621	< .0001 ***
	Ileum / Rectum	0.541657	0.020644	10	1	-16.087	< .0001 ***
	Colon / Rectum	0.761155	0.02901	10	1	-7.16074	<b>0.00023</b> ***
FPD	Duodenum / Jejunum	1.11096	0.131047	10	1	0.892047	0.893511
	Duodenum / Ileum	1.373847	0.162057	10	1	2.692599	0.125156
	Duodenum / Colon	0.88665	0.104588	10	1	-1.01989	0.840781
	Duodenum / Rectum	1.030691	0.121579	10	1	0.256274	0.998876
	Jejunum / Ileum	1.236631	0.145871	10	1	1.800553	0.423593
	Jejunum / Colon	0.798094	0.094142	10	1	-1.91194	0.370455
	Jejunum / Rectum	0.927748	0.109436	10	1	-0.63577	0.965523
	Ileum / Colon	0.645378	0.076128	10	1	-3.71249	<b>0.026005</b> *
	Ileum / Rectum	0.750223	0.088495	10	1	-2.43632	0.182529
	Colon / Rectum	1.162455	0.137122	10	1	1.276164	0.710482

**Table S3 | ANOVA on homogeneity of group dispersions statistics.** Results of the permutation-based ANOVA on the average distance of samples to their group centroid in ordination space across 5 intestinal regions: duodenum, jejunum, ileum, colon and rectum; based on all four distance metrics: BC: Bray-Curtis, JC: Jaccard, WUF, Weighted Unifrac

	Df	Sum Sq	Mean Sq	F value	p-value
BC Dissimilarity	4	0.0024604	0.00061509	1.0519	0.4285
JC Dissimilarity	4	0.0084444	0.0021111	1.4296	0.2938
WUF Dissimilarity	4	0.00019583	4.8957e-05	1.4289	0.294
UUF Dissimilarity	4	0.023794	0.0059485	0.5713	0.6897

**Table S4 | Pairwise PERMANOVA on difference in microbiome community composition between intestinal regions.** Results from the pairwise permutational ANOVA to test for differences in microbiome composition between the individual 5 intestinal regions: duodenum, jejunum, ileum, colon and rectum; for all four dissimilarity matrices (BC: Bray-Curtis, JC: Jaccard, WUF: weighted Unifrac, UUF: unweighted Unifrac). Significant effects and p-values are in bold.

	pairs	Df	SumsOfSqs	F.Model	R2	p.value	p.adjusted
<b>BC</b>							
Dissimilarity	Duodenum / Jejunum	1	1.055839	630.342	0.993694	0.1	1
	Duodenum / Ileum	1	1.254399	2285.559	0.998253	0.1	1
	Duodenum / Colon	1	1.28015	601.1893	0.99339	0.1	1
	Duodenum / Rectum	1	1.276866	564.0198	0.992958	0.1	1
	Jejunum / Ileum	1	0.52723	310.6447	0.987287	0.1	1
	Jejunum / Colon	1	0.711394	217.0381	0.981904	0.1	1
	Jejunum / Rectum	1	0.906032	265.5237	0.985159	0.1	1
	Ileum / Colon	1	0.347015	161.2861	0.9758	0.1	1
	Ileum / Rectum	1	0.603721	264.0883	0.98508	0.1	1
	Colon / Rectum	1	0.13148	34.00431	0.894749	0.1	1
<b>JC</b>							
Dissimilarity	Duodenum / Jejunum	1	1.239279	213.4954	0.981609	0.1	1
	Duodenum / Ileum	1	1.365487	664.4711	0.994016	0.1	1
	Duodenum / Colon	1	1.371427	189.464	0.979324	0.1	1
	Duodenum / Rectum	1	1.368894	178.5812	0.978092	0.1	1
	Jejunum / Ileum	1	0.822723	139.8098	0.972185	0.1	1
	Jejunum / Colon	1	0.980078	88.5502	0.95678	0.1	1
	Jejunum / Rectum	1	1.128877	98.20607	0.960863	0.1	1
	Ileum / Colon	1	0.622518	85.06272	0.955088	0.1	1
	Ileum / Rectum	1	0.892548	115.2378	0.966454	0.1	1
	Colon / Rectum	1	0.300987	23.28048	0.853375	0.1	1
<b>WUF</b>							
Dissimilarity	Duodenum / Jejunum	1	0.019647	247.675	0.984106	0.1	1
	Duodenum / Ileum	1	0.023895	2183.562	0.998171	0.1	1
	Duodenum / Colon	1	0.032549	433.4679	0.990856	0.1	1
	Duodenum / Rectum	1	0.038693	349.3531	0.98868	0.1	1
	Jejunum / Ileum	1	0.008563	105.4117	0.963441	0.1	1
	Jejunum / Colon	1	0.012955	89.11374	0.957042	0.1	1
	Jejunum / Rectum	1	0.018823	103.9686	0.962952	0.1	1
	Ileum / Colon	1	0.003524	45.7653	0.919623	0.1	1
	Ileum / Rectum	1	0.006337	56.25135	0.933611	0.1	1
	Colon / Rectum	1	0.0027	15.27334	0.792459	0.1	1
<b>UUF</b>							
Dissimilarity	Duodenum / Jejunum	1	0.123394	3.098193	0.436476	0.1	1
	Duodenum / Ileum	1	0.329698	12.99735	0.764669	0.1	1
	Duodenum / Colon	1	0.353095	6.57213	0.621647	0.1	1
	Duodenum / Rectum	1	0.474881	22.24861	0.847611	0.1	1
	Jejunum / Ileum	1	0.158569	4.661539	0.538188	0.1	1
	Jejunum / Colon	1	0.263749	4.228368	0.513877	0.1	1

Jejunum / Rectum	1	0.322266	10.74429	0.728708	0.1	1
Ileum / Colon	1	0.187892	3.921374	0.495037	0.1	1
Ileum / Rectum	1	0.205459	13.2273	0.76781	0.1	1
Colon / Rectum	1	0.079877	1.819842	0.312696	0.1	1

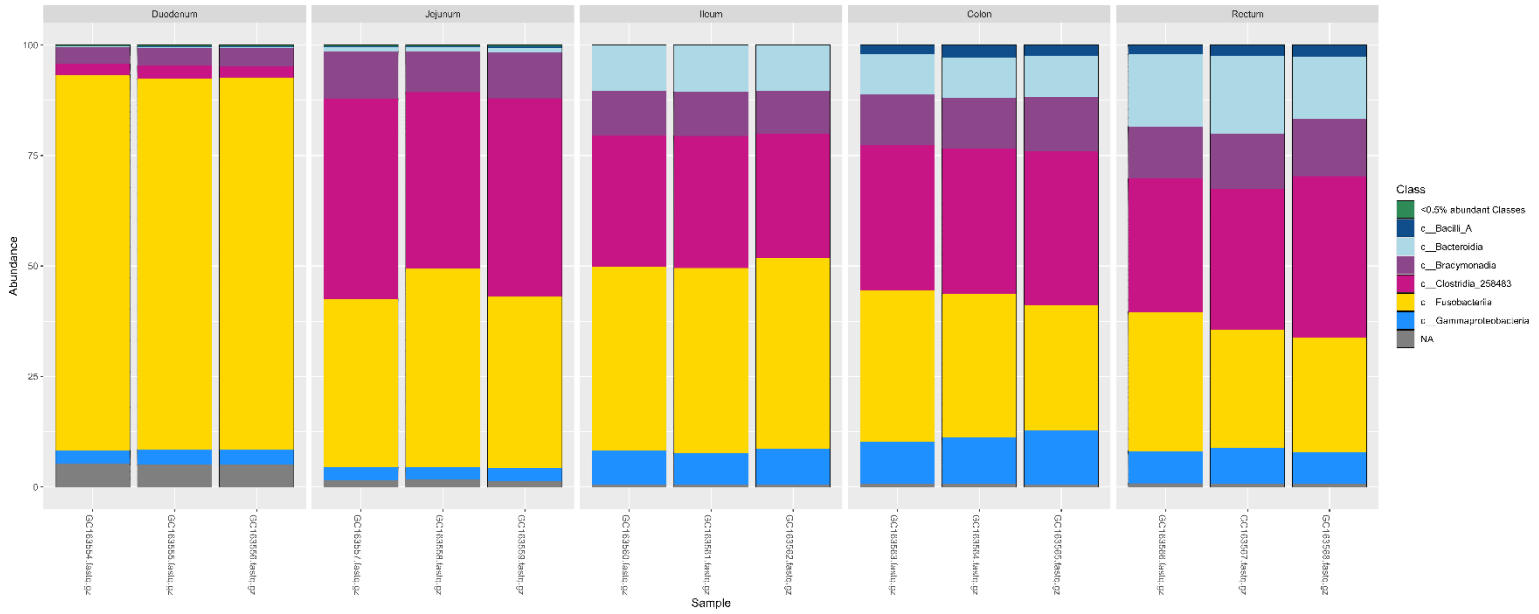


**Fig. S2 | Community composition across the intestinal tract at class level.** Bar plots showing the relative abundances (%) of each detected bacterial class per sample. classes with a relative abundance < 0.5% are grouped.

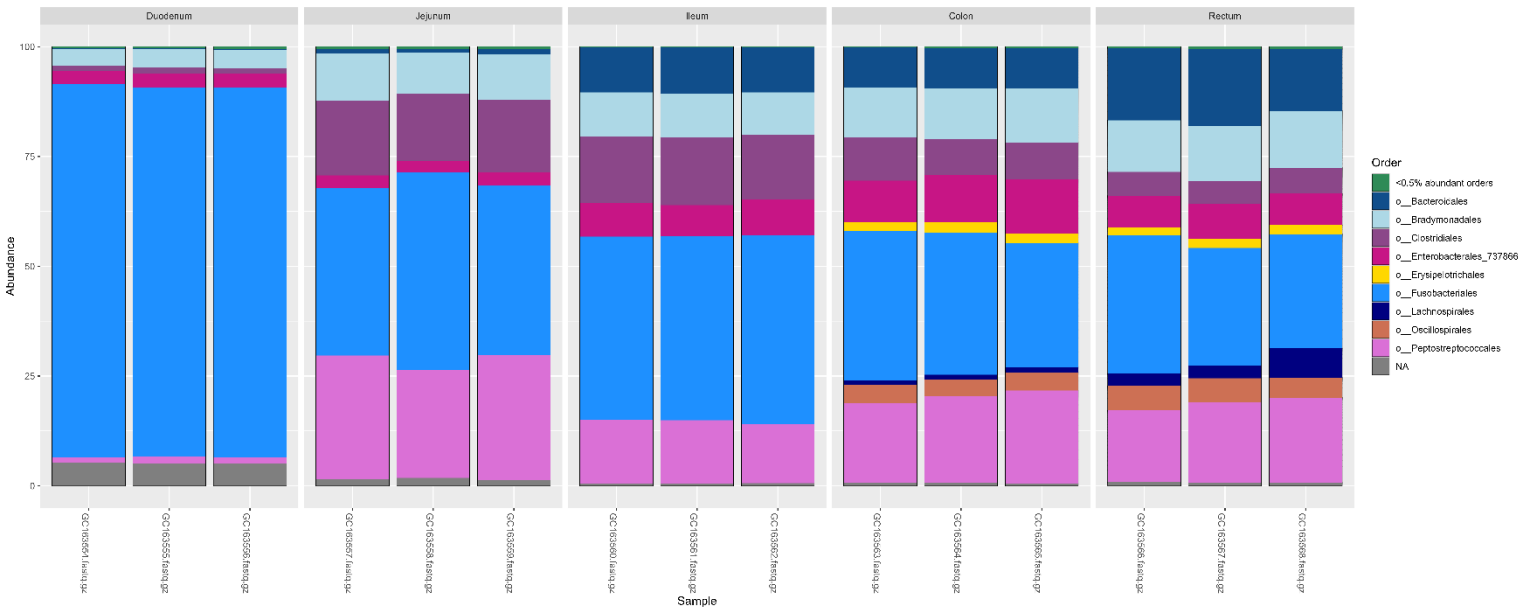


**Fig S3 | Community composition across the intestinal tract at order level.** Bar plots showing the relative abundance (%) of all detected bacterial orders per sample. Orders with a relative abundance < 0.5% are grouped.

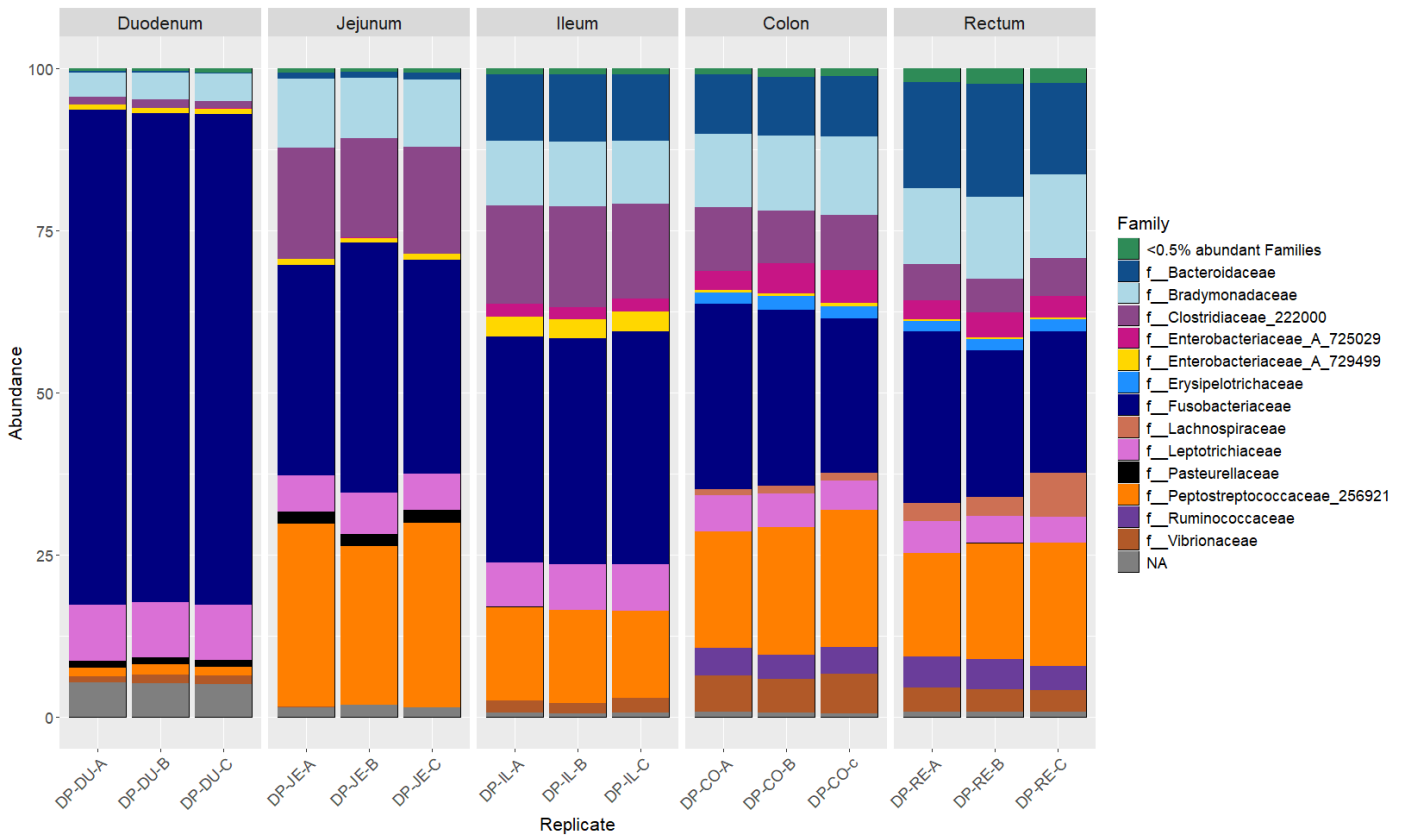


**Figure S4 | Microbiome composition of killer whale De Panne along its intestinal tract at family level.** Bar plots show the relative abundances (%) of bacterial families per replicate grouped by anatomical site: Duodenum, Jejunum, Ileum, Colon, and Rectum for killer whale De Panne. Families with a relative abundance < 0.5% are pooled under the category “<0.5% abundant Families”.



The student declares that the submitted thesis text (including graphs) is original work, written using the wording of the student and reflecting the student's English language proficiency. The text acknowledges, to the best of the ability and knowledge of the student, previous ideas and data.

## **Generative AI**

Generative AI has strictly been used according to KU Leuven guidelines and appropriate references have been added. I take full responsibility for the content of this thesis.

**AFDELING**  
Straat nr bus 0000  
3000 LEUVEN, BELGIË  
tel. + 32 16 00 00 00  
fax + 32 16 00 00 00  
[www.kuleuven.be](http://www.kuleuven.be)

